UNCERTAINTY ASSESSMENT IN RESERVE ESTIMATION OF A NATURALLY FRACTURED RESERVOIR

A THESIS SUBMITTED TO
THE GRADUATE SCHOOL OF NATURAL AND APPLIED SCIENCES
OF
MIDDLE EAST TECHNICAL UNIVERSITY

BY

ÖZLEN ERIÇOK

IN PARTIAL FULFILLMENT OF THE REQUIREMENTS
FOR
THE DEGREE OF MASTER OF SCIENCE
IN
THE DEPARTMENT OF PETROLEUM AND
NATURAL GAS ENGINEERING

DECEMBER 2004

Approval of the Graduate School of Natural and Applied Sciences

_____

Prof. Dr. Canan ÖZGEN
Director

I certify that this thesis satisfies all the requirements as a thesis for the degree of Master of Science.

_____

Prof. Dr. Birol DEMIRAL
Head of Department

This is to certify that we have read this thesis and that in our opinion it is fully adequate, in scope and quality, as a thesis for the degree of Master of Science.

_____

Prof. Dr. Fevzi GÜMRAH
Supervisor

Examining Committee Members

Prof. Dr. Birol DEMIRAL (Chair Person, METU) _____

Prof. Dr. Fevzi GÜMRAH (METU) _____

Prof. Dr. Nurkan KARAHANOGLU (METU) _____

Assoc. Prof. Dr. Serhat AKIN (METU) _____

Yildiz KARAKEÇE (TPAO) _____

I hereby declare that all information in this document has been obtained and presented in accordance with academic rules and ethical conduct. I also declare that, as required by these rules and conduct, I have fully cited and referenced all material and results that are not original to this work.

Özlen ERIÇOK

ABSTRACT

UNCERTAINTY ASSESSMENT IN RESERVE ESTIMATION OF

A NATURALLY FRACTURED RESERVOIR

ERIÇOK, Özlen

M.S., Department of Petroleum and Natural Gas Engineering

Supervisor : Prof. Dr. Fevzi GÜMRAH

December 2004, 169 pages

Reservoir performance prediction and reserve estimation depend on various petrophysical parameters which have uncertainties due to available technology. For a proper and economical field development, these parameters must be determined by taking into consideration their uncertainty level and probable data ranges.

For implementing uncertainty assessment on estimation of original oil in place (OOIP) of a field, a naturally fractured carbonate field, Field-A, is chosen to work with. Since field information is obtained by drilling and testing wells throughout the field, uncertainty in true ranges of reservoir parameters evolve due to impossibility of drilling every location on an area. This study is based on defining the probability distribution of uncertain variables in reserve estimation and evaluating probable reserve amount by using Monte Carlo simulation method. Probabilistic reserve estimation gives the whole range of probable

original oil in place amount of a field. The results are given by their likelyhood of occurance as P10, P50 and P90 reserves in summary.

In the study, Field-A reserves at Southeast of Turkey are estimated by probabilistic methods for three producing zones; Karabogaz Formation, Kbb-C Member of Karababa formation and Derdere Formation. Probability density function of petrophysical parameters are evaluated as inputs in volumetric reserve estimation method and probable reserves are calculated by @Risk software program that is used for implementing Monte Carlo method.

Outcomes of the simulation showed that Field-A has P50 reserves as 11.2 MMstb in matrix and 2.0 MMstb in fracture of Karabogaz Formation, 15.7 MMstb in matrix and 3.7 MMstb in fracture of Kbb-C Member and 10.6 MMstb in matrix and 1.6 MMstb in fracture of Derdere Formation. Sensitivity analysis of the inputs showed that matrix porosity, net thickness and fracture porosity are significant in Karabogaz Formation and Kbb-C Member reserve estimation while water saturation and fracture porosity are most significant in estimation of Derdere Formation reserves.

Keywords: Uncertainty, Probability, Monte Carlo Method, Probability Density Function, Cumulative Probability Distribution, Matrix, Fracture, Reserve Estimation, Volumetric Method

ÖZ

DOGAL ÇATLAKLI BIR REZERVUARIN REZERV TAHMININDE BELIRSIZLIK DEGERLENDIRMESI

ERIÇOK, Özlen
Yüksek Lisans, Petrol ve Dogal Gaz Mühendisligi Bölümü
Tez Yöneticisi : Prof. Dr. Fevzi GÜMRAH

December 2004, 169 sayfa

Rezervuar performansi ve rezerv tahmini, mevcut teknolojiye bagli olarak belirsizlik içeren birçok petrofizik parametreye dayalidir. Uygun ve ekonomik bir saha gelistirme için bu parametreler belirsizlik düzeyleri ve olasi veri araliklari göz önüne alinarak saptanmalidir.

Bir sahanin orjinal yerinde petrol miktarinin (OOIP) tahmininde belirsizlik degerlendirmesinin uygulanmasi için çalismak üzere dogal çatlakli karbonat bir saha olan Field-A seçilmistir. Saha bilgileri, saha genelinde kuyularin sondaji ve test edilmesiyle saglanabildiginden, tüm sahada sondaj yapmanin imkansizligi sebebiyle rezervuar parametrelerinin gerçek deger araliklarinda belirsizlik ortaya çikmaktadir. Bu çalisma, rezerv tahminindeki belirsiz degiskenlerin olasilik dagilimlarini tanimlamak ve olasi rezerv miktarini Monte Carlo

simülasyonu metoduyla ölçmek üzerinedir. Istatistiksel rezerv tahmini bir sahanin olasi tüm yerinde petrol miktarini vermektedir. Sonuçlar olasilik ihtimallerine göre özet olarak P10, P50 ve P90 rezervleri olarak verilmistir.

Çalismada, Türkiye'nin güneydogusunda bulunan Field-A rezervi istatistiksel metotlarla üç üretim zonu için tahmin edilmistir; Karabogaz Formasyonu, Karababa Formasyonunun Kbb-C Üyesi ve Derdere Formasyonu. Petrofizik parametrelerin olasilik dagilim fonksiyonlari hacimsel rezerv tahmini metoduna girdi olarak degerlendirilmis ve olasi rezervler Monte Carlo metodunun uygulanmasi için @Risk programi kullanilarak hesaplanmistir.

Simülasyon sonuçlari, P50 rezerv tahminine göre Field-A'nin Karabogaz Formasyonu matriksinde 11.2 MMstb ve çatlaginda 2.0 MMstb, Kbb-C Üyesi matriksinde 15.7 ve çatlaginda 3.7 MMstb ve Derdere Formasyonu matriksinde 10.6 MMstb ve çatlaginda 1.6 MMstb yerinde petrol oldugunu göstermistir. Girdilerin duyarlilik analizi, matriks gözenekliligi, net kalinlik ve çatlak gözenekliliginin Karabogaz Formasyonu ve Kbb-C Üyesinde önemli, Derdere Formasyonu rezervinde ise matriks su doymuslugu ve çatlak gözenekliliginin önemli oldugunu göstermistir.

Anahtar Kelimeler: Belirsizlik, Olasilik, Monte Carlo Metodu, Olasilik Dagilimi Fonksiyonu, Kümülatif Olasilik Dagilimi, Matriks, Çatlak, Rezerv Tahmini, Hacimsel Metod

To My Family

and

Yafeko

ACKNOWLEDGEMENTS

I would like to express my deepest gratitude to my supervisor Prof. Dr. Fevzi GÜMRAH for his encouraging support and trust, to my managers, Yildiz KARAKEÇE and Mustafa YILMAZ for their advices and ideas during the study.

I would like to express my gratitude to my family for their generous attitude and support.

I would also like to thank TPAO Production Group members for their help and Schlumberger, Calgary engineers for their ideas.

The technical assistance of my colleagues in TPAO and METU are gratefully acknowledged.

TABLE OF CONTENTS

LIST OF TABLES

TABLE

LIST OF FIGURES

FIGURE

NOMENCLATURE

Symbol	Description	Unit
a	matrix block dimension	cm
A	area	m^2
A_{fD}	Areal fracture density	1/cm
B_{oi}	initial formation volume factor of oil	rbbl/stb
c.d.f	cumulative probability distribution	
f_i	frequency of a class interval	
FMI	Fullbore Formation Microimager log	
h	net thickness	m
Hcpt	hydrocarbon pore thicknes	m
K_f	Fracture permeability	darcy
l	matrix block length	cm
L_{fD}	Linear fracture density	1/cm
min	minimum value	
mode	modal value	
max	maximum value	
Mstb	10^3 stb	
MMstb	10^6 stb	
n	number of data points in a sample pool	
ntg	net to gross thickness ratio	fraction
OOIP	original oil in place	stb
p.d.f	probability density function	
ppm	salinity	parts / million
psi	pressure	pounds/ $inch^2$
psia	atmospheric pressure	
psig	gauge pressure	

Symbol	Description	Unit
r	Pearson Product-Moment Correlation Coefficient	fraction
rbbl	reservoir blue barrel stb	stock tank barrel
s	standard deviation of a sample data set	
SPI	secondary porosity index	
S_{wi}	initial water saturation	fraction or %
S_{wim}	initial water saturation of matrix	fraction or %
S_{wif}	initial water saturation of fracture	fraction or %
V_{fD}	Volumetric fracture density	1/cm
$\bar{x}$	arithmetic mean	
x_i	i^{th} value of the data	
x'_i	class mark	
$Ø_f$	Fracture porosity	fraction or %
$Ø_{ND}$	density-neutron log porosity	fraction or %
$Ø_m$	Matrix porosity	fraction or %
$Ø_S$	sonic log porosity	fraction or %
μ	population mean	
s^2	population variance	
s	standard deviation of population	
?	resistivity	ohm
?	error function	

CHAPTER 1

INTRODUCTION

The subject of this study is to understand the effects and importance of reservoir variables in calculation of original oil in place amount. It is not hard to say that there is as much uncertainty as we have few data regarding these variables. To be able to make an economic planning and improvement of an oil field, facts and limits must be fully understood and defined in terms of reservoir structure and petrophysical properties.

Characteristics of an oil field can only be defined by application of detailed testing of reservoir properties. To evaluate the petrophysical and hydrocarbon properties some series of laboratory testing must be performed on hydrocarbon and rock samples. Proper sampling is not always possible because of the very own characteristics of reservoir structure. So whether high technology tools are used and detailed testing is implemented or not there will always be some uncertainty in characterization of field because of the limited amount of reservoir properties' representative samples that could be gathered.

Since planning and improvement are all based on economics and time limitations of a company, calculations of reserves and producible oil amounts must be performed in time and since it is known that there are uncertainties on the variables of calculations a method must be used to assess the uncertainty. Statistical calculations are widely used to make reservoir characterization in petroleum industry via making a generalization of the hydrocarbon and rock properties.

In this study, a fractured carbonate oil field, Field-A is used to implement statistical methods by using its recorded production and petrochemical data. Original oil in place amount of the field, in matrix and fracture system is

calculated by statistical approach. Monte Carlo simulation technique is chosen which gives the opportunity to make several runs of calculations in order to get representative approach to the reservoir properties.

CHAPTER 2

LITERATURE REVIEW

Petroleum reserves classification systems have evolved significantly over the last 10 years [1]. The February 2000 resource classification (Figure 2.1) published jointly by the Society of Petroleum Engineers (SPE), World Petroleum Congress (WPC), and American Association of Petroleum Geologists (AAPG,[2]) is now accepted as an industry standard framework for characterizing hydrocarbon assets and opportunities.

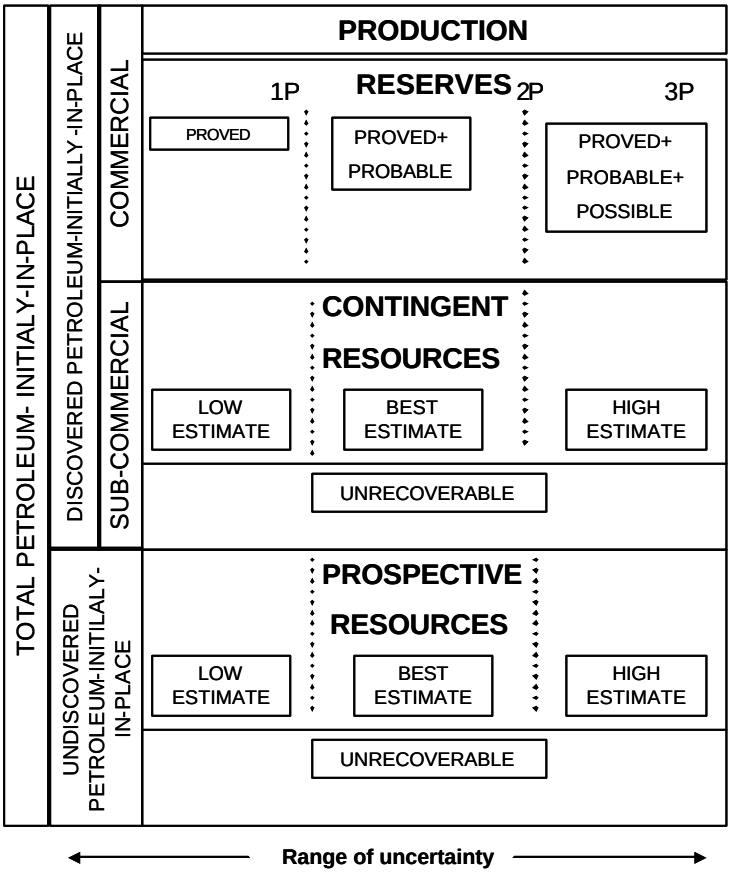

Figure 2.1 SPE/WPC/AAPG Resource Classification [1]

As it can be seen in Figure 2.1 , total hydrocarbons in place are divided mainly in two categories as resources and reserves. Resources are generally accepted to be all volumes of hydrocarbons contained in the sub-surface, plus those volumes already produced [3]. An example definition, by the Canadian Institute of Mining, Metallurgy and Petroleum (CIM, [4]), is as follows:

"*Resources are the total quantities of oil and gas and related substances that are estimated, at a particular time, to be contained in, or that have been produced from known accumulations, plus those estimated quantities in accumulations yet to be discovered*."

Reserves constitute a sub-set of resources and, despite the number of different reserve definitions currently in use, there are four key criteria which frequently constitute the basis of the definitions [3]. These reflect the requirement that in order to be "reserves", the volumes of hydrocarbons must be:

i) discovered
ii) recoverable
iii) commercial and
iv) remaining

SPE also explains reserves as, "*Reserves are estimated volumes of crude oil, condensate, natural gas, natural gas liquids and associated substances anticipated to be commercially recoverable from known accumulations from a given date forward, under existing economic conditions, by established operating practices, and under current government regulations"* [5]. In summary, official reserves definition suggests that reserves can be classified in three groups such as "proved", "probable" and "possible".

2.1 Estimating Reserve Volumes

Reserves frequently are estimated (1) before drilling or any subsurface development, (2) during the development drilling of the field, after some performance data are available, and (3) after performance trends are well established [6]. While the ultimate recovery estimates may become accurate at some point in the late life of a reservoir, the reserve estimate at that time still may have a significant risk.

Reserve estimating methods usually are categorized into three families: (1) analogy, (2) volumetric, and (3) performance techniques. The performance technique methods usually are subdivided into simulation studies, material-balance calculations, and decline trend analysis [6]. Level of uncertainty in these techniques becomes lesser from analogy to performance techniques, where analogy method is based purely on statistics of a similar field when the prospect in study has none or insufficient wells.

2.1.1 Deterministic and Probabilistic (Statistical) Methods

Reserves of a field can be calculated in two ways as *deterministic* and *probabilistic (statistical)* methods. If the value of a variable is known or can be predicted with certainty at the time of decision making, the variable is called a deterministic variable [7]. The deterministic calculation of reserves is where specific values of each input parameter are multiplied together to determine a single estimate of reserves [3]. In this case, the deterministic method has to give the best estimate by highest confidence and this is only possible when enough and quality data are supplied. But, deterministic approach gives only a single number and, therefore, provides no information regarding uncertainty. Arguments presented in favor of the deterministic approach are:

i) simple to apply;

ii) easy to audit;
iii) based on specific criteria;
iv) conservative at proved level; and,
v) avoids misleading pseudo-accuracy [3].

In the statistical approach, each input parameter is defined by an uncertainty distribution (probability density function). The basis for the distribution is generally three input variables (e.g. low, most likely, high), which may be identical to those values used in the deterministic approach, an estimate of the levels of certainty associated with the low and high values, and an assumption of the type (shape) of the distribution. The distributions are then combined together using statistical methods with some assumptions regarding the level of dependence between parameters [3]. Arguments presented in favor of the statistical approach are:

i) mathematically correct;
ii) documents whole range of uncertainty;
iii) assigns values to level of uncertainty;
iv) leads to greater consistency of results.

As a result, in calculation of reserves by statistical methods, results can be given by cumulative probability levels which mean all the possible reserves add up to 100 %. For providing common understanding reserve estimations are generally summarized by three certainty levels as P10, P50 and P90 reserves. In these terms, P leads to probability and as it gets lesser the level of certainty gets higher. By P10 it is meant that there is 10 % uncertainty but 90 % confidence that the reserves are equal or less than that estimation. Generally, P50 estimates are close to deterministic estimates but it is also possible to see the variation in estimates depending on the variation in the reservoir parameters by probabilistic approach [8, 9, 10].

There are principally two methods for statistical calculations, Monte Carlo simulation and decision tree analysis. Monte Carlo technique considers entire ranges of the variables of original oil in place (OOIP) formula rather than deterministic figures [11].

In reserve calculation of a field there are several uncertain variables. In a traditional oil reservoir with rather homogeneous porosity and structure, uncertain variables that are most affecting the reserves volume can be listed as area, matrix pay thickness, hydrocarbon saturation and original formation volume factor of oil. But in a naturally fractured reservoir which has unique differences from a homogeneous reservoir there are more variables causing uncertainty in reserve estimation which is fracture parameters.

The degree of uncertainty of reserve estimation variables, range of values they have and probability that they show a value in those ranges must be described in order to see the effects of uncertainty in calculations. Best estimates, by other means, the most probable and certain values can be used resulting to a deterministic calculation of reserves. But, considering that there are limited data in contrast to every possible data point throughout the field, there is always a level of uncertainty which can only be reduced by drilling a new well and collecting more and more data.

It would be meaningful if a whole picture of possible inputs and outcomes are described to see the range of reserves that can exist in the field. This can be performed by using concepts of statistics. The statistical tool, Monte Carlo simulation is relevant in evaluating oil in place calculations based on a statistical approach.

One of the main considerations in calculating the oil in place is that the variables must be independent. But actually petrophysical variables are not independent [12]. High porosity fraction will also be led to high permeability. It is important to

determine which factors cause variability or uncertainty in calculations. The dependence can be investigated by sensitivity analysis [13].

2.2 Review of Basic Concepts in Statistics

Statistics is the science of data. This involves collecting, classifying, summarizing, organizing, analyzing and interpreting data. The objects upon which the measurements or observations are made are called experimental units, and the properties being measured are called variables [14].

All data are either qualitative or quantitative in nature. Quantitative data are data that can be measured on a numerical scale. In general, qualitative data take values that are nonnumeric that can only be classified. The statistical tools which are used to analyze data depend on whether the data are quantitative or qualitative. Thus, it is important to be able to distinguish between the two types of data [14].

2.2.1 Population and Sample

In statistics, the data set that is the target of interest is called a population. Many populations are too large to measure (because of time and cost); others can not be measured because they are partly conceptual, such as the set of quality measurements. Thus, it is often required to select a subset of values from a population and to make inferences about the population based on information contained in a sample [14].

A sample is a subset of data selected from a population. Probability theory is used to infer the nature of a population from information contained in a sample. The sample data is observed and then the likelihood of observing these particular measurements is considered for populations possessing various characteristics. A random sample of N experimental units is one selected from the population in

such a way that every different sample of size N has an equal probability (chance) of selection [14].

2.2.2 Random Variable

The variable measured in generating a population, denoted by the symbol x, is called a random variable. Observing a single value of x is equivalent to selecting a single measurement from the population [14]. Random variables may be thought of as those variables whose values can not be predicted with certainty at the time of decision making. For each possible value of the random variable there is associated a likelihood, or probability of occurrence [7].

Random variables are sometimes called stochastic variables to denote the fact that the likelihoods of the values occurring are stochastic, or probabilistic in nature. If the value of a variable is known or can be predicted with certainty at the time of decision making, the variables are called deterministic variable [7].

In reserves estimation, examples of random variables can be given as the possible values of net pay thickness of wells, porosity, hydrocarbon saturation, etc. The numerical values of a random variable can be positive or negative. Each value (or range of values) will have a certain probability of occurrence. Different values of the random variable can have the same probability of occurrence. The adjective “random” is named from the “random sampling” process that is used in Monte Carlo simulation. The value of a variable can be realized anywhere within a range of possibilities [7].

2.2.3 Numerical Description of Data Sets

2.2.3.1 Measures of Central Tendency

Averages are used to represent a set of data. Several different types of averages can be calculated. These include: the arithmetic mean; the median; the mode; and the geometric mean. All of these averages tend to be centrally located within the data; hence they are referred to as measures of central tendency [15].

One of the most common measures of central tendency is the mean or arithmetic average, of a data set. It is calculated by the following equation:

$$\bar{x} = \sum x_i / n \qquad 2.1$$

where, x_i = i^{th} value of the data

n = number of data points in a sample pool

$\bar{x}$ = arithmetic mean

The mean of a population, or equivalently, the expected value of x (E(x)), is usually unknown in a practical situation and its value needs to be inferred based on the sample data. The mean of a population is denoted by μ [14].

Data can be classified in ranges and number of data in a class (range) gives its frequency in that class. By classifying data and defining the distribution of frequency throughout the whole data range is an explanatory way of describing the data. If the data are in a frequency distribution, an arithmetic mean can be calculated from the following:

$$\bar{x}' = \sum f_i x_i' / n \qquad 2.2$$

where, f_i = frequency of a class interval

x'_i = class mark (the midpoint of class) of the i^{th} class interval

When a group of data is arranged in order of magnitude, the median, or set of numbers, is found by taking the middle value (when there is an odd number of values) or the arithmetic mean of the two middle values (when there is an even number of values) [15].

A mode is the value which occurs with the greatest frequency. A distribution can have a single mode, several modes, or no modes. If all the class intervals of a distribution occur at the same frequency, then the distribution is said to have no modes [15].

2.2.3.2 Measures of Dispersion

It is frequently designed to determine how a group of data is dispersed or spread about its average. Measures of dispersion include: the range; the mean deviation; the standard deviation; and the variance. The range of a sample of n measurements is the difference between the largest and smallest measurements in a sample. The mean deviation (M.D) is sometimes called the average deviation and is given by the following [15]:

$$M.D. = \sum \left| x_i' - \bar{x} \right| / n \qquad 2.3$$

If the data exist as a frequency distribution, then the mean deviation is calculated by:

$$M.D. = \sum f_i \left| x_i' - \bar{x} \right| / n \qquad 2.4$$

The variance of a set of measurements is defined to be the average of the squares of the deviations of the measurements about their mean. Thus, the population variance would be the mean or expected value of $(x-\mu)^2$:

$$\text{Population variance} = E[(x-\mu)^2] = s^2 \qquad 2.5$$

where, E = expected value of population variance

x = value of a data in a population

μ = population mean

s^2 = population variance

The concept of a variance is important in theoretical statistics, but its square root, called a standard deviation, is the quantity most often used to describe data variation [1]. The standard deviation in a sample data set is found by:

$$s = \sqrt{\sum \left(x_i - \bar{x} \right)^2 / n} \qquad 2.6$$

where, s = standard deviation of a sample data set

x_i = i^{th} value of data in sample pool

$\bar{x}$ = mean of sample pool

n = number of data in sample pool

For data in the form of a frequency distribution the standard deviation is:

$$s = \sqrt{\sum f_i \left(x_i' - \bar{x} \right)^2 / n} \qquad 2.7$$

The abbreviation n is used in the denominator of Equations 2.5 and 2.6 when the entire population is being sampled, i.e. when n equals the total possible number of

data points. When only a subset of the population is being sampled, n should be replaced with n-1. However, when n gets larger than about 30, there is very little error introduced by using N [15]. Population's standard deviation is inferred by sample's standard deviation, and it is denoted by the symbol s.

2.2.4 Probability and Probability Distribution

The classical definition of probability involves a group or a set of equally likely outcomes. A graphical or mathematical representation of the range and likelihoods of possible values that a random variable can have is probability distribution. Probability distributions can be discrete or continuous, depending on the nature of the variable. The horizontal scale of a probability distribution is the measure of the variable, in whatever units or scale are appropriate. The height of a probability distribution above the horizontal axis (amplitude) is proportional to the probability of the values along the horizontal axis [7].

Figure 2.2 shows an example of a continuous probability distribution. More formally, this is called a probability density function (p.d.f.). It is continuous in the sense that any value of recoverable reserves within the range of x_{min} and x_{max} is possible. That is, there is a continuum of possible values of x between the minimum and maximum values. The curve, f(x), is a mathematical function such that when the area is determined under the distribution by integrating f(x) from x_{min} to x_{max} the resulting area will be 1.0, dimensionless [7].

The area under all probability density distributions is, by definition, one. Another characteristic of all probability distributions is that the probabilities are always positive (or zero), but never negative. This means the probability distribution curve, or function, never goes below the horizontal axis. By use of appropriate proportionality constants and/or some integration the vertical scale can be converted to a numerical scale that is proportional to the probability of occurrence of a value or range of values of the random variable. This leads us to the general

statement given earlier that the height of the curve above the x-axis is proportional to the probability of occurrence. Thus, in Figure 2.2 it is concluded that values of x towards the low end of the range and under the high points of the curve are the most probable values. As x gets larger the curve gets lower and lower which implies that the larger ranges of x become decreasingly less probable. The probability of occurrence of a value of x which is less than x_{min} or greater than x_{max} is zero [7].

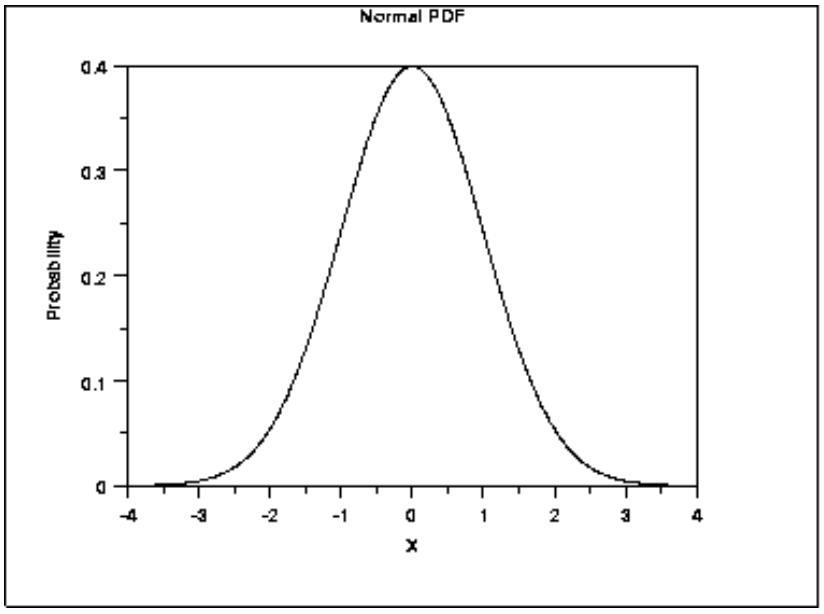

Figure 2.2 Normal probability density function

2.2.5 Frequency Distributions

It is often necessary to take large numbers of raw data and summarize them for further processing. For example, when a core is drilled from a well, porosity and permeability measurements are usually made from samples taken at one foot intervals throughout the core. The values of porosity and permeability are the raw data and as such are not very useful. When the raw data are summarized, they

begin to take on more meaning and utility. There are several ways of summarizing data like frequency distribution [15].

A useful graphical method for describing quantitative data is provided by a relative frequency distribution. This type of the graph shows the proportions of the total set of measurements that fall in various intervals on the scale of measurement. The area over a particular interval under a relative frequency distribution curve is proportional to the fraction of the total number of measurements that falls in that interval [14]. If a frequency distribution is constructed, operations such as reading area under the curve, etc. without taking the final step of mathematically converting to probability density functions can be performed [7].

Since the theoretical probability distribution for a population is usually unknown, sample from the population is obtained. The objective is to describe the sample and use this information to make inferences about the probability distribution of the population. Stem-and-leaf plots and histograms are two of the most popular graphical methods for describing samples (Figure 2.3). Both methods display the frequency (or relative frequency) of observations that fall into specified intervals (or classes) of the variable's values. For small data sets with measurements with only a few digits, stem-and-leaf plots can be constructed easily by hand. Histograms, on the other hand, are better suited to the description of larger data sets, and they permit greater flexibility in the choice of classes. Both however can be generated by using the computer. A histogram consists of a set of rectangles and is referred to as a bar graph [14,15].

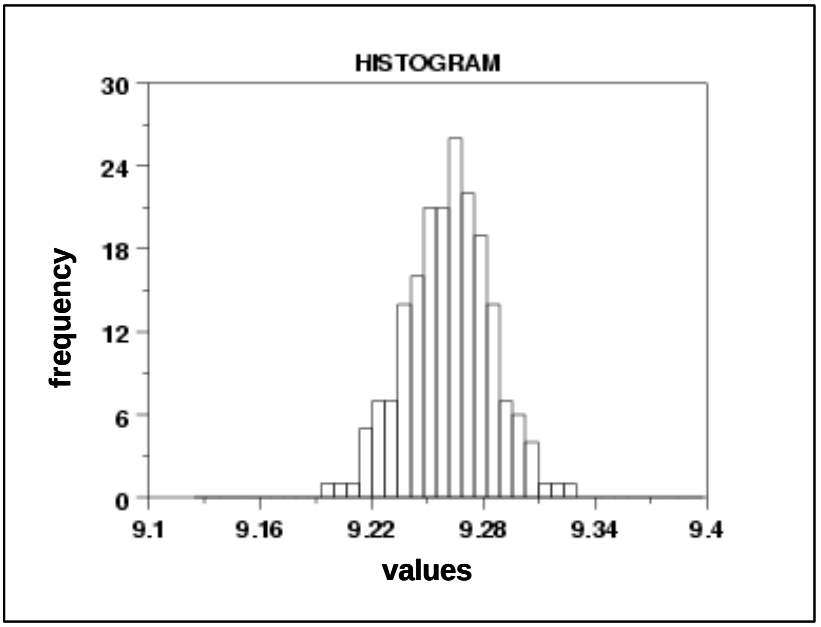

Figure 2.3 A histogram of a data set

2.2.6 Cumulative Frequency Distributions

A distribution is expressed in an equivalent graphical form called a cumulative distribution. A cumulative density distribution (Figure 2.4) is exactly equivalent-in information content-to a probability density function (i.e., probability distribution). A cumulative frequency distribution is equivalent to a frequency histogram [7]. Cumulative frequency distribution (sample) is the estimator of the cumulative density distribution (population).

There are two principal reasons for expressing distributions in their cumulative frequency form:

1. If there is a cumulative frequency distribution, any probabilities desired under the probability distribution without having to revert to integrating a probability density function can be read.

2. In Monte Carlo simulation, the cumulative form of the probability distribution is the basis for sampling possible values for random variables [7].

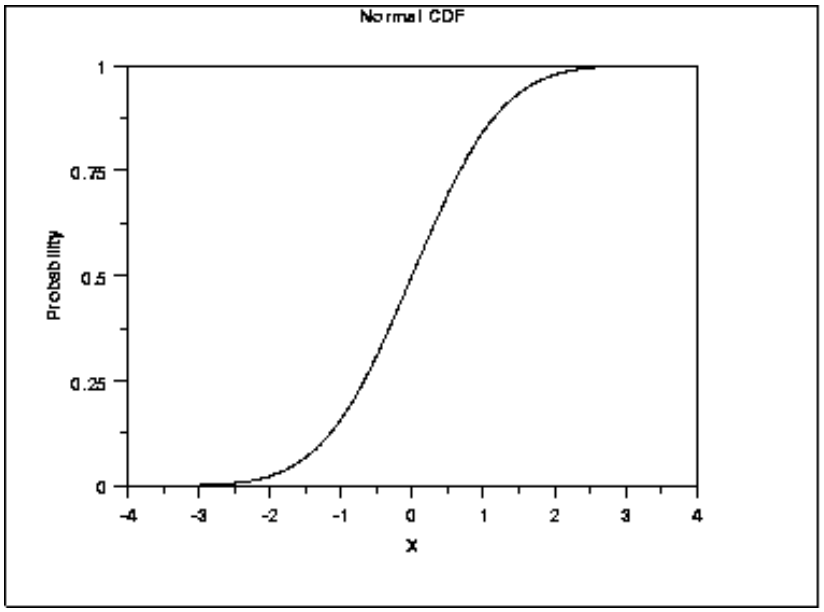

Figure 2.4 Normal cumulative density distribution

The method to convert a distribution to its equivalent cumulative form consists of moving from left end of the distribution to the right end and computing the total area less than or equal to various values of the random variable within the range. These cumulative areas (probabilities) are then plotted on a graph as functions of the values of the random variable corresponding to each cumulative area [7]. The same applies to cumulative probability distribution. For example, on cumulative distribution plot of a variable such as oil in place, most probable amount would be the smallest oil in place calculation. It can be said that there is 90 % or less then 90 % probability that the reserves are 30 MMstb or there is 50 % or less than 50 % probability that the reserves are 15 MMstb, which are denoted as P90 and P50 reserves.

2.2.7 Basic Probability Distribution Functions

The probability plot is a graphical technique for assessing whether or not a data set follows a given distribution. The data are plotted against a theoretical distribution in such a way that the points should form approximately a straight line. Departures from this straight line indicate departures from the specified distribution.

The correlation coefficient associated with the linear fit to the data in the probability plot is a measure of the goodness of the fit. Estimates of the location and scale parameters of the distribution are given by the intercept and slope. Probability plots can be generated for several competing distributions to see which provides the best fit, and the probability plot generating the highest correlation coefficient is the best choice since it generates the straightest probability plot.

For distributions with shape parameters (not counting location and scale parameters), the shape parameters must be known in order to generate the probability plot. For distributions with a single shape parameter, the probability plot correlation coefficient (PPCC) plot provides an excellent method for estimating the shape parameter.

2.2.7.1 Location, Scale and Shape Parameters

A probability distribution is characterized by location and scale parameters. Location and scale parameters are typically used in modeling applications [16].

For example, Figure 2.2 shows a probability density function for the standard normal distribution, which has the location parameter equal to zero and scale parameter equal to one.

The effect of the location parameter is to translate the graph, relative to the standard normal distribution, 10 units to the right on the horizontal axis. A

location parameter of -10 would have shifted the graph 10 units to the left on the horizontal axis.

The effect of a scale parameter greater than one is to stretch the pdf. The greater the magnitude, the greater the stretching. The effect of a scale parameter less than one is to compress the pdf. The compressing approaches a spike as the scale parameter goes to zero. A scale parameter of 1 leaves the pdf unchanged (if the scale parameter is 1 to begin with) and non-positive scale parameters are not allowed.

The standard form of any distribution is the form that has location parameter zero and scale parameter one. For the normal distribution, the location and scale parameters correspond to the mean and standard deviation, respectively. However, this is not necessarily true for other distributions.

Many probability distributions are not a single distribution, but are in fact a family of distributions. This is due to the distribution having one or more shape parameters.

Shape parameters allow a distribution to take on a variety of shapes, depending on the value of the shape parameter. These distributions are particularly useful in modeling applications since they are flexible enough to model a variety of data sets.

Kurtosis is based on the size of a distribution's tails. The following formula can be used to calculate kurtosis [17]:

$$kurtosis = \frac{\sum (x-m)^4}{n * s^4} - 3 \qquad 2.8$$

2.2.7.2 Normal Distribution

The general formula for the probability density function of the normal distribution is [16]:

$$f(x) = \frac{e^{-(x-m)^2/(2s^2)}}{s\sqrt{2p}} \qquad 2.8$$

where, μ = location parameter

s = scale parameter

The formula for the cumulative distribution function of the normal distribution is:

$$F(x) = \Phi\left(\frac{x - mean}{s}\right) \qquad 2.9$$

where, ? = error function

Mean :	The location parameter μ.
Median :	The location parameter μ.
Mode :	The location parameter μ.
Range :	Infinity in both directions.
Standard Deviation :	The scale parameter s.
Coefficient of Variation :	s / μ
Skewness :	0

Kurtosis : 3

Probability density function and cumulative density function plots of normal distribution are given in Figures 2.2 and 2.4.

2.2.7.3 Uniform Distribution

The general formula for the probability density function of the uniform distribution is [16]:

$$f(x) = \frac{1}{B-A} \quad \text{for A = x = B} \qquad 2.10$$

where, A = location parameter

B-A = scale parameter

The formula for the cumulative distribution function of the uniform distribution is:

$$F(x) = x \quad \text{for } 0 = x = 1 \qquad 2.11$$

Mean : $(A + B)/2$ 2.12

Median : $(A + B)/2$ 2.13

Range : $B - A$ 2.14

Standard Deviation : $\sqrt{\frac{(B-A)^2}{12}}$ 2.15

Coefficient of Variation : $\frac{(B-A)}{\sqrt{3}(B+A)}$ 2.16

Skewness : 0

Kurtosis : 9/5

Probability density function and cumulative density function plots of uniform distribution are given in Figures 2.5 and 2.6.

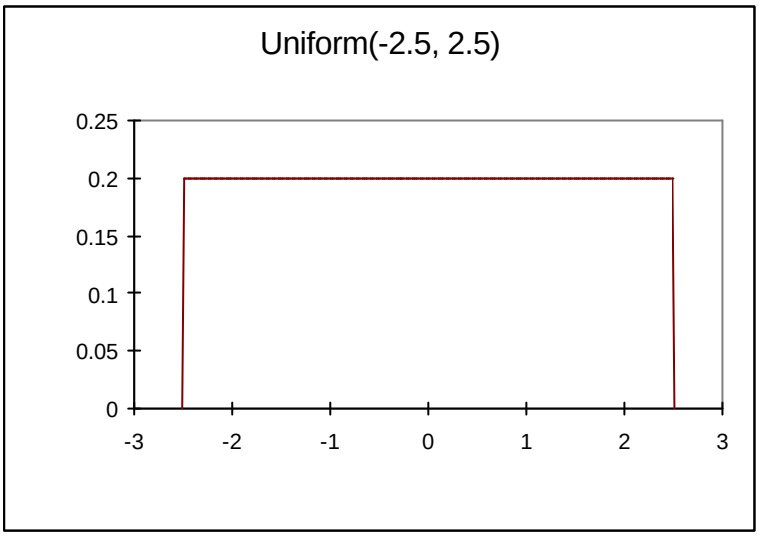

Figure 2.5 Probability density function of uniform distribution

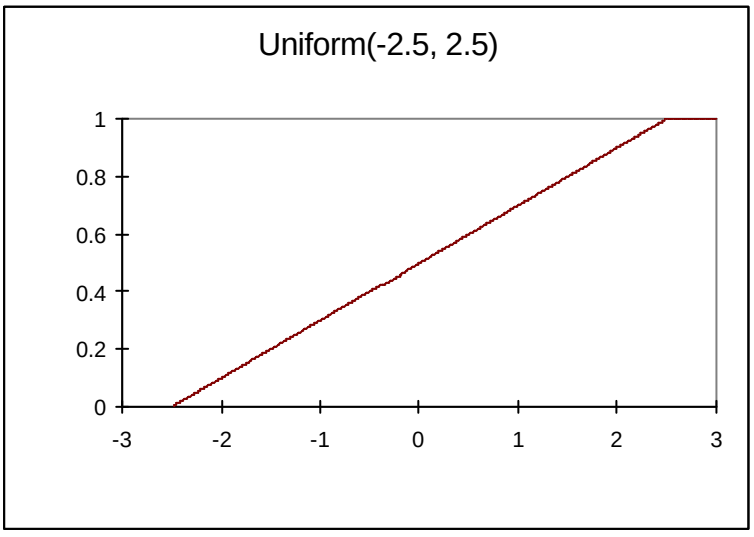

Figure 2.6 Cumulative distribution function of uniform distribution

2.2.7.4 Triangular Distribution

The Triangular Distribution is typically used as a subjective descryption of a population for which there is only limited sample data. It is based on knowledge of the minimum and maximum and an inspired guess as to what the modal value might be. Despite being a simplistic description of a population, it is a very useful distribution for modeling processes where the relationship between variables is known, but data is scarce (possibly because of the high cost of collection) [17].

The general formula for the probability density function of the triangular distribution is [61]:

$$f(x) = \frac{2}{(\max) - (\min)} \qquad \text{for x = mode} \qquad 2.17$$

$$f(x) = \frac{2(x - \min)}{(\max - \min)(\mathrm{mod} - \min)} \qquad \text{for x < mode} \qquad 2.18$$

$$f(x) = \frac{2(\max - x)}{(\max - \min)(\max - \mathrm{mod})} \qquad \text{for x > mode} \qquad 2.19$$

where, min = minimum value

mode = modal value

max = maximum value

The formula for the cumulative distribution function of the triangular distribution is:

$$F(x) = \frac{(\mathrm{mod} - \min)}{(\max - \min)} \qquad \text{for x = mode} \qquad 2.20$$

$$F(x) = \frac{(x - \min)^2}{(\mathrm{mod} - \min)(\max - \min)} \quad \text{for x < mode} \qquad 2.21$$

$$F(x) = 1 - \frac{(\max - x)^2}{(\max - \mathrm{mod})(\max - \min)} \quad \text{for x > mode} \qquad 2.22$$

$$\text{Mean} = \frac{(\min + \mathrm{mod} + \max)}{3} \qquad 2.23$$

$$\text{Variance} = \frac{\min^2 + \mathrm{mod}^2 + \max^2 - \min * \mathrm{mod} - \min * \max - \mathrm{mod} * \max}{18} \qquad 2.24$$

Kurtosis = 2.4

Probability density function and cumulative density function plots of triangular distribution are given in Figures 2.7 and 2.8.

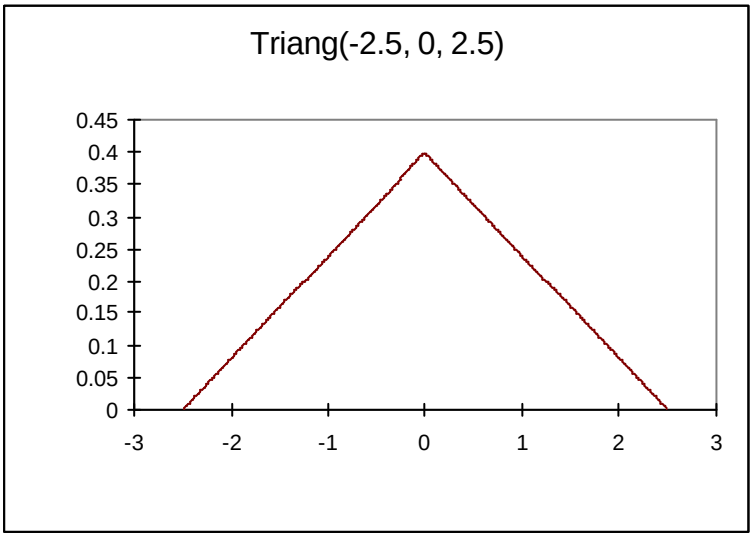

Figure 2.7 Probability density function of triangular distribution

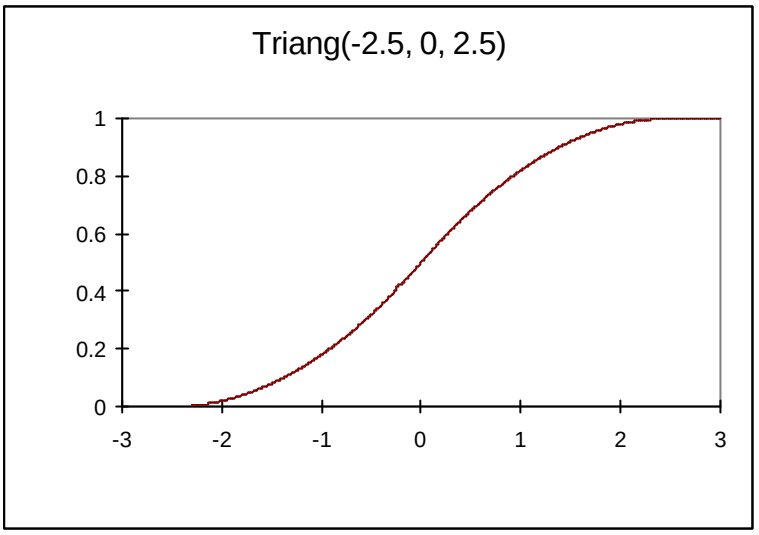

Figure 2.8 Cumulative distribution function of triangular distribution

2.2.7.5 Lognormal Distribution

A variable X is lognormally distributed if Y = LN(X) is normally distributed with "LN" denoting the natural logarithm. The general formula for the probability density function of the lognormal distribution is [16]:

$$f(x) = \frac{e^{-((\ln((x-q)/m))^2/(2s^2))}}{(x-q)s\sqrt{2p}} \qquad \text{for x = ? ; μ, s > 0} \qquad 2.25$$

where, ? = location parameter

s = scale parameter

μ = shape parameter

The case where ? = 0 and μ = 1 is called the standard lognormal distribution. The case where ? equals zero is called the two-parameter lognormal distribution. The formula for the cumulative distribution function of the lognormal distribution is:

$$F(x) = \Phi\left(\frac{\ln(x)}{s}\right) \qquad \text{for x = 0, s > 0} \qquad 2.26$$

where, ? = error function

The formulas below are with the location parameter equal to zero and the scale parameter equal to one.

Mean	= $e^{0.5s}$	2.27
Median	= Scale parameter μ (= 1 if scale parameter not specified).	
Mode	= $\frac{1}{e^{s^2}}$	2.28
Range	= Zero to positive infinity	
Standard Deviation	= $\sqrt{e^{s^2}(e^{s^2}-1)}$	2.29
Skewness	= $\left(e^{s^2}+2\right)\sqrt{e^{s^2}-1}$	2.30
Kurtosis	= $\left(e^{s^2}\right)^4+2\left(e^{s^2}\right)^3+3\left(e^{s^2}\right)^2-3$	2.31
Coefficient of Variation	= $\sqrt{e^{s^2}-1}$	2.32

Probability density function and cumulative density function plots of triangular distribution are given in Figures 2.9 and 2.10.

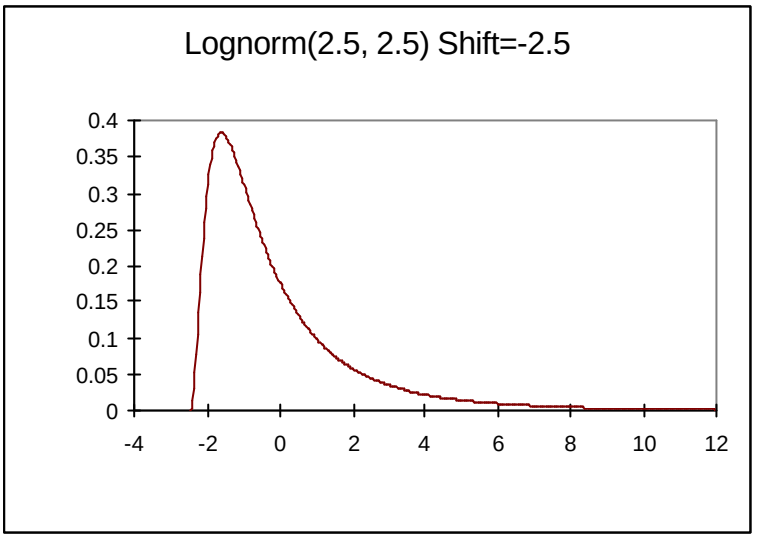

Figure 2.9 Probability density function of lognormal distribution

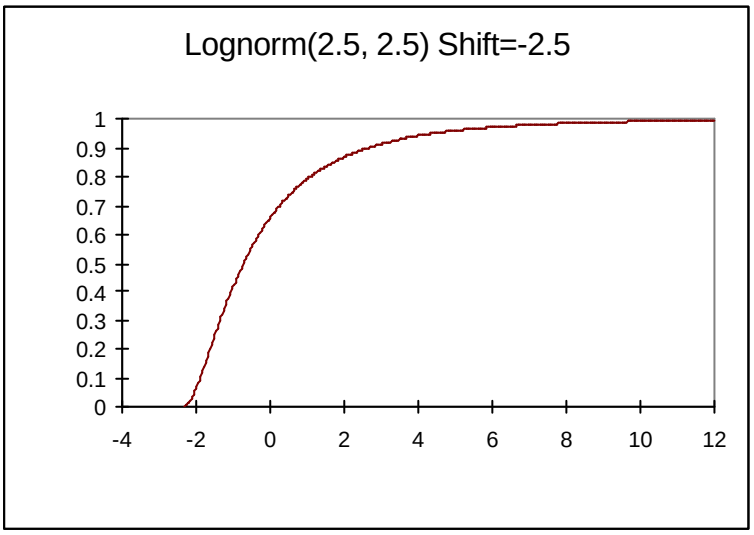

Figure 2.10 Cumulative distribution function of lognormal distribution

2.2.8 Correlation Coefficient

The *Pearson Product-Moment Correlation Coefficient* (r), or correlation coefficient for short is a measure of the degree of linear relationship between two variables. In correlation the emphasis is on the degree to which a linear model may describe the relationship between two variables [15].

The computation of the correlation coefficient is most easily accomplished with the aid of a statistical calculator. The correlation coefficient may take on any value between plus and minus one.

$$-1.00 = r = +1.00 \qquad 2.33$$

The sign of the correlation coefficient (+ , -) defines the direction of the relationship, either positive or negative. A positive correlation œefficient means that as the value of one variable increases, the value of the other variable increases; as one decreases the other decreases. A negative correlation coefficient indicates that as one variable increases, the other decreases, and vice-versa.

Taking the absolute value of the correlation coefficient measures the strength of the relationship. A correlation coefficient of r = 0.50 indicates a stronger degree of linear relationship than one of r = 0.40. Likewise a correlation coefficient of r = -0.50 shows a greater degree of relationship than one of r = 0.40. Thus a correlation coefficient of zero (r = 0.0) indicates the absence of a linear relationship and correlation coefficients of r = +1.0 and r = -1.0 indicate a perfect linear relationship.

2.3 Uncertainty Assessment by Monte Carlo Simulation

The most common mathematical basis for the statistical calculation of reserves is the Monte Carlo method. Monte Carlo simulation method used in oil and gas exploration and exploitation investments appeared in petroleum literature in the beginning of 1976 [18]. Monte Carlo simulation takes on special importance in

the field of reserve estimation, which introduces significant and vital area of interest to any reservoir engineer. Monte Carlo simulation allows each variable to vary between some minimum and maximum value according to some prescribed distribution, and then solves the problem for a large set of these input variables. The results of Monte Carlo simulation are then presented in graphical form as a probability distribution for the dependent variable. This probability is then interpreted by using statistical methods to determine the likelihood of a particular solution occurring or not occurring [13].

In many engineering problems there may be a multitude of input parameters that are not known very accurately and thus have uncertain values. Uncertainty in a variable can occur for a number of reasons. For example, the method of measuring a parameter may have to be predicted into the future, or there may be a limited amount of data for a certain parameter. In any case, the best that can be done for a variable with an uncertain value is to choose a reasonable range over that range.

The choice of the particular distribution for a certain variable should be guided by the engineer's knowledge of that variable. Within the Monte Carlo simulation method, the selection of a value for an independent variable is accomplished by using the fact that the integral of the probability distribution will lie between 0 and 1 and will be monotonic in behavior. Thus the selection of a random number between 0 and 1 will yield a distinct random value for the variable between the selected minimum and maximum [15].

Once the independent variables have been determined then the dependent variable, i.e. an evaluation criteria that has been chosen, can be calculated. The process is then repeated a large number of times. The values of the dependent variable are then grouped in class intervals and relative and cumulative probability plots are constructed [15].

The following sequences of steps summarize Monte Carlo simulation method:

i. Establish distributions for each parameter or independent variable.

ii. Set up equations which will allow the calculation of the independent variables. This is done by determining expressions for the integrals of probability distributions. It should be recognized that the integral of a probability distribution is the cumulative frequency of the distribution.

iii. Generate a random number for each independent variable. A different random number must be determined for each independent variable.

iv. Use the random numbers to calculate values for the independent variables.

v. Calculate dependent variable and store the result in a class interval.

vi. Return to step 3 and repeat 3 through 5 a large number of times.

vii. Construct relative and cumulative frequency diagrams.

A common criticism of the method is that it is not exactly repeatable; however, it is simply a matter of running enough passes to ensure an acceptable level of repeatability. The key advantages of the method over other statistical approaches are:

i. no constraints on input and output distributions; and,
ii. Can accommodate dependencies [3].

2.4 Reserve Estimation in a Fractured Reservoir

Reserve estimates in naturally fractured reservoirs present a unique challenge to the reservoir engineer. Reservoir storage capacities and thus reserves in a

fractured reservoir come from two major sources: fracture capacity and matrix capacity. Most fractured reservoirs consist of a combination of these two capacities [19].

The principal methods of reserves determination; i.e. analogy, volumetric method and performance analysis apply to dual porosity reservoirs as well as to single porosity systems. Each of these methods is applicable based upon the information available to the reserves estimator at the time the estimate is made. All reserve estimates contain some degree of uncertainty. Reserve estimates may be modified from time to time as the amount of reliable geologic and engineering data increases and interpretation of these data changes [19].

Fractures can be an important feature of hydrocarbon reservoirs where their presence (either naturally occurring or induced) increase the productive capacity. Many low matrix permeability reservoirs would not be commercially attractive without a natural or induced fracture system. While there is no question at to the importance of fractures with respect to formation permeability there is the matter of contribution that fractures make to the reservoir storage capacity or more specifically the porosity. The assignments of porosity in a dual porosity system (e.g., matrix and fractures) may be critical in estimating the in place reserves and ultimate production of hydrocarbons. In general, there appears to be a general tendency to assign too much porosity to the fracture system often resulting in grossly optimistic production and economic predictions [20].

2.4.1 Fracture Porosity and Permeability

Fractured reservoir rocks are made up of two porosity systems; one intergranular formed by void spaces between the grains of the rock and a second formed by void spaces of fractures and vugs. The first type is called primary porosity and is typical of sandstone and limestone. The second type is called secondary porosity

or, when referring to only vugs or fractures, vugular porosity/fracture porosity. Matrix and fracture capacities comparison is given in Figure 2.11.

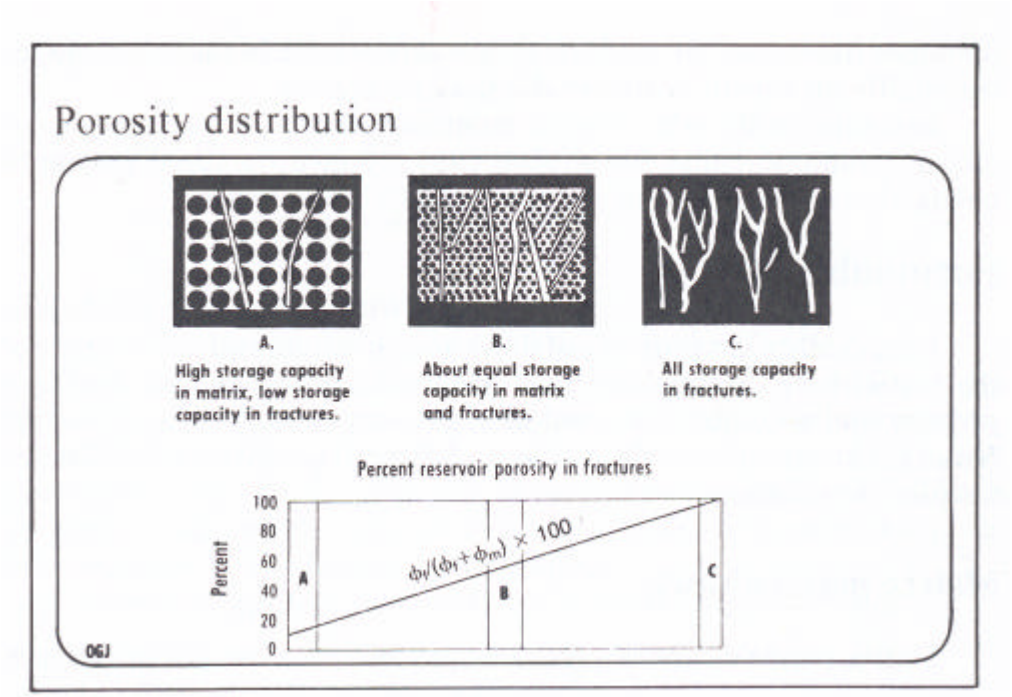

Figure 2.11 Schematic sketches showing porosity distribution in fractured reservoir rocks [21].

Fracture porosity is a function of size of the matrix blocks between the fractures (related to fracture density) and fracture width. Fracture width (opening) is the distance between the fracture walls. The width of the fracture opening may depend (in reservoir conditions) on depth, pore pressure and rock type. The fracture width varies between 10 – 200 microns, but statistics have shown that the most frequent range is between 10 – 40 microns (Figure 2.12). Permeability of a fracture is also associated with fracture width. Fracture permeability is dependent on the conductivity measured during the flow of fluid through a single fracture or through a fracture network, independent of the surrounding rock (matrix). So fracture permeability can be expressed in terms of fracture porosity and width [20, 21].

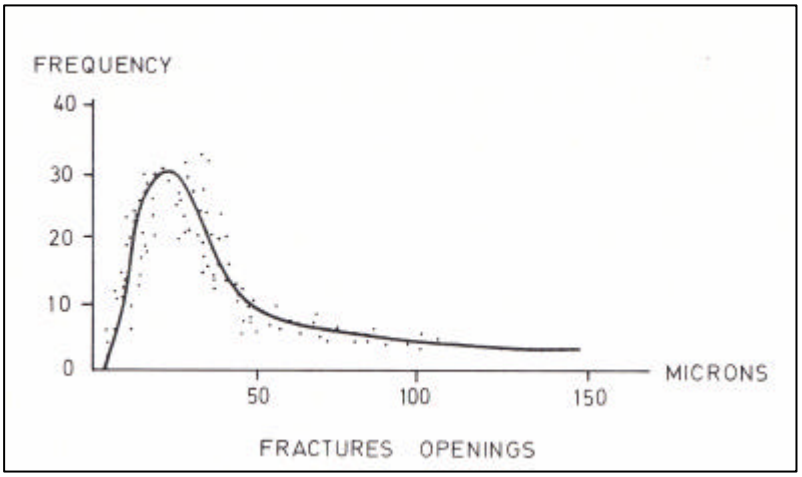

Figure 2.12 Statistical frequency curve of fracture opening width [21].

Fracture density expresses the degree of rock fracturing through various relative ratios. If the ratio refers to the bulk volume, the fracture density is called volumetric fracture density. If the ratio refers to the area or to a length the fracture density is called areal or linear fracture density. In literature fracture density vs. lithology is recorded as listed below [21]:

Table 2.1 Fracture density vs. lithology [21]

Rock lithology	Fracture density, 1/m
Medium-grained sandstone	9.0
Fine-grained sandstone	50.0
Glauconitic sandstone	19.5
Calcareous sandstone	9.5
Flaggy bedded limestone	30.0
Algal limestone	33.0
Massive limestone	12.3
Medium-grained limestone	12.0
Fine-grained limestone	27.0
Thick-bedded limestone	24.0

Table 2.1 Fracture density vs. lithology (continued)

Rock lithology	Fracture density, 1/m
Argillaceous limestone	60.0
Argillite	56.0
Volcanic rock	48.0
Thin-bedded marl	20.0
Massive porphyrite	36.4
Conglomerate	44.0

The complex matrix-fracture structure could be reduced to matrix blocks of simple geometry (parallelepipeds, cubes spheres, etc.) separated by uniform spaced intervals which represent fracture voids. Various block geometries and the direction of fluid flow in the system are shown on Figure 2.13. The size and shape of the blocks depend on fracture density and type of fracture [21].

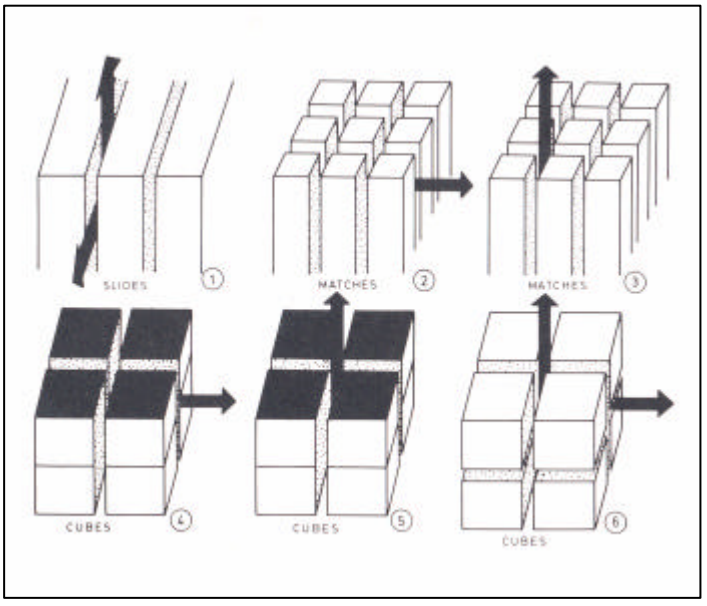

Figure 2.13 Simplified geometric matrix blocks [38].

For the models in Figure 2.13, the basic parameters, fracture porosity $Ø_f$, and fracture density $A_{fD,}$ are presented in Table 2.2. Permeability K_f is expressed as a function of porosity block dimension *a*, or fracture opening *b* through dimensional and dimensionless equations [21].

In the case of Model-5 of Figure 2.13 and Table 2.2 (rotated so that flow is horizontal):

- Areal fracture density

$$A_{fD} = (n*l) / \text{surface} = 2a / a^2 = 2 / a \qquad 2.38$$

where, n = number of blocks parallel to the fracture
a = block dimension, cm
l = length, cm

- Linear fracture density 2.39

$$L_{fD} = n / l = 2 / a$$

- Volumetric fracture density

$$V_{fD} = 6a^2 / a^3 \qquad 2.40$$

- Fracture porosity

$$Ø_f = 2b / a \qquad 2.41$$

where, b = fracture opening, cm

Table 2.2 Parameters of simplified matrix models [21]

MODEL		DIMENSIONLESS EQUATIONS				DIMENSIONAL EQUATIONS			
Nº	TYPE	A_{fD}	ϕ_f	$k_f(\phi_f,a)$	$k_f(\phi_f,b)$	A_{fD} cm^{-1}	ϕ_f %	$k_f(\phi_f,a)$ darcy	$k_f(\phi_f,b)$ darcy
1	SLIDES	$\frac{1}{a}$	$\frac{b}{a}$	$\frac{1}{12}a^2\phi_f^3$	$\frac{1}{12}b^2\phi_f$	$\frac{1}{a}$	$\frac{1}{100}\frac{b}{a}$	$8{,}33\,a^2\phi_f^3$	$8{,}33\times10^{-4}b^2\phi_f$
2	MATCHES	$\frac{1}{a}$	$\frac{2b}{a}$	$\frac{1}{96}a^2\phi_f^3$	$\frac{1}{24}b^2\phi_f$	$\frac{1}{a}$	$\frac{1}{100}\frac{2b}{a}$	$1{,}04\,a^2\phi_f^3$	$4{,}16\times10^{-4}b^2\phi_f$
3	MATCHES	$\frac{2}{a}$	$\frac{2b}{a}$	$\frac{1}{48}a^2\phi_f^3$	$\frac{1}{12}b^2\phi_f$	$\frac{2}{a}$	$\frac{1}{100}\frac{2b}{a}$	$2{,}08\,a^2\phi_f^3$	$8{,}33\times10^{-4}b^2\phi_f$
4	CUBES	$\frac{1}{a}$	$\frac{2b}{a}$	$\frac{1}{96}a^2\phi_f^3$	$\frac{1}{12}b^2\phi_f$	$\frac{1}{a}$	$\frac{1}{100}\frac{2b}{a}$	$1{,}04\,a^2\phi_f^3$	$4{,}16\times10^{-4}b^2\phi_f$
5	CUBES	$\frac{2}{a}$	$\frac{2b}{a}$	$\frac{1}{48}a^2\phi_f^3$	$\frac{1}{12}b^2\phi_f$	$\frac{2}{a}$	$\frac{1}{100}\frac{2b}{a}$	$2{,}08\,a^2\phi_f^3$	$8{,}33\times10^{-4}b^2\phi_f$
6	CUBES	$\frac{2}{a}$	$\frac{3b}{a}$	$\frac{1}{162}a^2\phi_f^3$	$\frac{1}{18}b^2\phi_f$	$\frac{2}{a}$	$\frac{1}{100}\frac{3b}{a}$	$0{,}62\,a^2\phi_f^3$	$5{,}55\times10^{-4}b^2\phi_f$

UNITS: K (Darcy), a (cm), b (microns); ϕ_f (percent units)

- Fracture permeability

$$K_f = Ø_f * b^2 / 12 = Ø_f * (Ø_f\, a/2)^2 / 12 = (1 / 48)* a^2 * Ø_f^3 \qquad 2.42$$

- Fracture porosity and permeability in a single fracture system

$$Ø_f = (12 / b^2) * K_f \qquad 2.43$$

- Fracture porosity and permeability in a multi-fracture system

$$Ø_f = (12 * K_f * A_{fD}^2)^{1/3} \qquad 2.44$$

2.4.2 Matrix and Fracture Porosity in a Reservoir

In a fractured reservoir the total porosity ($Ø_t$) is the result of the simple addition of the primary and secondary porosities,

$$Ø_t = Ø_1 + Ø_2 \qquad 2.45$$

This total porosity is equivalent to the static definition of rock storage or total void space. The two porosities are expressed by the conventional definitions,

$Ø_1$ = matrix void volume / total bulk volume 2.46

$Ø_2$ = fracture void volume / total bulk volume 2.47

and are relative to the total bulk volume (matrix + fractures).

In the correlation of the matrix porosity ($Ø_m$) and the fracture porosity ($Ø_f$), the fact that the matrix porosity refers only to the matrix bulk may be taken into consideration,

$Ø_m$ = volume voids of the matrix / matrix bulk volume 2.48

while the fracture porosity,

$$Ø_2 \tilde{} Ø_f \qquad 2.49$$

In this case the primary porosity, as a function of matrix porosity, is expressed by,

$$Ø_1 = (1- Ø_2)* Ø_m \qquad 2.50$$

The most important fracture subdivision related to fracture porosity concerns two categories: macrofractures and microfractures. Macrofractures are extended

fractures with wide openings which develop through various layers; while microfractures (or fissures) are fractures with narrow openings and limited extent, often limited to a single layer. Depending on the type of rock and state of stress, either the macrofractures or the microfractures will be more predominant. The most probable secondary porosity ranges are [21]:

a. Macrofracture network where $Ø_f$ = 0.01 – 0.5 %
b. Isolated fissures where $Ø_f$ = 0.001 – 0.01 %
c. Fissure network where $Ø_f$ = 0.01 – 2 %
d. Vugs (in karstic rocks) where $Ø_f$ = 0.1 – 3 %

The maximum secondary porosity based on the magnitude of total porosity is also given by various empirical correlations from which the following can be inferred [21]:

$$Ø_{fmax} < 0.1\ Ø_t \text{ when } Ø_t < 10\ \% \qquad 2.51$$

$$Ø_{fmax} < 0.04\ Ø_t \text{ when } Ø_t > 10\ \% \qquad 2.52$$

2.4.3 Estimation of Fracture Properties

Fractured reservoirs can be regarded as dual porosity media where on a small scale reservoir volume is provided by matrix and vug porosity (primary) in combination with porosity provided by the microfracture network (secondary), whereas, on a larger scale, fluid flow pathways and a component of secondary porosity are provided by an interconnected network of subseismic and seismic faults [22].

Typical fractured reservoirs are composed of brittle rock with low intergranular porosity. They are characterized by high permeabilities and low bulk porosities. The occurrence and extent of fractures in typical reservoir rock is controlled by such factors as initial shear strength, internal friction, rock ductility, effective

confining stress, temperature, depth of burial, rock type, bed thickness and adjacency to other beds. Fracture patterns are likewise controlled by many variables [19, 22].

Fracture porosity is generally overestimated particularly in dual porosity systems [20]. Fractures have such a dramatic impact on reservoir performance that their hydrocarbon storage capacities tend to be inflated. Many reservoirs that produce at high initial rates decline drastically after a short period of time. This occurs because the producible oil has been stored in the fracture system. Consequently, it is important to estimate oil in place reasonably within the fracture system. If the permeability of the matrix is very low, then the oil bleed of from the matrix into the fractures will be very slow and the oil originally within the fractures will be produced in a reasonably span of time [24].

Porosities can be subdivided into four groups; intergranular, dissolution, microporosity and fractures [25]. In literature it is stated that fracture porosity is rarely greater than one percent of the bulk volume [20,24]. Factors that are generating fracture porosity are fracture density and fracture width.

There are direct and indirect sources of information for evaluation and description of a fractured reservoir. Direct sources of information are:

a. Core analysis

In order to obtain the fracture parameters by core analysis techniques the first and most important factor is to have a whole core to work on but there are several technical shortcomings in taking a whole core from a fractured interval. In laboratory the total pore volume is measured by injecting water into the core.

Fracture width can be analyzed in laboratory on cores but this can result in misleading from several standpoints. Fractures may be observed and reported but

commentary may be missing as to whether the fractures are open or closed. Fractures that are open in cores may be closed in situ from mineralization or by tar or kerogen materials. Overburden pressures must be taken into account since the width of a fracture at reservoir conditions will be a function of the net confining pressure, i.e., "the effective compressive stresses are the difference between the total compressive stresses and the pore pressures" [20, 26]

b. Oriented Cores

Oriented cores provide a direct measurement of fracture orientation by placing the fractured core in the laboratory at its reservoir positions.

c. Drill Cuttings

Drill cuttings can be used to measure small fractures only if the cuttings are not broken along fractures. It is nearly impossible to analyze the fracture parameters by cuttings since they may not show any fracture indication even if the rock is fractured. A carefully designed analysis can only measure the microfractures existing in the cuttings and it is not possible to generate data about wider fractures which have a more important value on basis of oil in place (storage) evaluation of the efficient fracture system of reservoir.

d. Downhole Cameras

This technique simply composes of submersing a camera into the wellbore to detect fractures but it has many technical constrains such as temperature, pressure etc.

Indirect sources of information for evaluating naturally fractured reservoirs include the drilling history, log analysis, well testing, and production history [24]. These information techniques are explained below :

a. Drilling History

Mud losses during the drilling operation and drilling speed can supply information about existence of fractures.

b. Log Analysis

While conventional logs can be used for quantitative analysis of fractures there are specific logs designed for detecting fracture parameters. Among the conventional logs the most common ones to indicate the fracture existence are sonic and density-neutron logs which are interpreted parallel to observe fractures.

Sonic log is used to determine porosity and lithology. The velocity of sound or traveltime along well walls is measured by propagating an acoustic pulse from a transmitter toward one or more receivers. In density logging, gamma rays that had been send to the borehole and returned are counted. If there are high amount of rays returned it is said that they had not loose their energy because of high pore space. Neutron log counts the hydrogen atoms in the formation which means that there is a pore space in the formation whether filled with hydrocarbon or water. This log is also affected by hydrogen atoms in the rock. Generally density and neutron logs are overlaid to estimate the lithology and average effective porosity [27].

When a secondary porosity exists, i.e. of the vuggy type or when there are large fractures, in addition to the porosity of the rock matrix, the sonic porosity that is read, $Ø_S$, is lower than the density-neutron porosity, $Ø_{ND}$. Indeed, the sonic log does not see the vuggy porosity because acoustic energy is mainly channeled through solid porous rock. Therefore, a secondary porosity index (SPI) can be defined as:

$$SPI = Ø_{ND} - Ø_S \qquad 2.53$$

In the case of fractures, the secondary porosity index is usually small because the fractures represent only a small portion of the total volume of the rock in sedimentary formations [28].

The most effective log technique in identifying fractures is Fullbore Formation Microimager (FMI) log. Interpretation of this log gives a photographic view of the wellbore. FMI log is simply an electrical image log working by measuring the resistivity of the wellbore via four pads having electrots on them. Measured resistivity values are shown on a log plot by black and white or colored print. Colors show the change in resistivity where dark colors are indicating more conductive (less porous) parts (Figure 2.14).

FMI logs give the opportunity to interpret tectonic, sedimentary and diagenetic processes. Among them, tectonic processes include structural inclinations, fractures, faults and bends. If the fractures are open, they are filled with conductive mud thus, they can be recognized on the log plot as dark colored, linear, vertical or sloping, non-smooth features that are observed on a large range. Since they are not smooth because of the pad readings, a sinusoidal curve is drawn on them and by this way orientation, inclination, density and width of the fractures can be interpreted [27]. Figure 2.14 shows an FMI log plot on which fracture curves are drawn by red sinusoidal lines. Nearly vertical and large fractures are not natural but induced by drilling.

Interpretation of FMI logs provides information like fracture width and their density and direction in a formation. As discussed in Section 2.3.2 these values are giving the fracture porosity and permeability.

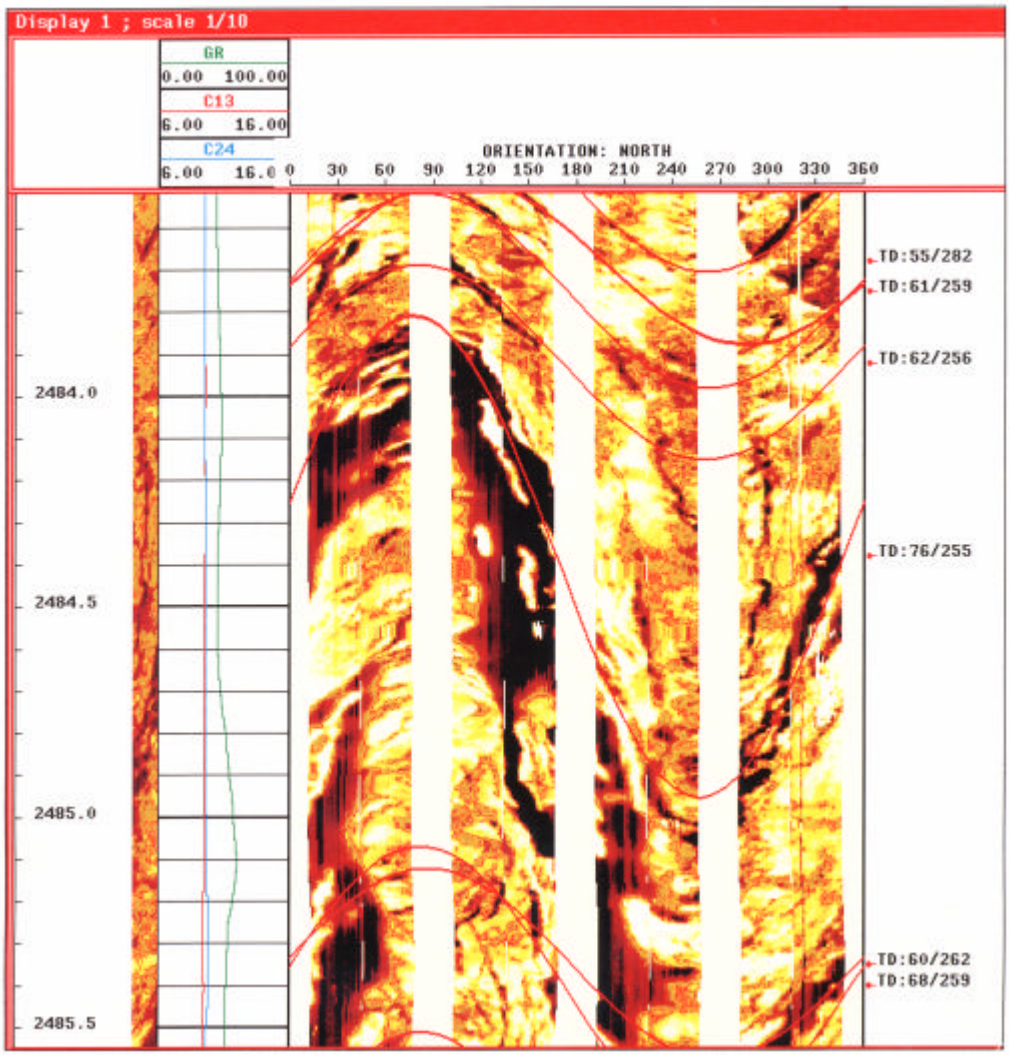

Figure 2.14 FMI interpretation plot, W-10

c. Production History

Production history of a field can give a qualitative information about the presence of fractures as obtaining a high production amount in contrast to low matrix porosity and permeability.

Without defining the fracture properties oil in place and productivity studies will have important problems since the production behavior changes severely by the

effect of fractures. Understanding the fluctuations on the trend of oil and water production in a bottom or edge water drive reservoir under given matrix porosity and permeability values is a key to evaluate the affect of fracture system and its storage capacity.

2.4.4 Volumetric Method in Fractured Reservoirs

Volumetric reserve estimates for naturally fractured reservoirs may be prepared much the same as for predominately matrix (single) porosity systems with a few exceptions. First the reserve estimator must determine if the reservoir has a single or dual porosity system. For a dual porosity system the reserve estimator must determine the reservoir volume for fractures and the matrix blocks of the reservoir. Next, the volumetric parameters of water saturation and formation volume factor are applied separately to the fracture and matrix portions of the reservoir to arrive at original hydrocarbons in place [19].

In fractured reservoirs the parameters for effective area, effective thickness, effective porosity and effective water saturation are substantially different for the fracture component. Reservoir height, area, and shape are strongly determined by fracture orientation and interconnection. In many cases the areal extent of the matrix component is dependant upon the interconnectedness of the fractures that intersect the matrix and ultimately connect to the remainder of the reservoir. Values for porosity and water saturation may also vary widely between the fracture and matrix components. Fractured reservoirs are complex systems that require special attention in preparing reserve estimates using the volumetric method [19].

In reserve estimation, fractured reservoir limits, both vertically and horizontally must be considered. In some cases vertical reservoir boundaries may extend into adjacent beds that serve as source rock fort the reservoir. Fracture trends may extend great distances from producing wells. In some instances wells on trend

have exhibited interference over several kilometers. In general, drainage areas for wells in fractured reservoirs are larger than for wells in single porosity reservoirs due to fracture permeability. Also, drainage areas in horizontal wells tend to be larger than for vertical wells in the same reservoir because of increased reservoir contact [19].

After all these factors are considered an initial volumetric estimate of reserves can be prepared. Separate estimates for fracture reserves and matrix reserves may be prepared and consolidated [19].

CHAPTER 3

RESERVOIR PROPERTIES AND GEOLOGY OF FIELD-A

Reserve estimation always includes some degree of uncertainty which is at its highest level at the beginning of the field history when only a discovery well is present. Uncertainty on field properties reduces during the development history of the field and the highest confidence in defining the properties is reached nearly at the end of the field production as each drilled well provides more information. But whether during the development or at the end of development there may always be some uncertain parameters that needs more complicated evaluation since they have heterogeneity. Naturally fractured reservoirs are the ones that have high heterogeneity because of their dual system. The field that is chosen as the basis of this study, which is named in this text as Field-A is a naturally fractured reservoir having such difficulties in evaluation.

Field-A is a highly fractured and structurally complex carbonate field with a strong aquifer providing bottom and edge water drive production mechanism. It is on production for 15 years and because of the strong aquifer and fractured reservoir zone near the oil-water contact, 92 % of the cumulative production is water. The amount of oil production for the wells are changing due to high heterogeneity of reservoir units. The neighboring wells show different production characteristics.

The areal dimensions of the field are 4.2 km*1.8 km. The reservoir structure of the field is anticlinal and the field is boundared from north and east by strike slip thrust faults directed toward NE-SW. Also it is separated into blocks by normal faults directed toward NE-SW. Production is performed from Late Cretaceous carbonates of Derdere Formation (Cenomanian-Turonian), Karababa Formation (Coniasian) and Karabogaz Formation (Cenomanian-Turonian). Source rock of the oil is Kbb-A Member of Karababa Formation and Karabogaz Formation.

Besides, Kbb-A Member, top of Karabogaz Formation ans Sayindere Formation are cap rocks for the reservoirs of structurally trapped oil [28]. The locations of the wells are given in Figure 3.1. Derdere Formation top contour map is given in Figure 3.2. Formation thicknesses are increasing from north-west to south-east and in the same manner porosity also increases [29].

Field-A can be stated as a member of a bigger structure which is separated into three fields by normal faults. Field-A is the member which is at the south of structure. Reservoir and fluid characteristics of the fields are similar to each other where they are producing from the same formations having similar petrophysical characteristics. These three fields are separated from each other by normal faults and lower zones which are under the water-oil contact and the zones having non-reservoir characteristics. Also, geochemical studies on the oil produced from the reservoir formations show that all three fields have the same oil properties. It is observed that at the northern field Karabogaz and Karababa Formations which will be described in detail in the following sections loses quality and mainly produces from Derdere Formation while by going towards the south their quality increases but the Derdere Formation which is main production zone in northern parts becomes to be invaded by water zone. The field at the north of Field-A is named as Analogy in this study and its data is used in case of lack of data of Field-A. Locations of wells in field Analogy are given in Figure 3.3

In this chapter production history, development, geology, rock and fluid properties of the field will be given. Also the data review and quality check will be explained.

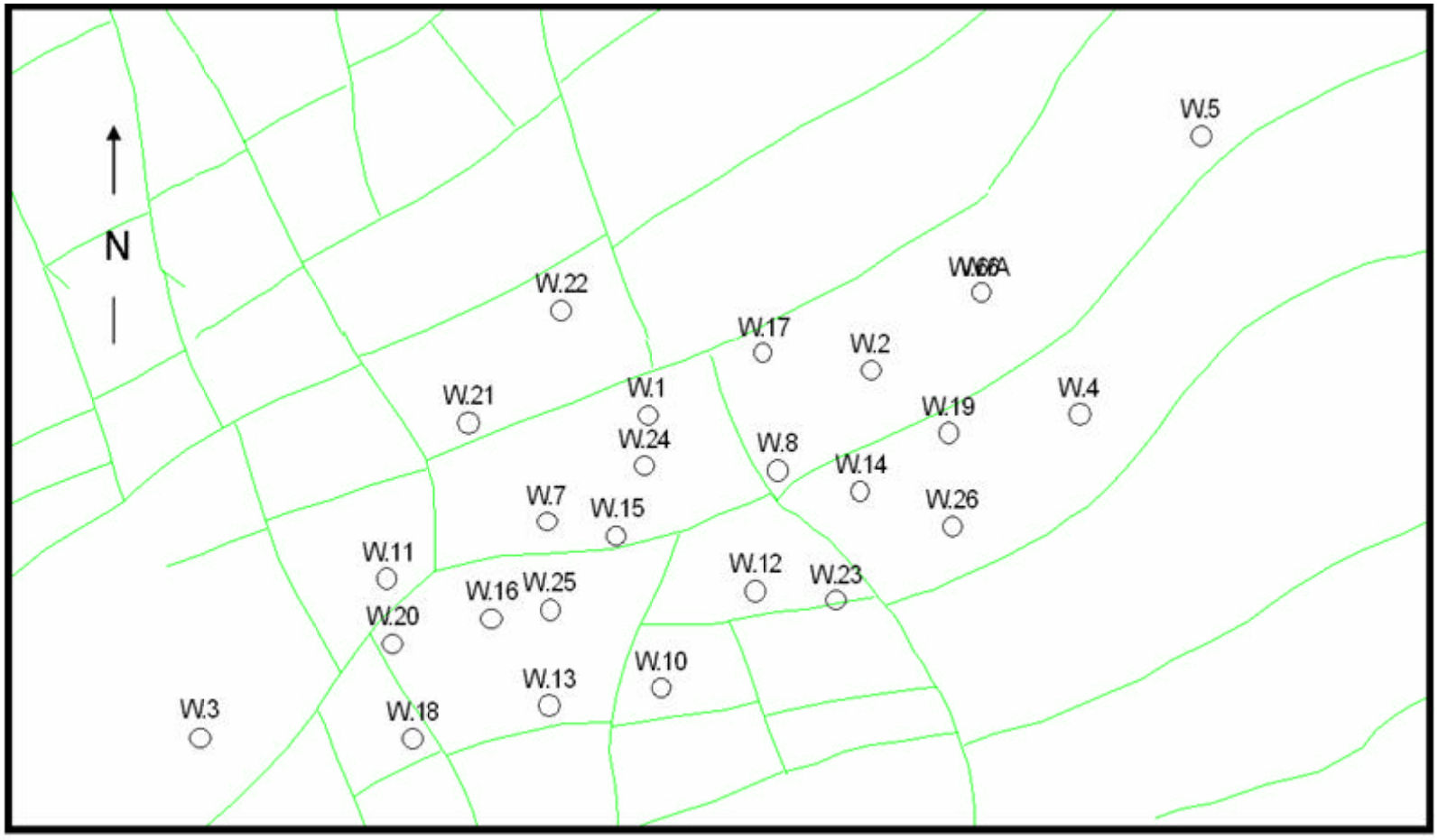

Figure 3.1 Location of the wells, Field-A

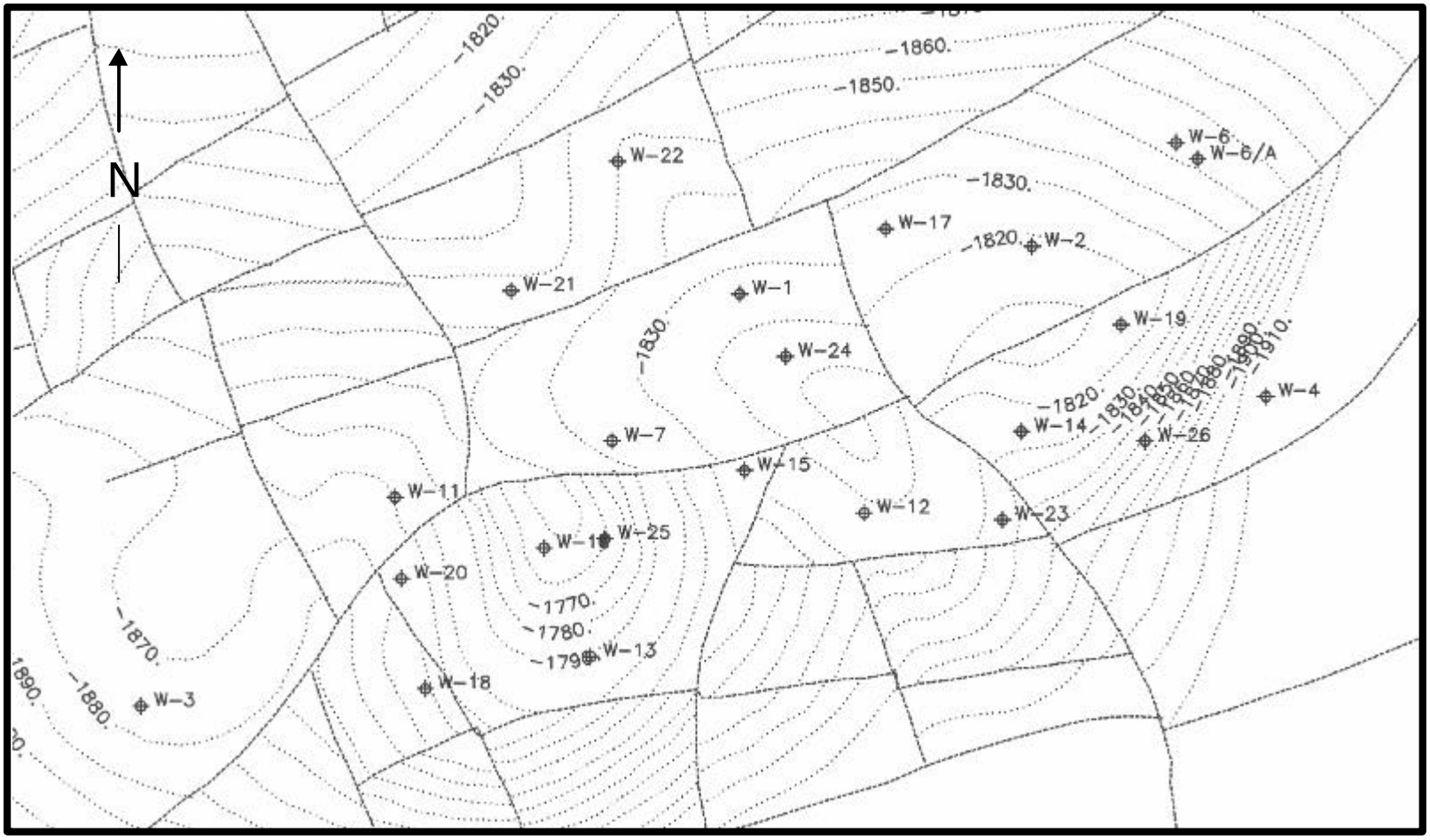

Figure 3.2 Derdere Formation top contour map, Field-A

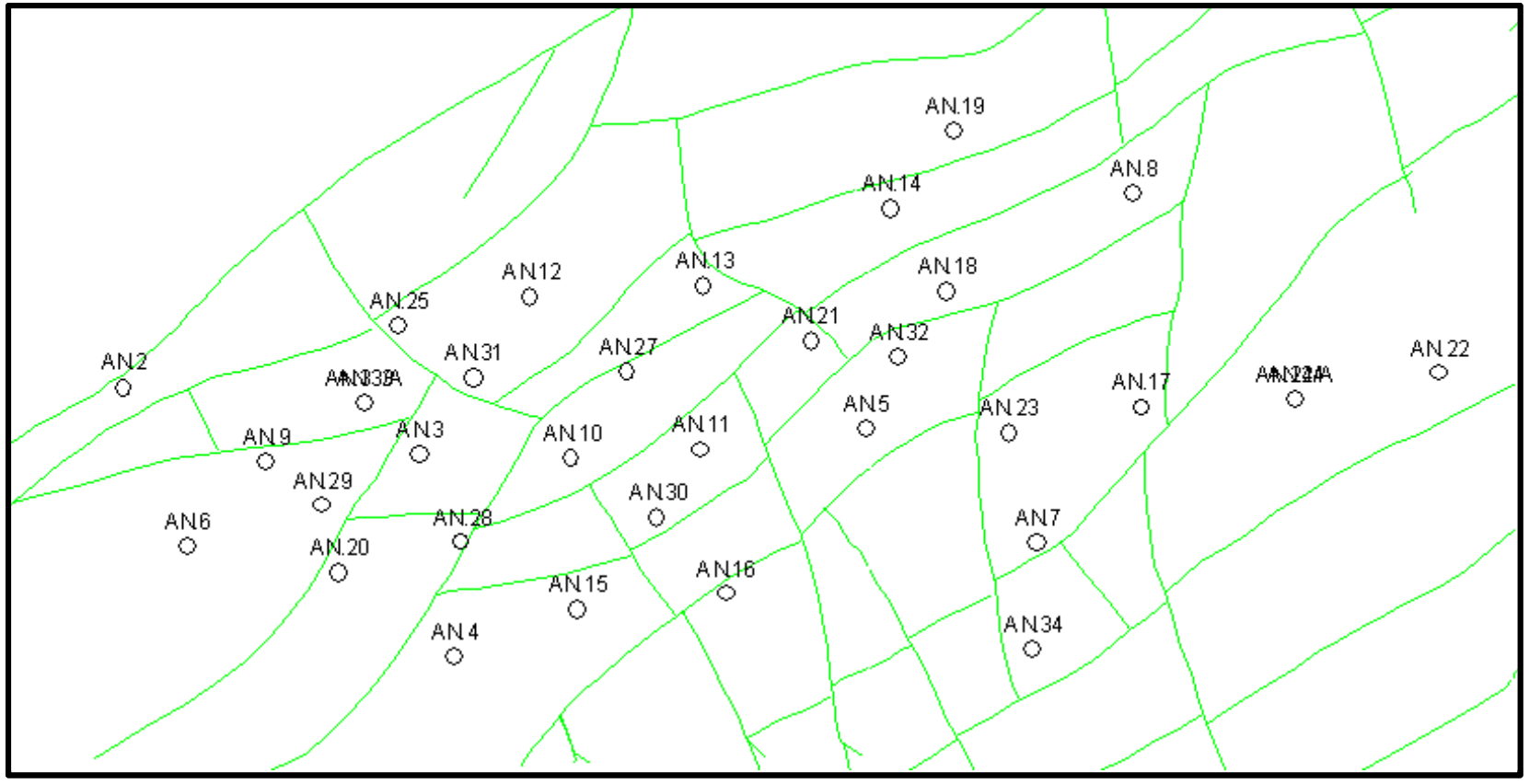

Figure 3.3 Location of the wells, field Analogy

3.1. History of the Field

Discovery well, W-1 of Field-A was drilled in 1989 and produced from Derdere Formation (Figure 3.4). Upon this well's good production level, 3 more wells were drilled in 1990 and since the aim was to discover the extension of the reservoir, W-3 was drilled at the west side while W-4 was drilled at south east of the field. W-2 produced from all of the three zones. W-3 was abandoned as dry well and since Derdere Formation of W-4 was water bearing, it produced from Kbb-C Member.

In 1991, 3 new wells were drilled which are W-5, 6 and W-7. W-7 produced from Derdere Formation while W-5 which was at east of the field abandoned since its Derdere Formation was water bearing and Kbb-C Member was oil show. W-6 could be produced from Kbb-C Member but with a low production level. Because of the low performance of these 3 wells development studies were stopped in 1992 and 1993.

In 1994, 3 more wells were drilled which were producing from Derdere, Karabogaz Formations and Kbb-C Member of Karababa Formation. At the end of 1994 production increased to 3200 bbl/day. In 1995, 2 wells were drilled and started production from Derdere Formation having high production performance.

Daily oil production increased to 5000 bbl/day at the end of 1995. In 1995 6 more wells were drilled upon increasing performance of the wells. These new wells started production from all of three oil bearing zones and production amount increased to 8000 bbl/day. In 1997 2 wells, in 1998 1 well, in 1999 2 wells, in 2000 1 well and in 2002 1 more well were drilled. As of November 2004, 21 wells are on production. Production intervals and formations of the wells are given in Table A.1 in Appendix-A. Shut-in wells are also given in Table A.1 by their last producing intervals.

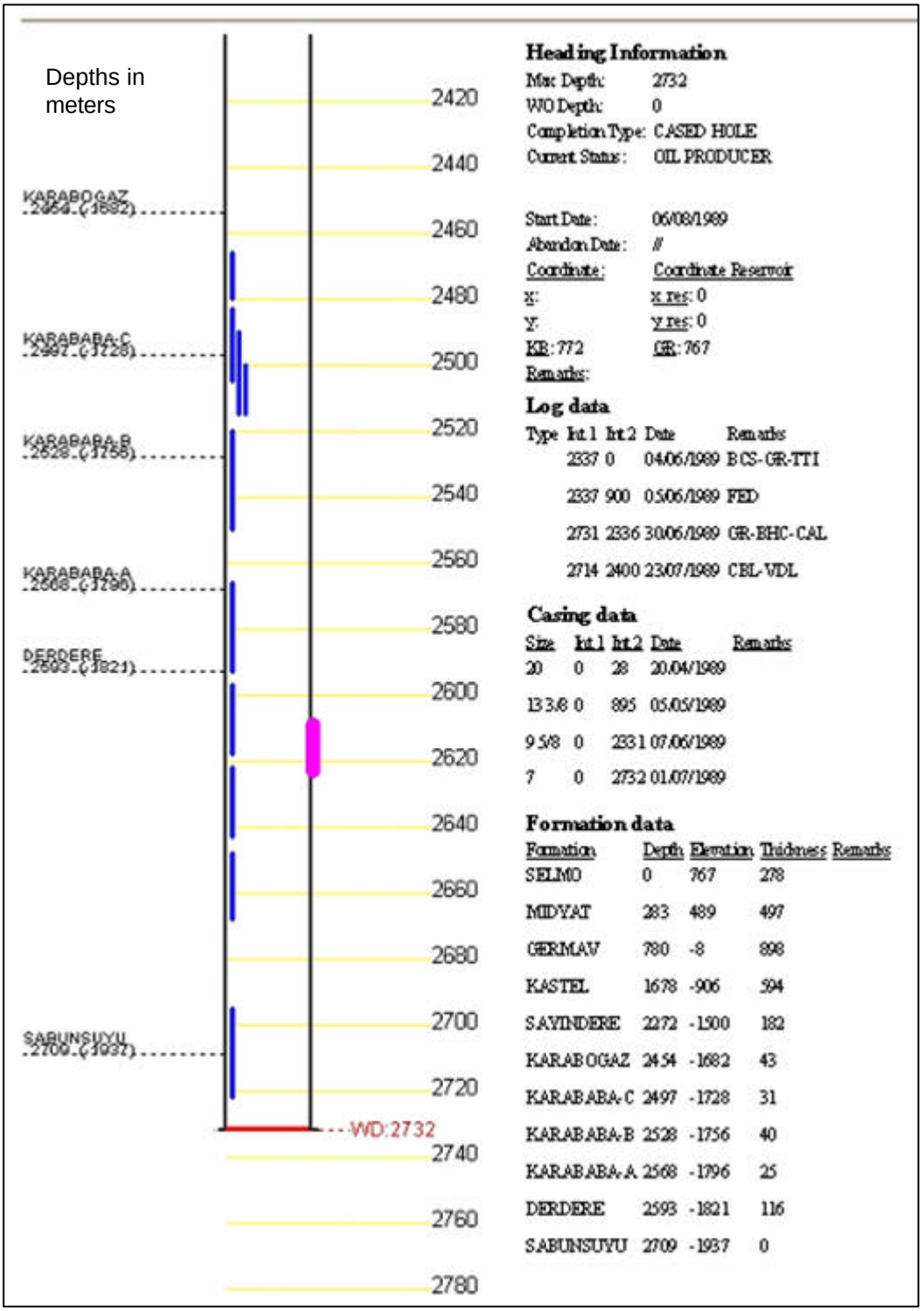

Figure 3.4 Diagram of the discovery well, W-1, Field-A

3.2. Geology

The field is located at SE of Turkey. Generalised cross section of the region (or field) is given in Figure 3.5. Several studies concerning stratigraphy and lithology of Field-A were implemented up to now. There are three formations showing reservoir properties. Field-A is producing from Derdere, Karabogaz and Kbb-C Member of Karababa Formation. Kbb-B member is productive according to fracture and matrix porosity and permeability development in a few wells. Lithologies of the target formations starting from Karabogaz Formation are given below. The reason to skip the other formations is that they are not oil bearing zones and they don't have effect on oil production. Stratigraphic cross section showing the zones are given in Figure 3.5.

a. Karabogaz Formation

Karabogaz Formation shows two different facies having lithologies as cherty limestones of open sea shelf environment and bioclastic limestones of shallow sea shelf environment. The first facies has no production capacity and Karabogaz Formation top is given as the top of second facies in this study. Average thickness of this formation (including both facies) is about 50 meters and it has unconformity with the Kbb-C Member below. Karabogaz Formation has comformity with the Sayindere Formation above. Lower section of the formation has a production potential due to limestones while the upper section can have the potential according to the fracture development [28].

b. Karababa Formation

This formation is divided into three sections which are named as Kbb-C, Kbb-B and Kbb-A beginning from the upper one.

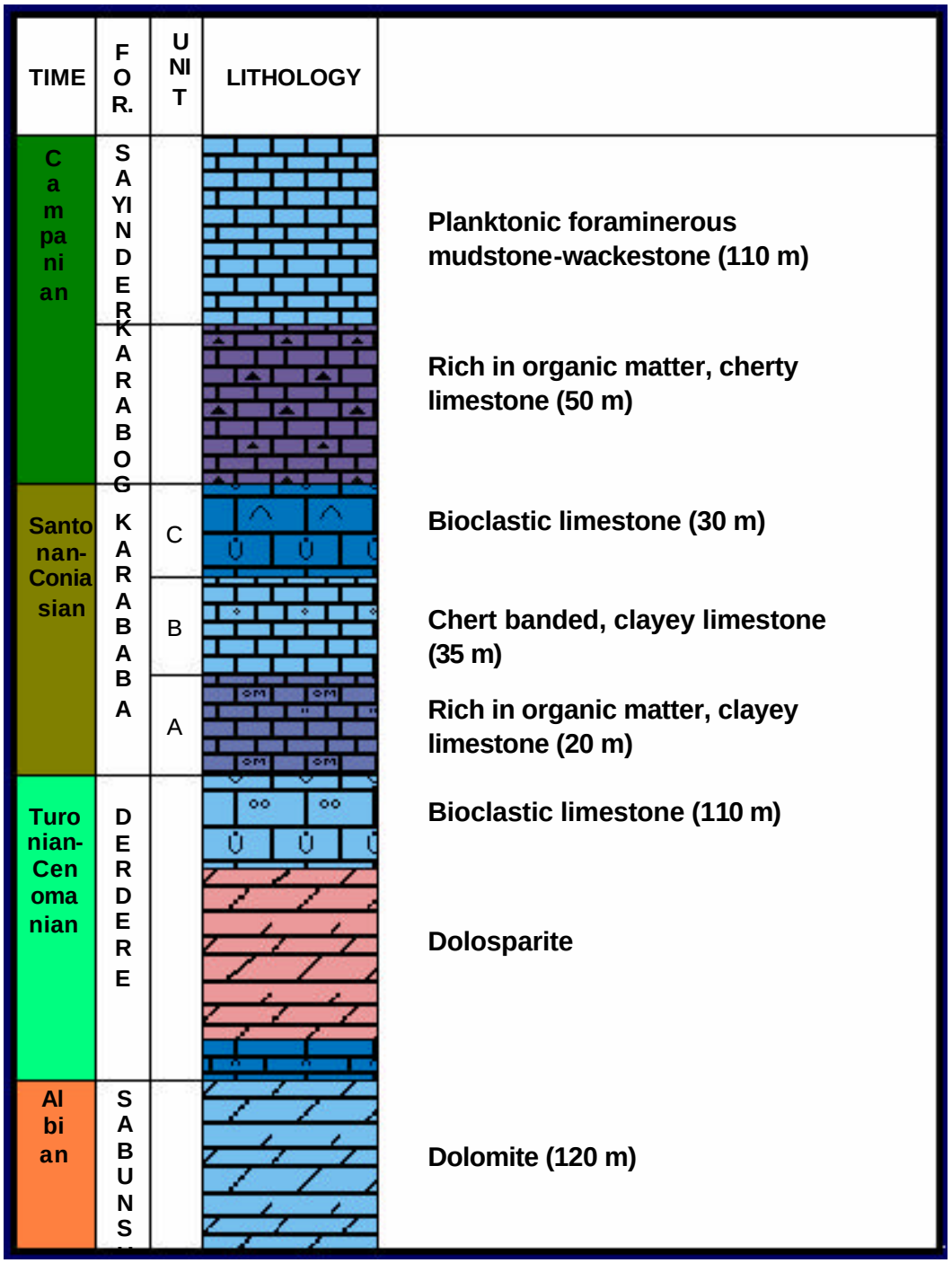

Figure 3.5 Stratigraphic cross section of Field-A

i. Kbb-C Member

Being discordant by Karababa Formation, this formation is the second best productive zone of the field. It is composed of limestones and the upper section of the formation has more production potential by the progress in porosity. Average thickness of the formation is 35 meters [28].

ii. Kbb-B member

Kbb-B Member has confirmity with Kbb-A Member below and Kbb-C Member above and it is composed of limestones with chirt bands at the top sections. These open shelf deposit limestones can only be produced in the wells which have high porosity development. Kbb-B Member has areal distribution over the field but reservoir characteristics of this unit has no areal distribution. Because of insufficient porosity and permeability this formation is not classed as reservoir zone. Its average thickness is 42 meters [28].

iii. Kbb-A member

Karababa-A Member has unconformity with Derdere Formation below and confirmity with Kbb-B Mmeber above. It is composed of limestones which are rich in organic material. These deep marine deposit limestones has no reservoir quality but have potential as source rock in the region. It has an average thickness of 27 meters [28].

c. Derdere Formation

Top contact of Derdere Formation has uncorfirmity with Kbb-A Member and also it is excepted that bottom contact has unconfirmity with Sabunsuyu Formation below and there exists an erosion process after the deposition of Sabunsuyu Formation. Facies evaluation of Derdere Formation shows that it is composed of

three main lithofacies from top to bottom. First of them is shallow marine limestones, the second is dolomites and the third is deep marine limestones. Limestones at the top section have thicknesses between 20-35 m. and are productive where matrix porosity and fracture network are well developed. The dolomites at the middle section whose thicknesses vary according to dolomitisation are transitive with the limestones above in some wells.Intracrystalline porosity of the dolomites are high thus this zone is an important reservoir section. Only one well is fully crossing Derdere Formation and the thickness of the unit in this well is 110 meters [28].

3.3 Reservoir Rock and Fluid Properties

3.3.1 Porosity

Porosity measurements were performed by using core and log properties. There are 9 cores from 26 wells in the fields. Also full-set logs were taken from 25 wells and 19 of them are interpreted. The results of core analysis are given in Table A.2.

Plugs are taken from cores to analyze permeability and porosity values of the reservoir rock. But, due to laboratory measurement techniques they must be whole and well shaped, which results in necessity of taking them from tight parts of the cores, by other means non-fractured parts. So, plug analysis results give the matrix parameters of a reservoir rock. These results show low matrix porosity properties. There are very few data obtained by core analysis. The other fact is that the recoveries of the cores are low. Field-A is known to be a highly fractured field which results in low recovery of the cores. Megascopic (visual) observations of the cores are also showing the signs of fractured formation.

Fractures are the secondary porosity of the field and they are very effective in producability of the oil. Evaluation of the core results shows us that the matrix

porosity is low and high production amount of the wells are supplied by fracture-matrix interaction.

From Derdere Formation there is only one core analysis done. Other analyses are belonging to Kbb-C Member and Karabogaz Formation. These data are far from giving enough information arealy. They are not satisfactory in making a porosity distribution analysis of the formations. But they give the indication to accept the fractured structure of production zones.

Matrix effective porosity interpretations are done by a complex log interpretation program. Data was recorded by 0.1524 meters intervals. Average log porosity values for Karabogaz Formation, Kbb-C Member and Derdere Formation are given in Tables A.3, A.4 and A.5 for the sections above the oil-water contact (-1860 m).

3.3.2 Permeability

Permeability values from core analysis results are given in Table A.2. Restrictions that were faced in porosity evaluation also apply to permeability values. For Derdere Formation there is only one data and the other formation's data are not satisfactory. Although there is limited data it can be said regarding these data that permeability values are very low as such under 0.1 md. Again the reason for this phenomenon can be explained by the recovery of the cores from tight matrix sections. Since more porous and fractured and because of that highly productive zones can not be analyzed due to low recovery of the cores, these measurements are not representing the exact permeability values of the reservoir rock.

Relative permeability analysis is not performed on any of the core samples. Using empirical correlations from literature is an option in defining relative permeability values.

3.3.3 Water and Hydrocarbon Saturation

The parameters used in calculating water saturation and depending on it the hydrocarbon saturation values are formation water salinity and Rw (water resistivity) which is related to salinity. Salinity values of Kbb-C Member and Karabogaz Formation show that their formation water are similar and the average salinity of them is in average around 50 000 ppm. Derdere Formation water has different characteristics and measured average salinity of this water is 14 000 ppm. Since they have different salinity values logs must be interpreted according to this distinction. Different Rw values are calculated for different types of zones.

The range of measured reservoir temperature is between 93-99 ^{0} C during logs were recorded. Logs were interpreted as taking Rw values between 0.15-0.20 ? for Derdere Formation and between 0.05-0.06 ? for Karababa Formation. Interpretation is performed by using Archie formula which is most proper method for clean carbonate formations. Via this formulae mobile and irreducible hydrocarbon saturation values are calculated. The average saturation values for these zones in each well are given in Table A.3, A.4 and A.5.

3.4 Production Mechanism of a Fractured Reservoir, Field-A

Field-A has a production mechanism of water drive. For a strict water drive, there is no gas cap [30]. Depending on the way that the water enters the reservoir, water drive reservoirs are sometimes characterized as either (1) bottom water drive or (2) edge water drive [30]. In a bottom water drive, the formation has enough vertical permeability so that the water can move vertically or perpendicular to the formation grain orientation. In this type of reservoir, since there is some vertical permeability, water coning can be a serious problem.

Production trend of a fractured reservoir is directly related to the transmissibility and storability of the fractures, matrix porosity and the interaction between matrix

and the fractures. In the early stages of the production, the fluid stored in the fractures will be produced and after production of the whole capacity of the fractures, flow from the matrix to the fractures will begin and production amount will depend on the degree of matrix capacity and its degree of feeding the fractures. The conventional reservoir formed by intergranular porosity is studied under the simplified assumption that the reservoir is homogeneous and the basic physical properties such as porosity and permeability, are always associated with a trend [20].

In a non-conventional reservoir that is naturally fractured there are discrepancies and discontinuities throughout the whole reservoir as the result of two distinct porosity systems in the same formation (Figure 2.4). In a double porosity system, when the flow is stabilized, the flow process towards a well is actually a flow only through the fracture network, whereas the flow from each matrix block is reduced to a steady-state supply of fluid to the surrounding fractures. The fractures assure the flow of hydrocarbons from the matrix where those hydrocarbons are stored to wells from which they will be later lifted to the surface. In general, the fractured network is divided into a number of zones, each of them practically saturated with only one phase, while inside each zone the matrix block may be saturated with one, two or even three phases. The matrix-fracture interaction and fluid exchange will depend on the relative position of the single block in the reservoir and the respective water-oil contact [20].

A fractured oil reservoir may have oil, water and gas-cap zone before any production begins, in agreement with the fracture saturation distribution [20]. In Field-A, before production begins, static equilibrium is obtained by the two phases existed in the reservoir, which are oil and water, inside the fractures and the matrix blocks. The two phase contacts in the fractured network are always sharp, distinct and horizontal [20]. Initially, above oil-water contact, matrix blocks are saturated with oil and interstial water while fractures are only saturated

with oil. Below oil-water contact, both matrix blocks and fractures are saturated with water.

As the production begins, water encroachment starts and water invades the zones above original oil-water contact. In this stage, by the most simplified approach, the reservoir is divided into three zones as water zone, water invaded zone and oil zone starting from the bottom. Related to the heterogeneities, the range of pressure drop may have different degrees inside a zone and further zonation can be made.

As water drive production mechanism takes place, drainage displacement of oil in matrix blocks by water in the fractures starts in case of oil wetted matrix block. It can not be concluded definitely that Field-A wetting phase is oil or water since there is no relative permeability measurements but can be said that the field has a heterogeneous wettability according to the production trend of the wells.

The presence of a strong water drive may maintain a reservoir pressure nearly equal to the initial reservoir pressure. Field-A has a strong bottom water drive production mechanism, so the pressure is not declining with the same rate as the production continues, but stabilizes after a certain period of time (Figure 3.6). Recovery of the field is the result of imbibition and drainage displacement through capillary and gravity forces.

In the oil zone, as a result of reservoir pressure being higher than bubble point pressure, the entire fracture matrix system is saturated with only one movable phase, oil. The matrix-fracture fluid interchange is the unique result of fluid expansion associated to reservoir depletion and compressibility of the fracture-matrix system fluids and rock. In the water-invaded zone there is saturation in water (interstitial and invaded) and saturation in residual oil [20].

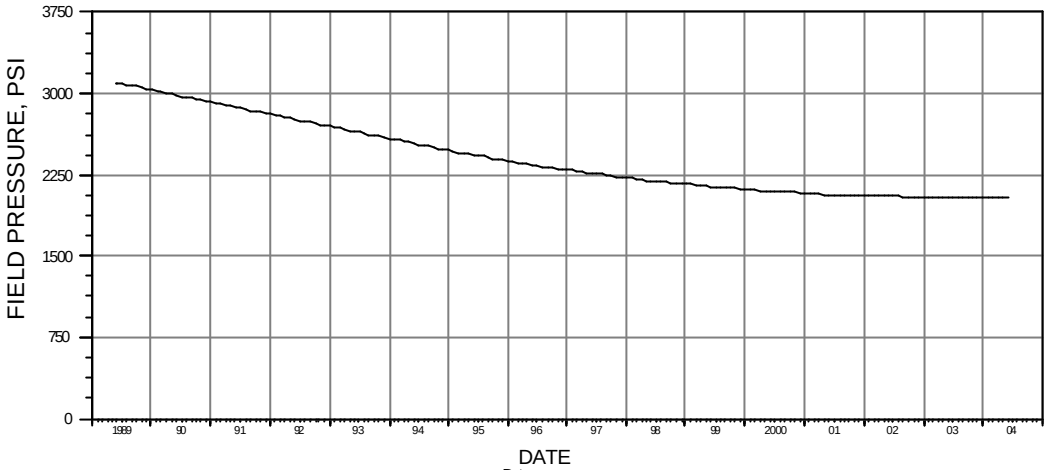

Figure 3.6 Average reservoir pressure at -1750 m. sub sea (original reservoir pressure is 3100 psi)

CHAPTER 4

STATEMENT OF THE PROBLEM

Field-A, a fractured carbonate field with bottom and edge water drive production mechanism will be investigated under the rules of uncertainty assessment by interpreting the valid reservoir rock and fluid analysis and production history. Original oil in place amount of Field-A will be evaluated in order to get the probability of observing all the possible values of it under the present set of data relating to its reservoir properties.

CHAPTER 5

METHOD OF SOLUTION

Traditionally, the analysis combine single point estimates of a model's variables to predict a single result. Estimates of model variables must be used because the values which actually occur are not known with certainty. In reality, however the combined errors in each estimate often lead to a real-life result that is significantly different from the estimated result. To be able to combine all the uncertainties in a model a simulation must be performed. For this reason in this study @Risk software is used for making Monte Carlo simulation.

5.1 Use of @Risk in Monte Carlo Simulation

@Risk is an "add-in" to Microsoft Excel. It links directly to Excel to add uncertainty analysis capabilities. So, it works with Excel style menus and functions. Uncertain values can be defined in as probability distributions as cell values. For each cell value a different type of distribution can be specified. Features of defining distribution types and running a Monte Carlo simulation is given in the following sections.

5.1.1 Developing a Model

If there is an uncertainty in a variable which means there are probabilities of occurrence then uncertainty can be summarized by using a probability distribution. Probability distributions give both the range of values that the variable could take (minimum to maximum) and the likelihood of occurrence of each value within the range. In @Risk, uncertain variables and cell values are entered as probability distribution functions, for example:

RiskNormal(100,10)

RiskUniform(20,30)

RiskExpon(A1+A2)

RiskTriang(10,20,30)

Before starting modeling dependent and independent variables must be decided. Independent variables' distribution functions are given by the user where the dependent variables' probability function is obtained by simulation of the independent variables. Independent variables' distribution functions are placed in a cell on the worksheet or formulas. Distribution functions can be fitted to a data set. Selecting the function "Define Distributions" (Figure 5.1) opens a menu window for selecting an appropriate distribution function for the variable.

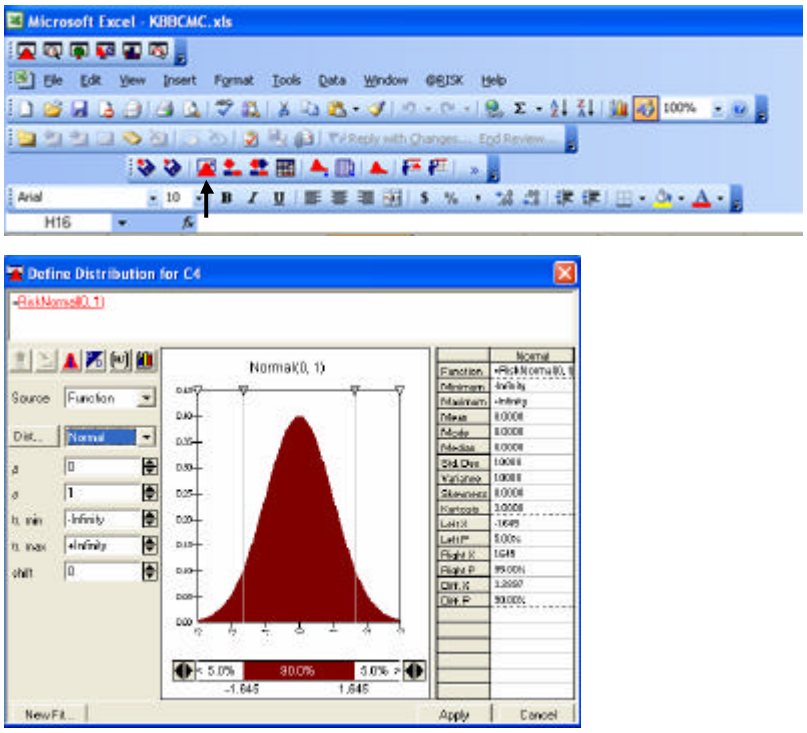

Figure 5.1 Selecting a distribution function for a variable

Statistical results of the given function are read at the right hand side of the pop-up window. A truncation interval can be given to the distribution to prevent extreme values that are technically incorrect. From this window also a function

can be given by the user upon his decision about the nature of the data. By the option “New Fit” a data column can be selected for fitting the statistically most correct distribution types. A menu window “Fit Excel data” provides selection of the data range to be fitted to a distribution (Figure 5.2). @Risk fits a series of distributions to the given data according to the rank of statistical correctness (Figure 5.3). User can choose any one of them upon his decision.

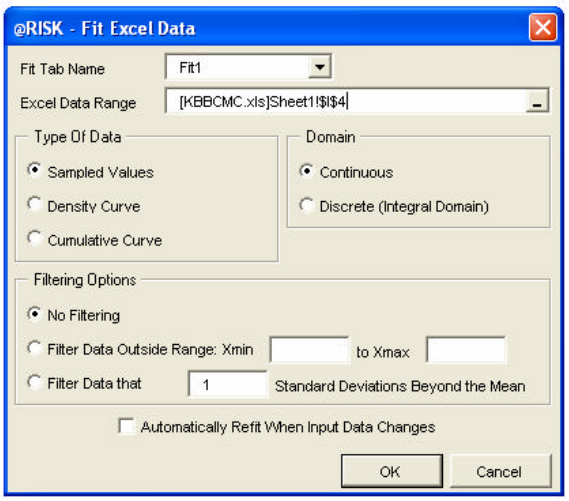

Figure 5.2 Selecting a data range for fitting distribution

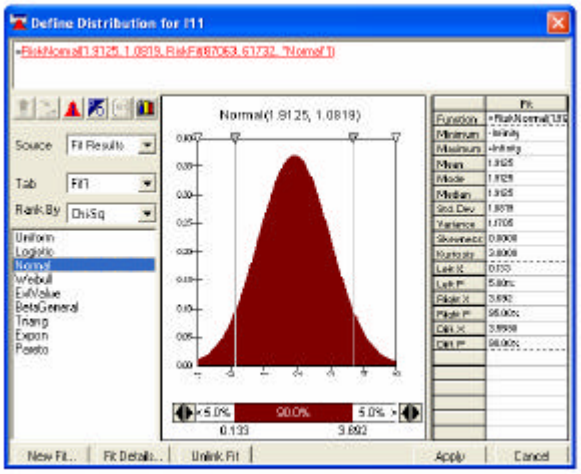

Figure 5.3 Fitted distributions menu of @Risk

Dependent variable again is given by a formula in a cell that is the function of independent variables. This cell must be selected as output cell by the function "Add Output". After distribution functions of the independent variables and the equation of the dependent variable is selected, simulation settings are defined by the function "Simulation Settings". Menu of this function gives the opportunity to the user as selection of simulation type, number of iterations, viewing the results as simulation continues, choosing only the marked inputs etc. (Figure 5.4)

After the simulation settings are chosen, by the function "Start Simulation" on the tool bar, @Risk makes runs the simulation with the given simulation settings and as the simulation is finished a statistics window showing input and output variables statistical results can be viewed (Figure 5.5). This menu also gives the graphical results (Figure 5.6) and detailed statistics with 5 % incremented percentiles.

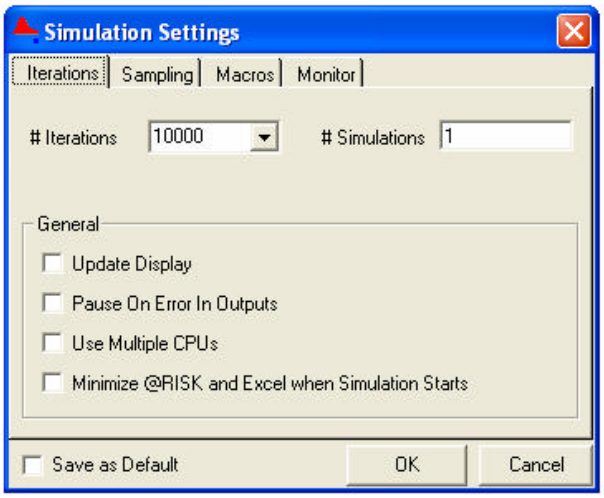

Figure 5.4 Simulation setting menu of @Risk

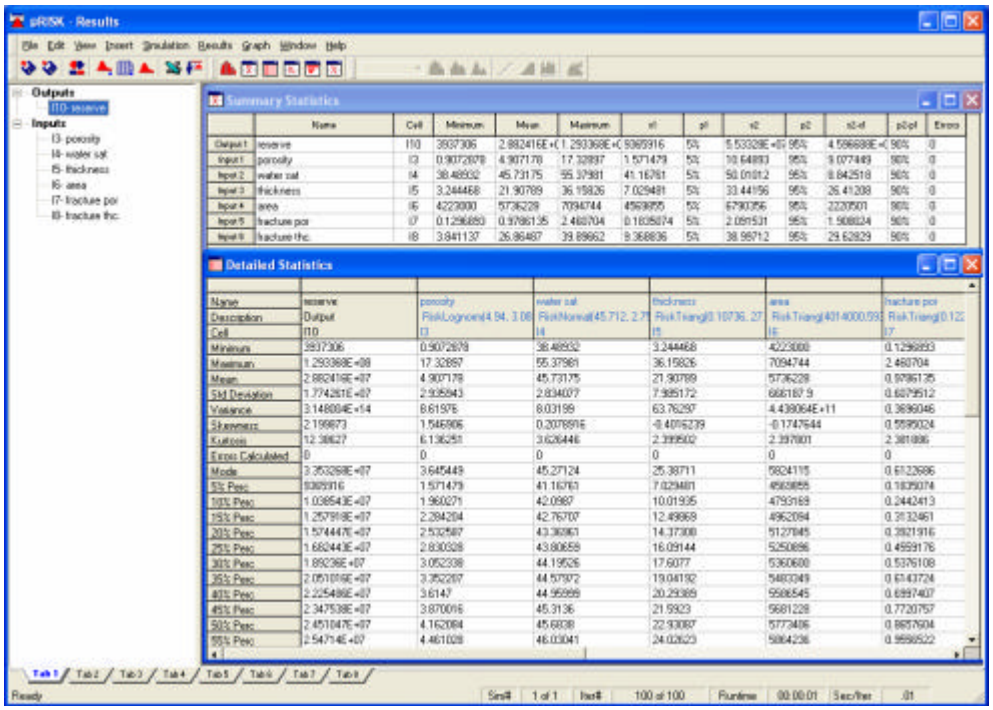

Figure 5.5 Statistics result page of simulation by @Risk

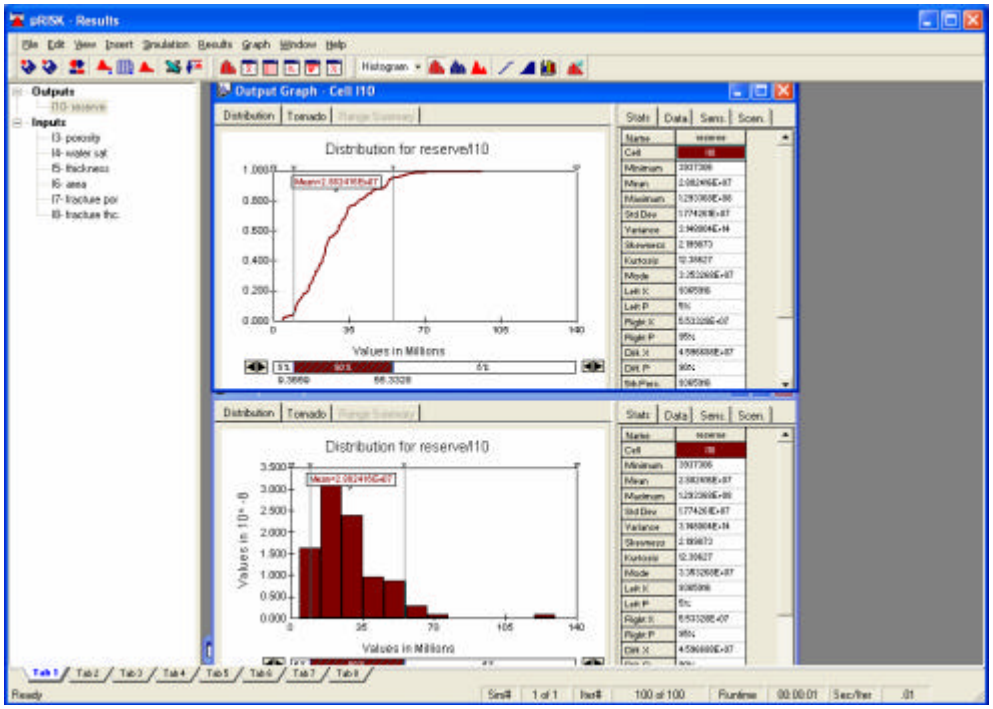

Figure 5.6 Graphical results of simulation by @Risk

@Risk provides sensitivity diagrams for understanding the impact of input variables on output variable. After the simulation of the output, sensitivity options can be chosen to see the relative effect of variables (Figure 5.7). Another tool commonly used to analyze probability results is a tornado chart. Nothing more than a bar graph turned sideways, tornado charts depict the correlation between the criteria (e.g.: OOIP) and some other variable, such as matrix porosity. The idea is to ascertain which variables are most important. Tornado charts pick up linear associations between the variables. Also simulation settings can be chosen such that sample data values beyond the reasonable range are not iterated.

In this study these simple and practical features of @Risk are used to simulate the uncertainty in original oil in place amount of Field-A. Simulation settings are set to Monte Carlo simulation and 10 000 iterations. Procedure in simulating the original oil in place by @Risk is follows:

1. Independent variables that are influencing the dependent variable (original oil in place) are determined. These variables are area, matrix and fracture porosities, matrix initial water saturation, and net thickness above 0 % porosity.

2. Data sets for each independent variable are prepared and distribution functions for them are defined.

3. Dependent variable is built by the volumetric method and then the cell is selected as output.

4. Simulation settings are chosen and simulation is run.

5. Results of the simulation showing probability distribution functions of independent and dependent variables and their detailed statistical information are taken and evaluated.

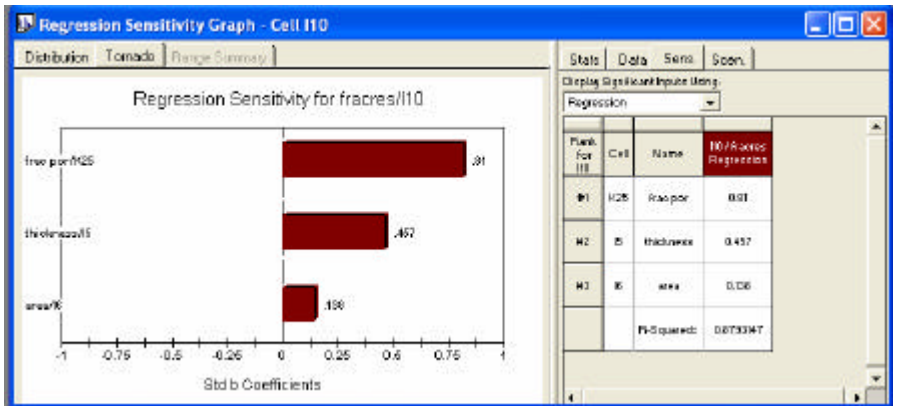

Figure 5.7 Sensitivity analysis by @Risk

CHAPTER 6

RESULTS AND DISCUSSION

Original oil in place (OOIP) of a field can be calculated by volumetric, material balance and decline analysis methods. Volumetric approach is chosen for capability to work with uncertainty assessment in this work.

Upon the facts on production mechanism of fractured reservoirs, production history of Field-A must be analyzed to validate the several geological and petrophysical observations indicating the fracture system combined with water drive production mechanism. The field has a strong aquifer providing a high productivity index for most of the wells, these wells are producing by electrical submersible pumps which permit high flow rates. But since a high pressure drawdown is created in the well by these pumps, aquifer water starts to invade the oil zone via high permeability fractures and water coning starts.

At the beginning of the field production, until 1992, it is observed that water cut is increasing steadily. As it was explained in section 3.1, in this period there were only 3 wells producing in the field. Since water coning started, production amount decreased in order to diminish the effects of water coning until 1994. By 1994, the field started to be developed further and commingled production from Derdere and Karababa Formations began to take place.

Derdere Formation has high reservoir quality in the area but in Field-A although it still persists these qualities, water table is very high and in several wells, this formation is highly saturated by water. Fractures cause the water to increase rapidly so water coning invades the zone after a short period of time. After a certain period these perforations are shut due to high water cut. For this reason Derdere Formation perforations are opened at the zones where matrix porosity

quality is good and if there is any large fracture that is detected from the logs, that intervals are not perforated to avoid sudden water increase.

Karabogaz and Karababa Formations are effected from an edge water drive at the flanks of the field. Some of the wells at the flanks (W-4, 6, 11 and 20) are directly opened to production from Kbb-C Member since Derdere Formation is under the oil-water contact at these parts. But the water production from these wells also increased rapidly showing that the field has an edge water drive also. Indeed, wells W-3 and W-5 could not produce from Karabogaz Formation or Kbb-C Member because of high water obtained in the tests. In other areas where edge water drive is not affecting them, Karabogaz and Karababa Formations can not be produced separately since their pressure is lower and can not supply a certain liquid level for pumps to produce. In such a situation Derdere Formation is also put into production for increasing the liquid level in the wellbore. So it is expected that water rate increases during the production since pressure drop must be prevented by producing from the high water bearing zones.

In Figure 6.1 this behavior is observed easily especially after 1995 and today although the net oil production is decreasing water cut is still increasing. Decline of the production is becoming steadier as it is dependent on the matrix-fracture interaction. Matrix blocks feed the fractures and a steady flow is obtained.

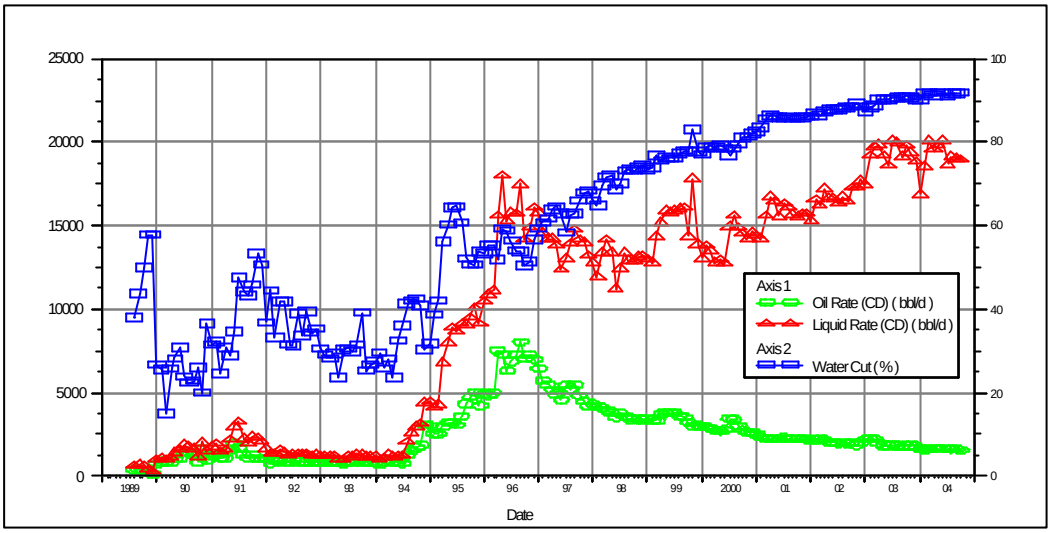

Figure 6.1 Production history of Field-A

6.1 Volumetric Method

To calculate the original oil in place (OOIP) in Field-A, volumetric approach is used. Reserve calculations are done for three zones; Karabogaz Formation, Kbb-C Member and Derdere Formation since wells are producing from these zones. Kbb-B member is productive in 4 wells due to fracture development in this zone. Since there is no core analysis in this zone it is not possible to define its permeability but production and swab test results suggest that this zone has not enough reservoir quality for production.

For estimation of OOIP for Field-A, first the uncertain variables must be stated. The reason for uncertainties and the assumptions to describe the probable values of these uncertain variables are explained also. OOIP, by volumetric method, has the formula below :

$$OOIP = A*h*\varnothing*(1-S_{wi})/B_{oi} \qquad 6.1$$

where, A= area

h = net thickness

$\varnothing$ = porosity (matrix or fracture)

S_{wi} = initial water saturation (matrix or fracture)

B_{oi} = initial formation volume factor of oil (matrix or fracture)

Matrix and fracture oil in place values can be calculated separately, giving the appropriate values for them in Equation 6.1. Knowing that Field-A has a fracture system the fracture reserves are added to the OOIP calculations of the matrix volume by using the variables related to fractures like fracture porosity, fracture water saturation and their volumetric distribution.

All of these variables have some sort of uncertainty due to their characteristics and measurement shortcomings. The petrophysical variables $\varnothing$, S_W and net reservoir thicknesses are normally not directly measured, but estimated from some physical properties measured in the well, applying some mathematical model of more or less empirical origin with its required parameter values based on physical measurements in the wells, on core material or on some other sources [24]. Besides, having only limited measurements that at most equal to the number of drilled wells there always will be uncertainty.

Measurements on these variables will be used as sample pool for those variables. By Monte Carlo simulation their probability range of P10, P50 and P90 will be estimated.

6.1.1 Area

Area of the field is stated by the seismic studies and drilling operations. Seismic interpretations give the border faults that can be accepted as the boundary of the field. Also original oil-water contact specified by the logs and test results, which is -1860 m. sub sea, is accepted as boundary where encountered. But unless a well

is drilled and tested outside these boundaries they can not be strictly stated as exact boundaries of the field. Field is mapped due to the faults drawn by seismic study and depth of the formation tops which were decided according to the existing wells formation depth knowledge. In this study, area of the field is given by three values as; low, average and high estimates. Karabogaz and Karababa Formation reserve areas are larger than Derdere Formation area. The reason is that there are producing wells from these formations while Derdre formation is under the oil-water contact.

Low estimate for Karabogaz and Karababa Formations (Figure 6.2) is given by accepting that the field area is bordered by a boundary drawn just at the outer edge of the related formation's produced wells. Average estimate case is the one that would be used in a deterministic study whose areal boundaries would be given again by produced wells, structure and oil-water contact (Figure 6.3). High estimate case is determined by structure and fault boundaries whether there is a drilled well or not (Figure 6.4).

For Derdere Formation low estimate is considered by the producing wells from this zone as in the former case (Figure 6.5). On the other hand average estimate is boundered by oil-water contact and fault structure (Figure 6.6). High estimate is given according to the structurally high but not tested zones and oil-water contact (Figure 6.7).

On these figures, wells which are outside of the given area are dry and area of a reservoir can not include dry wells. These values are given in @Risk as minimum, mean and maximum values of a triangular distribution (Table 6.1). Statistical results of cumulative distribution function of reserve area values calculated by @Risk are given in Table B.1 for Karabogaz Formation and Kbb-C Member and in Table B.3 for Derdere Formation.

Table 6.1 Lowest, average and highest possible reserve areas of Karabogaz Formation, Kbb-C Member and Derdere Formation, Field-A

RESERVE AREA, m^2			
Unit	Lowest possible	Average	Highest possible
Karabogaz Fm.and Kbb-c M.	4,014,000	5,930,000	7,263,000
	Probability distribution type		
	RiskTriang(4014000,5930000, 7263000)		
Derdere Fm.	Lowest possible	Average	Highest possible
	3,141,000	4,555,000	5,166,000
	Probability distribution type		
	RiskTriang(3141000,4555000, 5166000)		

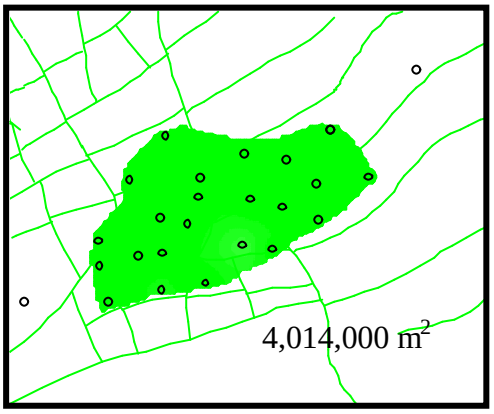

Figure 6.2 Lowest possible area of Karabogaz Formation and Kbb-C Member, Field-A (wells outside the area are dry wells)

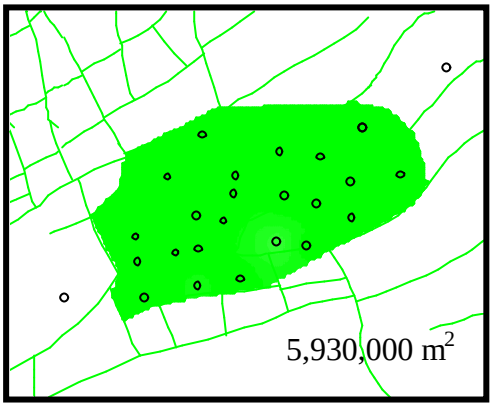

Figure 6.3 Average area of Karabogaz Formation and Kbb-C Member, Field-A

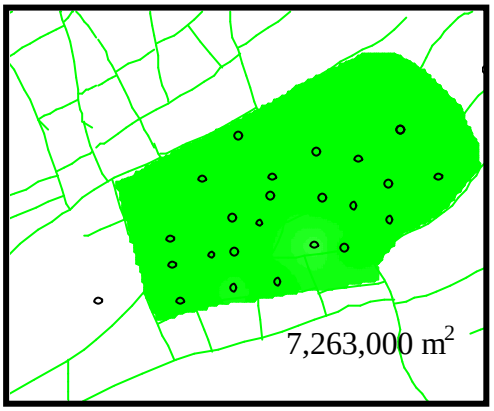

Figure 6.4 Highest possible area of Karabogaz Formation and Kbb-C Member, Field-A

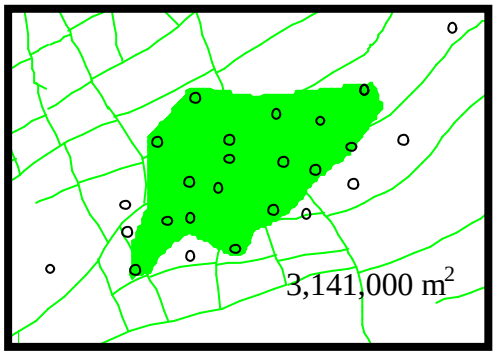

Figure 6.5 Lowest possible area of Derdere Formation, Field-A

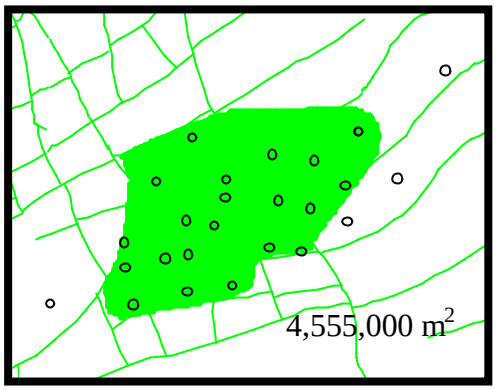

Figure 6.6 Average area of Derdere Formation, Field-A

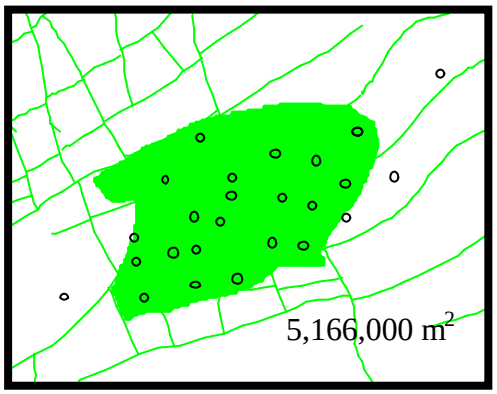

Figure 6.7 Highest possible area of Derdere Formation, Field-A

6.1.2 Matrix Porosity

Porosity measurements are done on the field by sonic and density-neutron logging. As it was explained, these logging techniques are not directly measuring the porosity of the rock but measuring some other variables like the time that sonic signals are reaching to the receiver or counting the electrons of some organic material, then converting these values to porosity values. This leads to

some level of uncertainty since measurement or calibration of the tools or interpretation of them may change by several factors.

The second sort of uncertainty of porosity which has key importance for this study and is related with OOIP is coming from limited and occasional application of logging on the field. Measurements are done as the wells are drilled so we have only that much measurement on the field and can not have certainty in describing the areal distribution of the porosity.

Logs taken from 19 wells are interpreted by SSI's LOGCALCII log interpretation software [31]. Log measurements are done in every 0.1524 meters, so there are enough measurements to create a sample pool for each reservoir zone. 100 % water saturation and 0 % porosity measurements have no value for describing a reservoir zone, so those values are omitted in plotting a frequency distribution of producing formations. Distribution types of the formations are selected according to their frequency histograms (Figures 6.8, 6.9 and 6.10). Frequency histograms are useful in determining the type of probability distribution of the variables.

Probability distribution curves are fit to the data by using @Risk program. @Risk gives the statistical information about the given data set such as mean, minimum, maximum values, standard deviation and cumulative probability values of the data by 5 % intervals (e.g. P10, P50, P90). Summary statistics of matrix porosity data sets and the fitted probability distribution types of each formation are given in Table 6.2. These distributions are then given to the simulation as inputs in calculation of original oil in place.

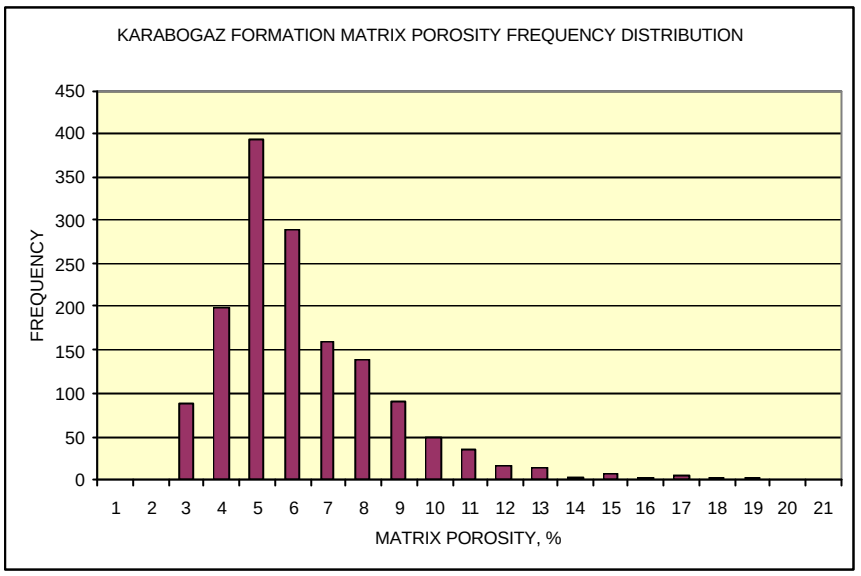

Figure 6.8 Histogram of Karabogaz Formation matrix porosity

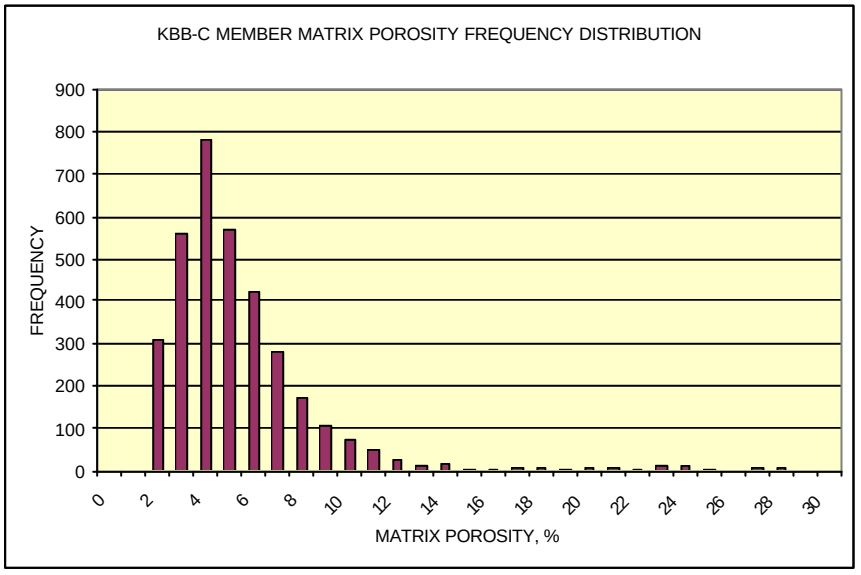

Figure 6.9 Histogram of Kbb-C Member matrix porosity

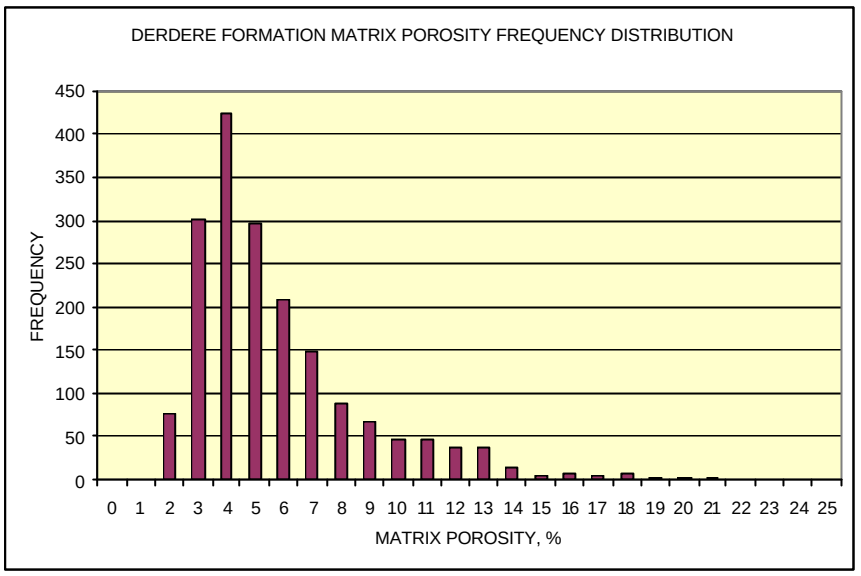

Figure 6.10 Histogram of Derdere Formation matrix porosity

Table 6.2 Probability distributions and summary statistics of matrix porosity

MATRIX POROSITY DISTRIBUTION FUNCTION OF PRODUCING FORMATIONS							
Formation	Statistical results						
$Ø_m$, %	Minimum	Maximum	Mean	Std Deviation	10% P	50% P	90% P
Karabogaz	0.867	17.437	4.905	2.270	2.474	4.453	7.918
Kbb-C	0.453	27.523	4.969	3.051	2.017	4.247	8.718
Derdere	0.555	20.572	5.205	2.226	4.478	4.547	9.089
Formation	Probability distribution function						
Karabogaz	RiskLognorm(4.9124, 2.3112, RiskTruncate(0, 17.844))						
Kbb-C	RiskLognorm(4.94, 3.0839, RiskTruncate(0, 27.845))						
Derdere	RiskLognorm(5.239, 3.1024, RiskTruncate(0, 20.757))						

Probability density function and cumulative probability distribution of matrix porosity values of formations are given in Figures 6.11, 6.12 and 6.13. Statistical results of cumulative distribution function of matrix porosity values calculated by @Risk are given in Tables B.1, B.2 and B.3 for Karabogaz Formation, Kbb-C Member and Derdere Formation.

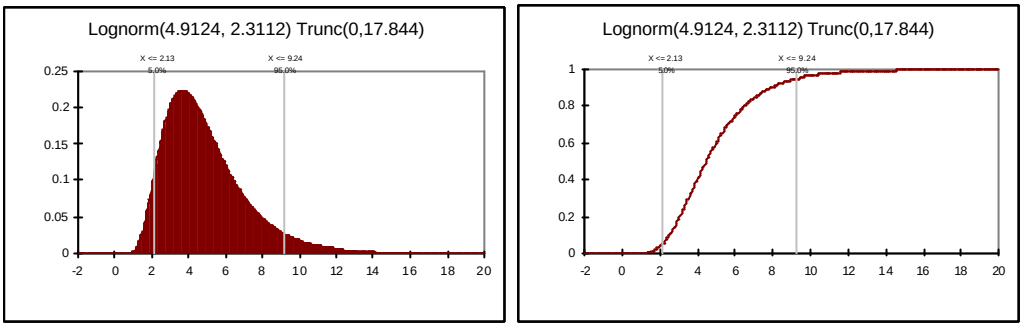

Figure 6.11 Matrix porosity distribution plots of Karabogaz Formation

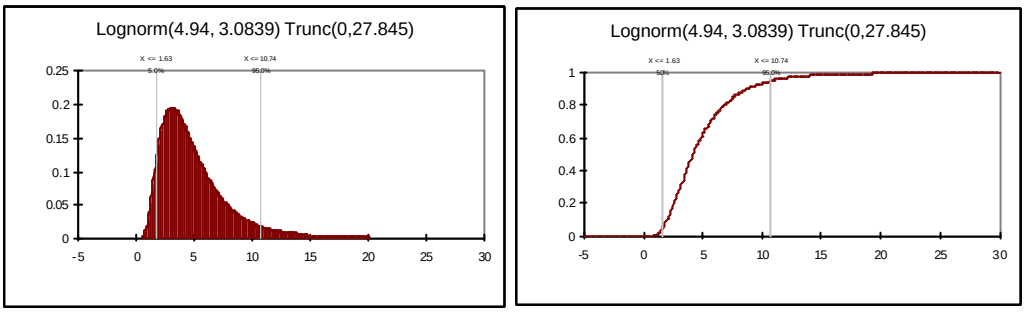

Figure 6.12 Matrix porosity distribution plots of Kbb-C Member

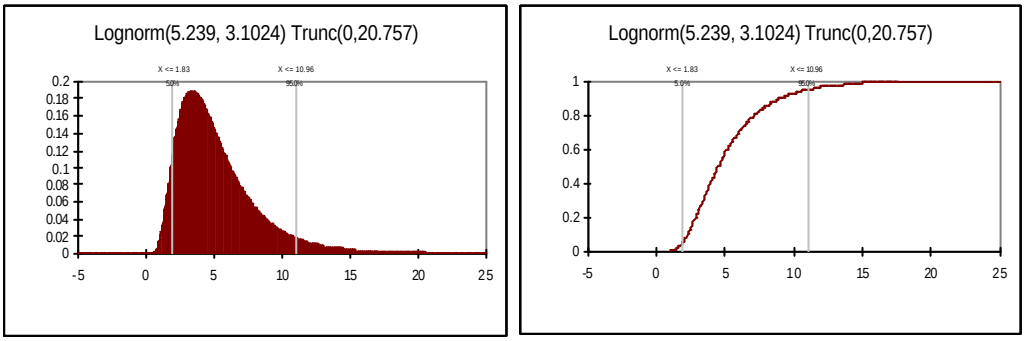

Figure 6.13 Matrix porosity distribution plots of Derdere Formation

6.1.3 Net Thickness

Net thickness will be the thickness of the reservoir formations that are having porosity greater than 0 % and water saturation less than 100 %. Since a stochastic approach is used, probability of the reservoir thickness will be calculated in this manner and no porosity cut-off value will be used to determine the reservoir thickness as it is generally applied in deterministic methods.

By sonic and density-neutron log measurements, thickness of the reservoir above zero porosity is taken for each well. Net thickness values are given in Tables A.3, A.4 and A.5. Frequency distribution plots of each formation are given in Figures 6.14, 6.15 and 6.16. Fitted net thickness probability distribution types and summary statistics of each formation are given in Table 6.3. After selecting the appropriate distribution types for the data sets, these distributions are given in simulation as input for reserves estimation.

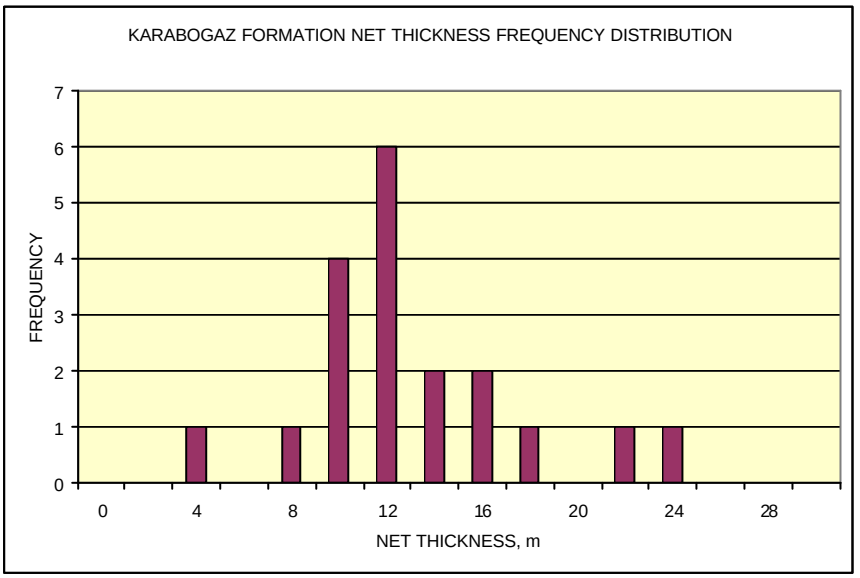

Figure 6.14 Histogram of Karabogaz Formation net thickness

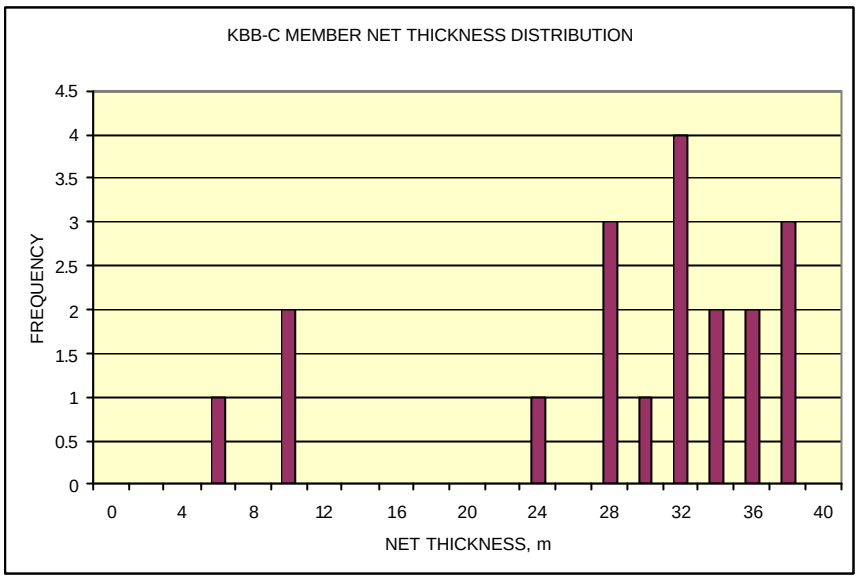

Figure 6.15 Histogram of Kbb-C Member net thickness

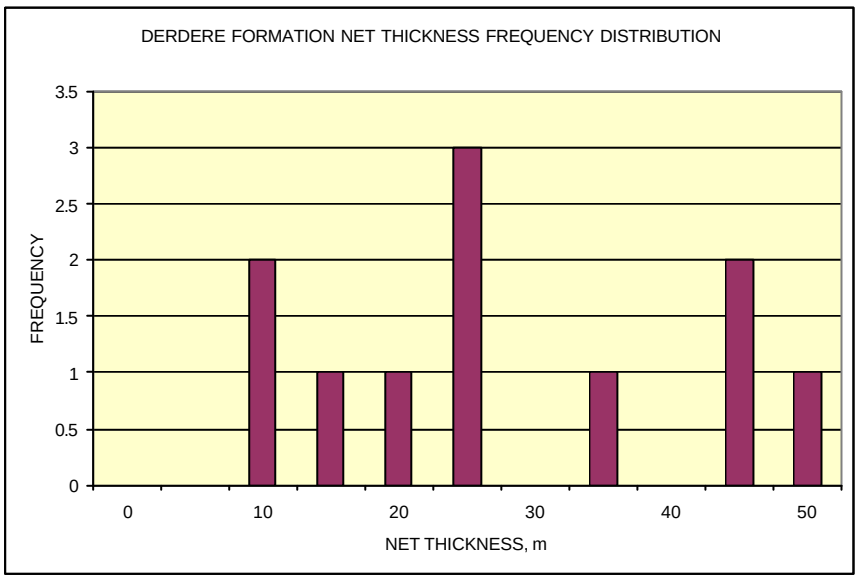

Figure 6.16 Histogram of Derdere Formation net thickness

Table 6.3 Probability distributions and summary statistics of net thickness

NET THICKNESS DISTRIBUTION FUNCTION OF PRODUCING FORMATIONS							
Formation	Statistical results						
H, m	Minimum	Maximum	Mean	Std Deviation	10% P	50% P	90% P
Karabogaz	1.347	25.254	12.295	4.969	5.904	11.934	19.244
Kbb-C	0.260	37.676	21.802	7.999	7.078	22.848	31.601
Derdere	5.282	49.589	26.860	9.288	14.548	26.492	39.711
Formation	Probability distribution function						
Karabogaz	RiskTriang(1.1049, 10.557, 25.273)						
Kbb-C	RiskTriang(0.10736, 27.777, 37.791)						
Derdere	RiskTriang(5, 25.34, 50)						

Probability density function and cumulative probability distribution of net thickness values of formations are given in Figures 6.17, 6.18 and 6.19. Statistical results of cumulative distribution function of net thickness values calculated by @Risk are given in Tables B.1, B.2 and B.3 for Karabogaz Formation, Kbb-C Member and Derdere Formation.

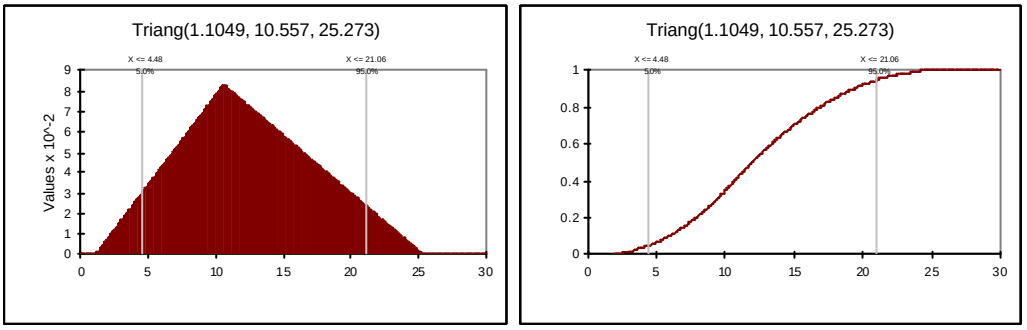

Figure 6.17 Net thickness distribution plots of Karabogaz Formation

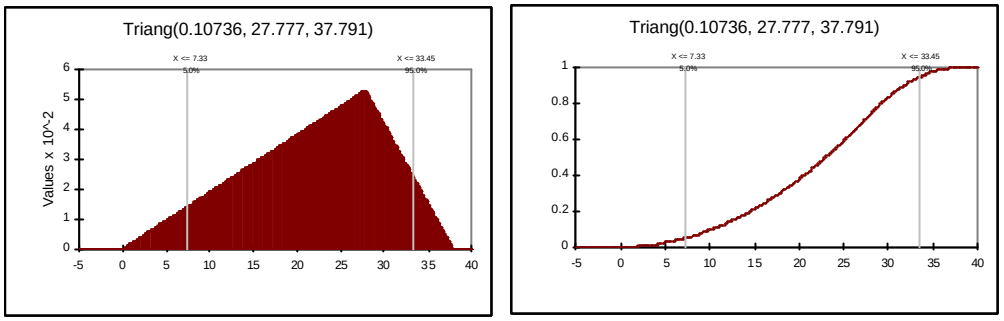

Figure 6.18 Net thickness distribution plots of Kbb-C Member

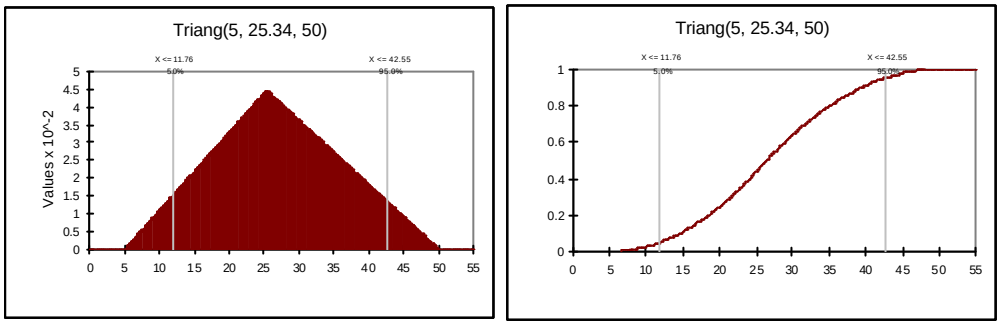

Figure 6.19 Net thickness distribution plots of Derdere Formation

6.1.4 Matrix Water Saturation

Water saturation measurements are done by interpreting resistivity log results. As a result of each log measurement in every 0.15 cm. a large sample pool is collected in each reservoir zone. Average values of initial water saturation below 100 % which are measured by logs are given in Appendix-A. Frequency distributions of initial matrix water saturation in reservoir zones are given in Figures 6.20, 6.21 and 6.22. Probability distribution types that are fitted by @Risk and resulting summary statistics of each formation's matrix water saturation data set are given in Table 6.4.

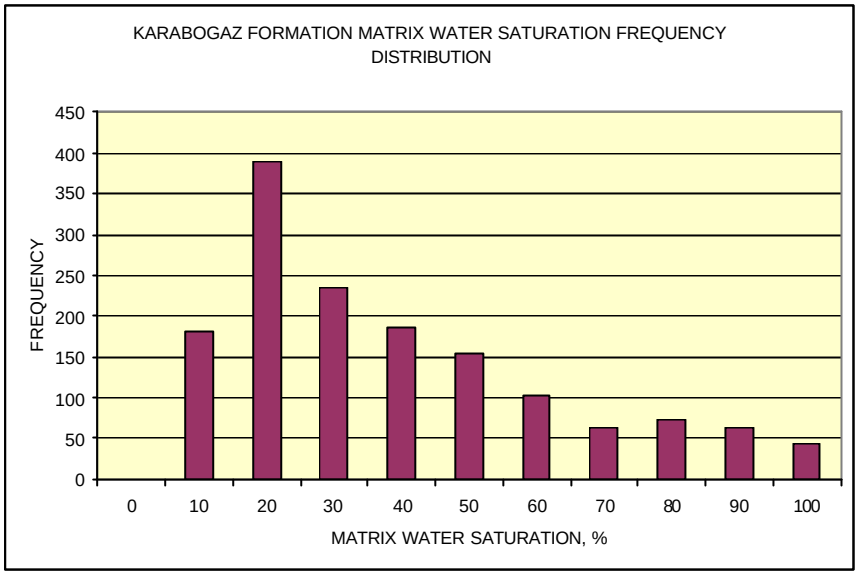

Figure 6.20 Histogram of Karabogaz Formation initial matrix water saturation

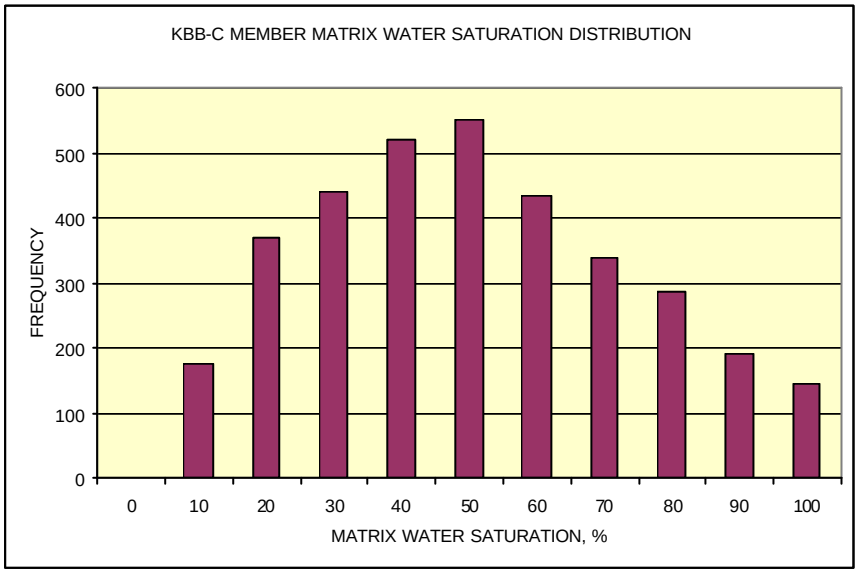

Figure 6.21 Histogram of Kbb-C Member initial matrix water saturation

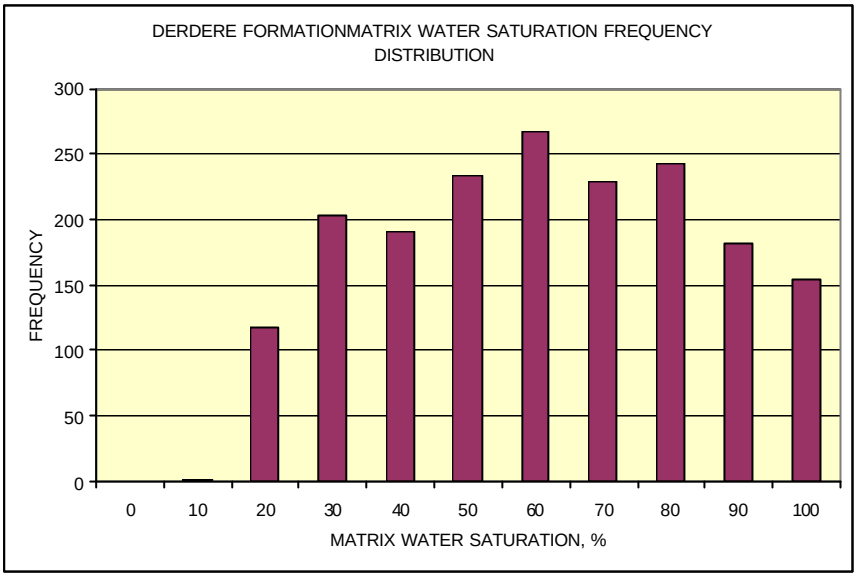

Figure 6.22 Histogram of Derdere Formation initial matrix water saturation

Table 6.4 Probability distributions and summary statistics of matrix residual water saturation

MATRIX INITIAL WATER SATURATION DISTRIBUTION FUNCTION OF PRODUCING FORMATIONS							
Formation	Statistical results						
S_{wi} , %	Minimum	Maximum	Mean	Std Deviation	10% P	50% P	90% P
Karabogaz	1.003	99.861	30.367	19.715	9.998	25.331	59.071
Kbb-C	35.454	56.972	45.736	2.754	42.205	45.746	49.233
Derdere	9.418	99.985	56.661	23.772	23.038	57.308	88.941
Formation	Probability distribution function						
Karabogaz	RiskLognorm(34.125, 29.032, RiskTruncate(0, 100))						
Kbb-C	RiskNormal(45.712, 23.758, RiskTruncate(0, 100))						
Derdere	RiskBetaGeneral(1.3776, 1.2748, 9.4096, 100.00)						

Probability density function and cumulative probability distribution of matrix initial water saturation values of formations are given in Figures 6.23, 6.24 and 6.25. Statistical results of cumulative distribution function of matrix initial water

saturation values calculated by @Risk are given in Tables B.1, B.2 and B.3 for Karabogaz Formation, Kbb-C Member and Derdere Formation.

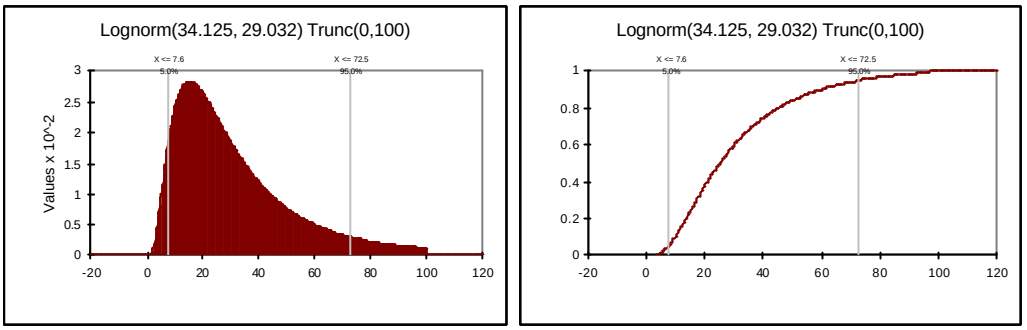

Figure 6.23 Matrix initial water saturation distribution plots of Karabogaz Formation

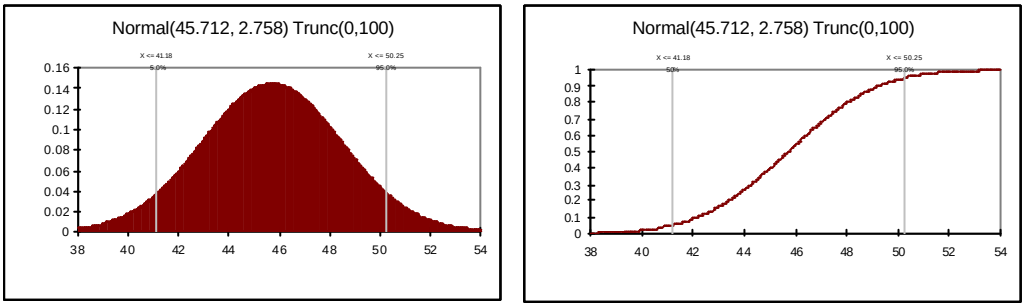

Figure 6.24 Matrix initial water saturation distribution plots of Kbb-C Member

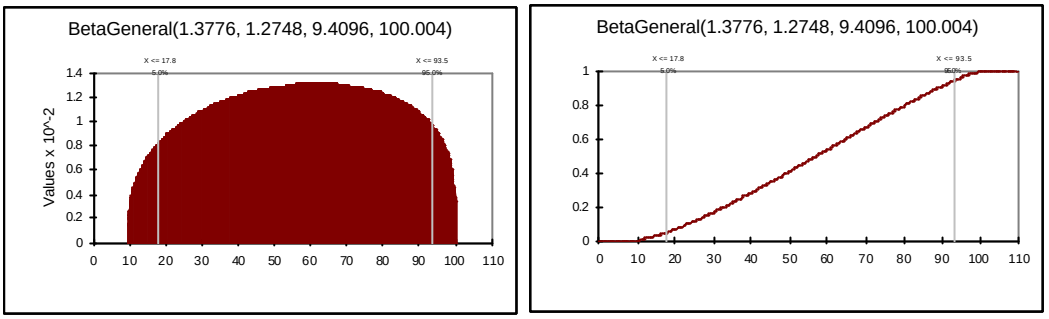

Figure 6.25 Matrix initial water saturation distribution plots of Derdere Formation

6.1.5 Fracture Porosity and Saturation

The tool that has the concept of measuring fracture density, width and distribution is simply the Fullbore Formation Microimager Logs (FMI). FMI logs are imaging tools of the wellbore and fracture parameters are obtained by interpretation of these logs with software programs. In Field-A, in four wells (W-10, 11, 13, 18) FMI logs were taken. W-10 and W-18 interpretation results are given as below [28] :

For Kbb-C Member:

- W-10 : fracture density, A_{fD} = 30 - 50 per meter
  fracture width, b = 0.3 - 1 mm
- W-18 : fracture density, A_{fD} = not given
  fracture width, b = 0.008 – 0.01 mm

For Derdere Formation:

- W-10 : fracture density, A_{fD} = 0 - 35 per meter
  fracture width, b = 0.3 - 1 mm
- W-18 : fracture density, A_{fD} = not given
  fracture width, b = 0.01 – 0.1 mm

Upon these results a range for fracture density and width can be given for these zones. Karabogaz Formation is considered to be having the same fracture properties with Kbb-C Member. Using Equation 2.38 and 2.41 the following equation is obtained:

$$Ø_f = b * A_{fD} \qquad 6.2$$

where, A_{fD} = fracture density, per mm.

b = fracture width, mm.

According to measured density and width of fractures probability distributions of these values are built. Probability distribution types of them for Karabogaz Formation, Kbb-C Member and Derdere Formation are given in Tables 6.5 and 6.6.

Table 6.5 Probability distributions and summary statistics of fracture density

FRACTURE DENSITY DISTRIBUTION FUNCTION OF PRODUCING FORMATIONS							
Formation	Statistical results						
A_{fD} ,1/mm	Minimum	Maximum	Mean	Std Deviation	10% P	50% P	90% P
Karabogaz and Kbb-C	0.030	0.050	0.040	0.004	0.034	0.040	0.046
Derdere	0	0.034	0.018	0.007	0.008	0.018	0.027
Formation	Probability distribution function						
Karabogaz and Kbb-C	RiskTriang(0.03, 0.04, 0.05)						
Derdere	RiskTriang(0, 0.018, 0.035)						

Table 6.6 Probability distributions and summary statistics of fracture width

FRACTURE WIDTH DISTRIBUTION FUNCTION OF PRODUCING FORMATIONS							
Formation	Statistical results						
b, mm	Minimum	Maximum	Mean	Std Deviation	10% P	50% P	90% P
Karabogaz and Kbb-C	0	1.000	0.273	0.231	0.034	0.240	0.620
Derdere	0	1.000	0.288	0.241	0.033	0.222	0.661
Formation	Probability distribution function						
Karabogaz and Kbb-C	RiskExpon(0.3215, RiskTruncate(0, 1))						
Derdere	RiskExpon(0.3425, RiskTruncate(0, 1))						

For Karabogaz Formation and Kbb-C Member probability density function and cumulative probability distribution plots are given in Figures 6.26 and 6.27, for They are given in Figures 6.28 and 6.29 for Derdere Formation. Statistical results of cumulative distribution function of fracture width and density values calculated by @Risk are given in Tables B.4 for Karabogaz Formation and Kbb-C Member and in Table B.6 for Derdere Formation.

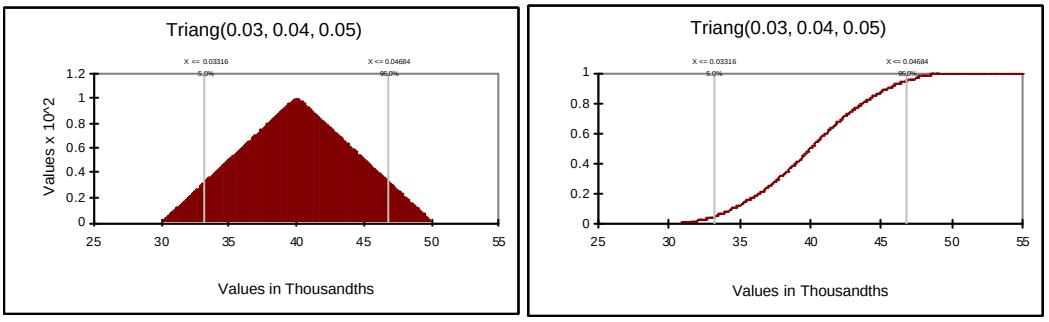

Figure 6.26 Fracture density distribution plots of Karabogaz Formation and Kbb-C Member

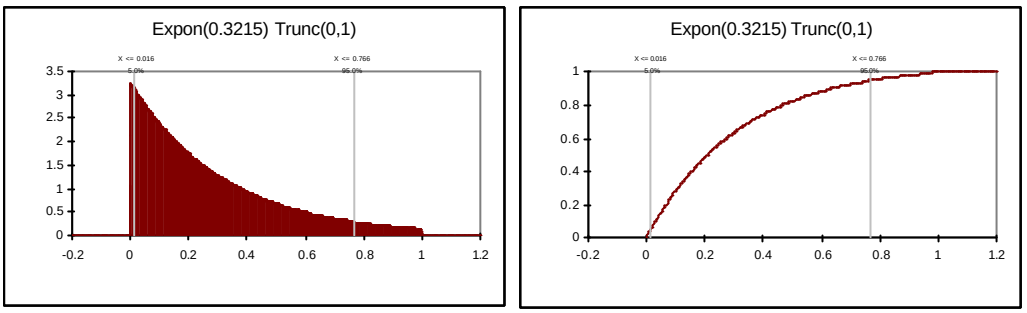

Figure 6.27 Fracture width distribution plots of Karabogaz Formation and Kbb-C Member

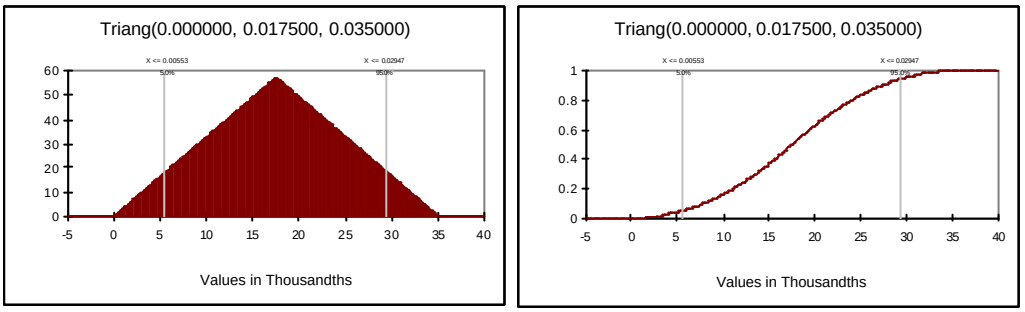

Figure 6.28 Fracture density distribution plots of Derdere Formation

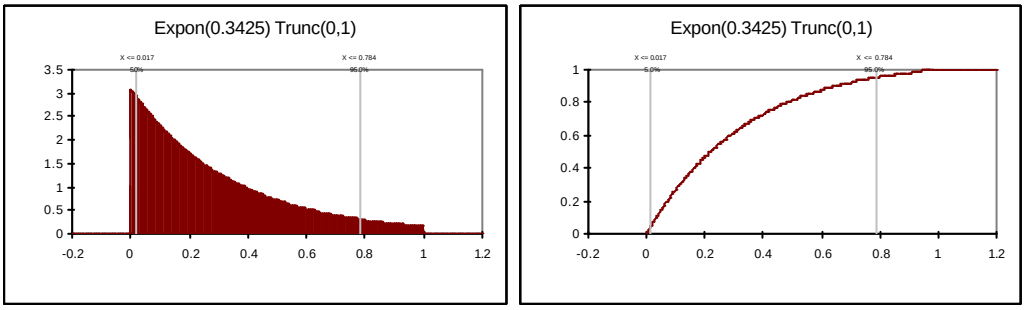

Figure 6.29 Fracture width distribution plots of Derdere Formation

Fracture density and width are independent variables of Equation 6.2 and the dependent variable which is fracture porosity is simulated by Monte Carlo method

to give the probability density function and cumulative distribution function. Resulting fracture porosity values and their ranges composed from 10000 calculations by Monte Carlo method

Table 6.7 Probability distributions and summary statistics of fracture porosity

FRACTURE POROSITY RESULTS BY MONTE CARLO SIMULATION							
Formation	Statistical results						
$Ø_f$, %	Minimum	Maximum	Mean	Std Deviation	10% P	50% P	90% P
Karabogaz and Kbb-C	0.045	1.986	0.670	0.470	0.105	0.588	1.364
Derdere	0.01	1.025	0.308	0.207	0.096	0.255	0.611

Results of the fracture porosity simulation are given as a histogram by 5 % frequency intervals of the fracture porosity range and cumulative probability distribution on Figure 6.30 for Karabogaz Formation and Kbb-C Member. Derdere Formation simulation results are given in Figure 6.31. Karabogaz and Kbb-C Member fracture porosity values are calculated up to 4.5 %. Since this value is incorrect as it is defined in literature (Section 2.3.2) the values above 2 % porosity which is given as the upper value for fissure network (it is even lesser for macrofractures), those values are discarded and the values in the range of 0-2 % porosity are given as a triangular distribution function for these zones. Fracture porosity of Derdere Formation has a lognormal probability distribution. Statistical results of cumulative distribution function of fracture porosity values simulated by Monte Carlo are given in Table B.4 for Karabogaz Formation and Kbb-C Member and in Table B.6 for Derdere Formation.

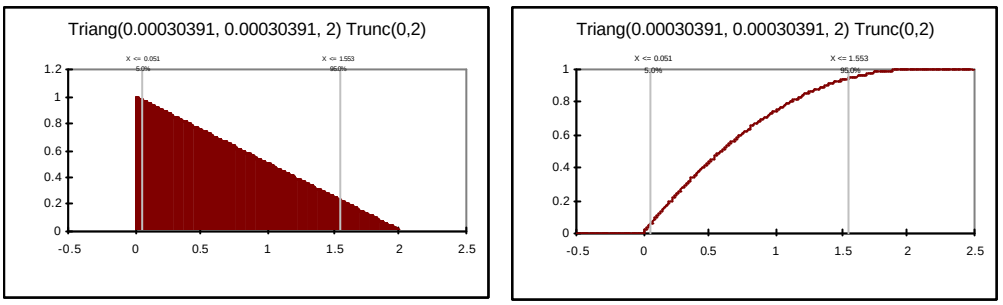

Figure 6.30 Fracture porosity distribution plots of Karabogaz Formation and Kbb-C Member

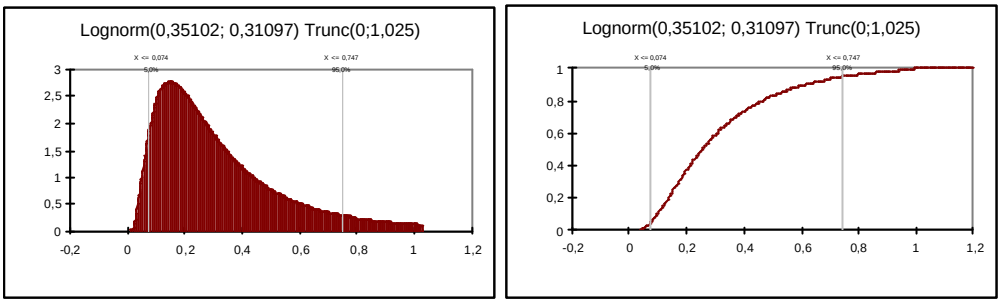

Figure 6.31 Fracture porosity distribution plots of Derdere Formation

In a fractured reservoir the two phase (oil-water) contact is sharp and horizontal in static and dynamic conditions since the transmissivity in a fractured network is high due to large permeability of fractures and any change in level is rapidly reequilibrated [20]. As a result, fractures in an oil zone will store oil and vice versa. Upon this issue fracture water saturation is taken as at most 1 % in the reservoir zones in this study. Sensitivity of initial water saturation of fracture network is very low on original oil in place calculations of fractures.

Naturally fractured reservoirs have unique characteristics in production depending on the storage and conductivity of fracture network. More detailed measurements

on fracture parameters decrease the level of uncertainty. In that case each production zone's production behavior can be modeled with more accuracy.

6.1.6 Fracture Porosity According to Production History

Because of their high permeability, fracture behavior can be noticed in production history of a well. Fractures affect production characteristics depending on their permeability, matrix-fracture interaction and water coning in a bottom water drive reservoir. Interpretation of oil production and water cut trends can give an idea on fracture porosity. It is known that in an oil zone fracture saturation is only oil and water saturation can be expected to be at most 1 %. On the contrary, matrix blocks which are separated by fractures are containing oil and residual water.

As the production begins, since the fractures have higher permeabilities than the matrix blocks the oil stored in them is produced first and since their storativity is low the amount of oil produced from the fractures will not be high comparing to the matrix reserves. Fractures often contribute most of the delivery capacity in a fractured reservoir [19]. After a fractured interval is perforated, the fractures cut by that perforation conducts the fluid (oil in oil zone and water in water zone) stored in them first and then the complicated phase of matrix feeding fractures begins.

This phase is effected by the porosity and permeability of the matrix, continuity of the fracture network, wettability of the reservoir rock and resulting drainage or imbibition displacement of the fluid in matrix pores, matrix block sizes between the fractures, matrix block shapes (Figure 2.13), reservoir pressure and aquifer influx rate etc. These phases can be seen on a production plot of a well, W-12, that produced from Derdere Formation at the beginning of production history (Figure 6.32). When the well is put on production, rate of production increases rapidly without water which contributes to the oil produced from fracture storage and when the matrix begins to feed the fractures water rate starts to increase.

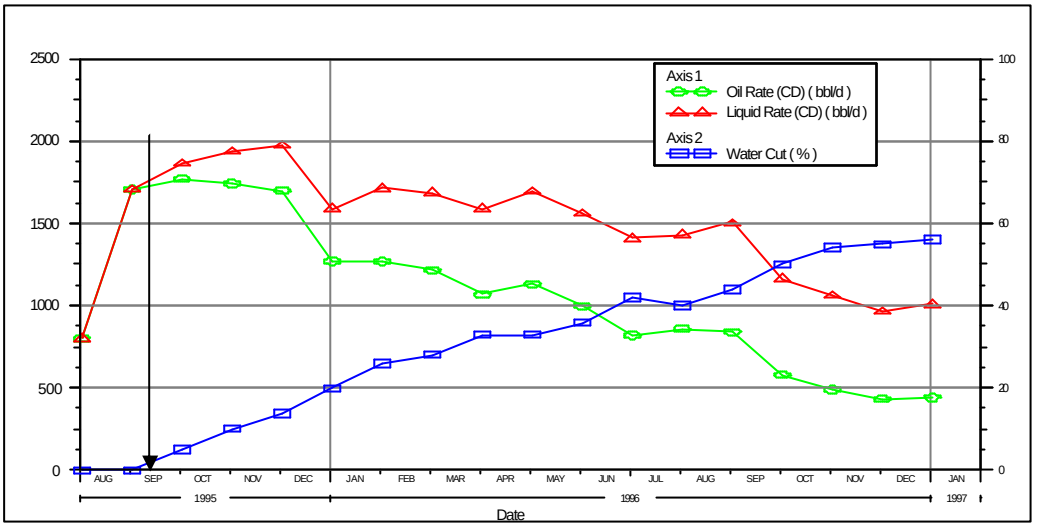

Figure 6.32 Production trend showing fracture behavior in W-12

Due to their high transmissibility aquifer water starts to increase rapidly in a fractured reservoir and after a certain period water begins to breakthrough resulting oil-water contact to increase. Heterogeneity in fracture network and matrix causes the oil-water contact to be at different levels throughout the field. If all the wells could be open to production at the same time from an uninvaded oil zone, the production behavior would be as oil produced without water initially, until the stored oil in the fractures are produced at the perforation levels and then the start of production of water and oil together that are reserved in the matrix blocks. Then aquifer water would breakthrough and water production would become higher. First wells drilled and put on production can show this trend but the wells that were put on production after water coning in the reservoir begin their production with a water cut since fractures would also be saturated with water in a water invaded zone.

When the production data of the field is checked it is seen that most of the wells are starting their production with a certain amount of water rate and it is hard to

separate the production behavior of the formations from each other since the production is commingled in most of the wells. The reason that water cut is seen at the beginning is that the Derdere Formation is invaded by water. In case of Karababa and Karabogaz Formation, production without water could be seen if they were put on to production without Derdere Formation. Only in one well (W-12) oil production from an uninvaded fracture could be seen for Derdere Formation. After Derdere Formation is totally invaded by water in some of the wells, invaded perforations are shut and Karababa and Karabogaz Formations continue their production. But until that time water coning occurs in the well and these formations also produce some amount of water.

In Field-A, Derdere Formation fracture production alone can not be seen. As it was explained in Chapter 3, Field-A is the continuing part of a structure consisting of three fields. The field at the north of Field-A was discovered and developed earlier than Field-A. By considering that both fields have the same reservoir and aquifer characteristics an analogy can be built. Analysis of the wells in this field which is named as Analogy (AN) in this text, suggests that production of fracture storage can be observed at the beginning of the production. This field has the same production formations but on the contrary of Field-A, these formations are not commingled generally.

An approach for collecting fracture porosity data is evaluated under the given conditions. First, to enrich the data set which would be meaningless when using only the Field-A data, both Field-A and Field-B data are collected. Via this data set, by checking the early oil production amount of the wells that were drilled at the beginning of the field history, fracture porosity values can be calculated by a simple volumetric approach. Drainage area in a naturally fractured reservoir is oriented along open fracture systems with significant areas included from nearby reservoir rock containing appreciable matrix porosity and permeability and intersected by the fracture system [19]. It is considered that fracture system has the same drainage area of the matrix since they are in interaction in recovery of

oil. Karabogaz Formation and Kbb-C Member of Karababa Formation have similar reservoir and production characteristics. Generally they are commingled in the wells. Because of the difficulty in creating separate data sets for each of them, they are considered to have similar fracture characteristics too.

For fracture porosity calculation of Karabogaz Formation and Kbb-C Member wells W-4, 11, 13, 26 and AN-6, 8, 16, 18, 29 are selected. For Derdere Formation fracture porosity calculations the selected wells are; W-12 and AN-9, 10, 14, 16, 17, 18, 20, 28. These wells' production graphics and decline curve analysis for the producing ones are given in Appendix-C. Fracture storage production amounts of the wells and their periods are given in Table 6.8. The proposed procedure to make an approach for evaluating fracture porosity using production data is given below:

1. Drainage areas of the wells are calculated by making the decline curve analysis of the wells. Ultimate recoveries of the wells are calculated by exponential decline.

2. Ultimate recovery amounts of each well are divided by their hydrocarbon pore thickness values and the drainage area is calculated. Hydrocarbon pore thickness (hcpt) is simply the hydrocarbon content a reservoir can store in a spot on the field. Hydrocarbon thicknesses are taken as the sum of net thicknesses of producing zones which are above 0 % porosity. These values for both fields are given in Table 6.8. Calculation of hcpt values is given below:

$$Hcpt = h*Ø_m*(1-S_{wim}) \qquad 6.3$$

where, h : net thickness value of the producing formations of each well, m

$Ø_m$: porosity of the matrix, fracture

S_{wim} : initial water saturation of the matrix, fracture

3. Dividing the producible oil amount of each well by their hcpt values gives the drainage area of the wells and so the drainage radius assuming cicular shapes. If no logging is present in a well, its drainage radius simply accepted as the interference radius of that well. Interference radius is the half of the average of the distances between wells. Maps of wells' drainage area are given in Figure 6.33 and Figure 6.34.

4. Accepting that the fracture system expands throughout the drainage area and oil produced without water as the perforations are opened is coming from the fracture system, dividing that amount of oil by the drainage area gives the fracture hcpt values.

5. Fracture hcpt values are different than the matrix hcpt values in terms of calculation of thickness. Before matrix-fracture interaction begins the fractures that are at the level of perforations produce first. So the thickness values will be the perforation thicknesses while calculating the fracture porosity by this procedure. Using these thickness values, 1 % water saturation as default and hcpt values, fracture porosities for each formation are calculated (Table 6.8). Equation of the procedure can be summarized as follows :

$\emptyset_f$ = fracture production / (drainage area * perforation interval) 6.4

Fracture porosities then can be generalized to the whole formation but the fracture parameters calculated in this way may contribute to less than or greater than the actual results for the upper zones and Derdere Formation. In Karabogaz Formation and Kbb-C Member the most fractured intervals that are detected in logs as sonic and density-neutron logs are perforated to enhance the production without permeability problems because of the low matrix quality and low formation pressure. But, since Derdere Formation is close to the water contact, large fractured intervals are not perforated in order to prevent early water breakthrough.

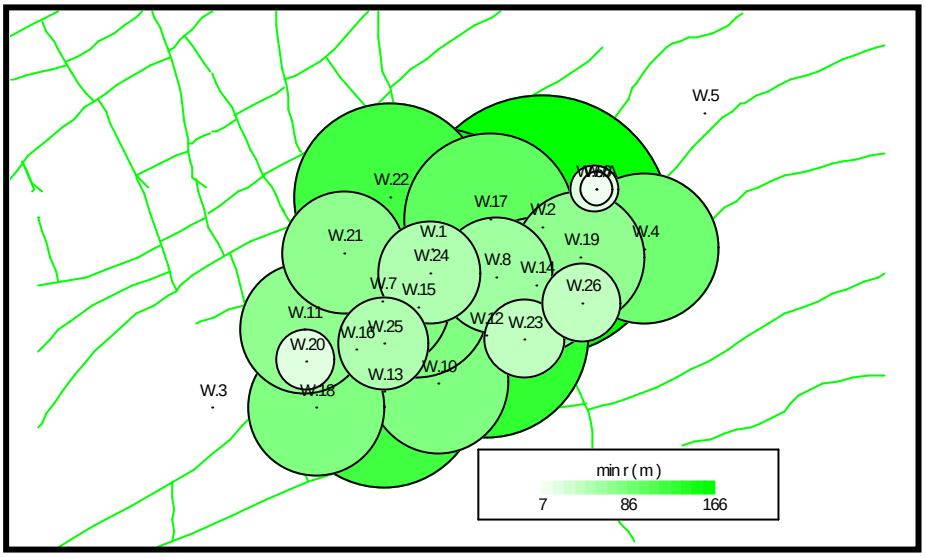

Figure 6.33 Drainage area of Field-A wells

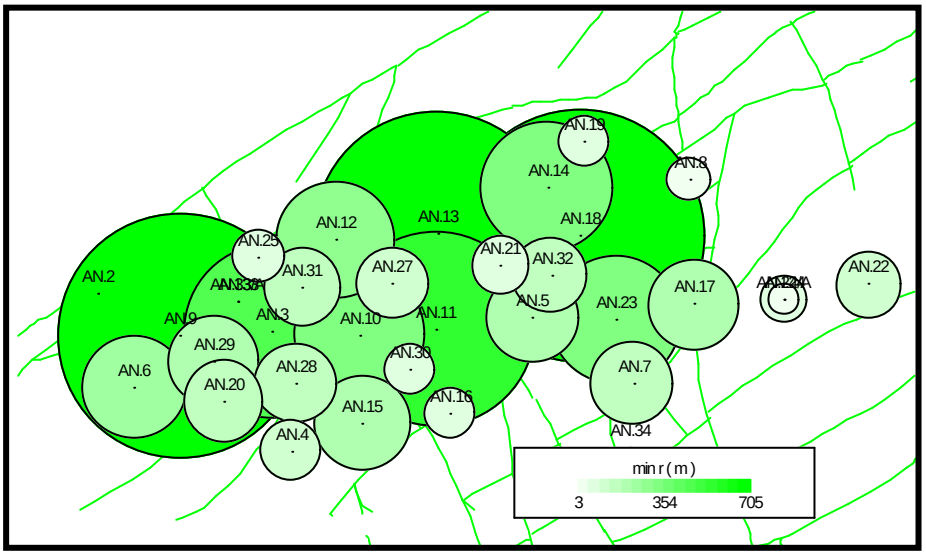

Figure 6.34 Drainage area of Analogy-1 wells

Table 6.8 Hcpt and drainage area values of wells

Well	Hcpt	Ultimate recovery, stb	Drainage area, m2	Fracture contribution		Perforation interval, m	$Ø_f$ %
				period, months	oil rec, stb		
W-4	3,80	990,889	45,607	8	107,359	36	1,16
W-11	1,76	549,601	54,617	2	20,911	34	0,20
W-13	5,25	2,374,340	79,145	3	154,970	34	1,02
W-26	3,95	391,241	17,324	2	6,951	43	0,16
AN-6	1,05	1,915,660	319,094	2	111,431	15	0,41
AN-8	0,83	51,523	10,857	6	27,096	17	2,59
AN-16	0,72	87,580	21,275	1	8,917	20	0,37
AN-18	0,03	1,020,540	5,949,748	28	312,448	25	0,04
AN-29*	-	1,586,780	149,225	18	250,961	25	1,19
W-12	6,80	2,988,690	76,871	2	75,990	31	0,56
AN-9	0,46	2,798,280	1,063,955	5	423,091	28	0,25
AN-10	2,31	4,822,130	365,104	3	400,866	32	0,61
AN-14	2,00	3,561,890	311,487	4	373,800	20	1,06
AN-17	2,44	2,454,310	175,926	4	80,364	22	0,37
AN-18	0,03	1,020,540	5,949,748	1	3,247	16	0,00
AN-20	2,91	1,504,740	90,440	1	1,487	7	0,04
AN-28	3,79	1,671,840	77,152	4	82,328	40	0,47
AN-32	2,78	1,231,230	77,461	3	49,906	32	0,36

*: Drainage area calculated by interference radius, log results are not available

After defining the fracture porosities by the proposed method given above, frequency distributions of them are plotted. Karabogaz Formation and Kbb-C Member fracture porosity distribution plots are given in Figure 6.35. Derdere Formation fracture porosity distribution plot is given in Figure 6.36. Probability distribution types fitted by @Risk and summary statistics of fracture porosities are given in Table 6.9.

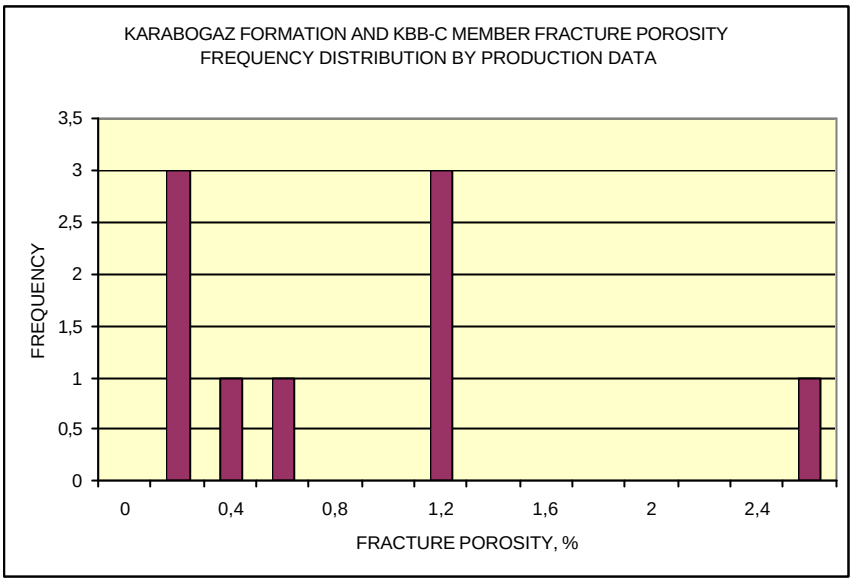

Figure 6.35 Histogram of Karabogaz Formation and Kbb-C Member fracture porosity obtained by production data

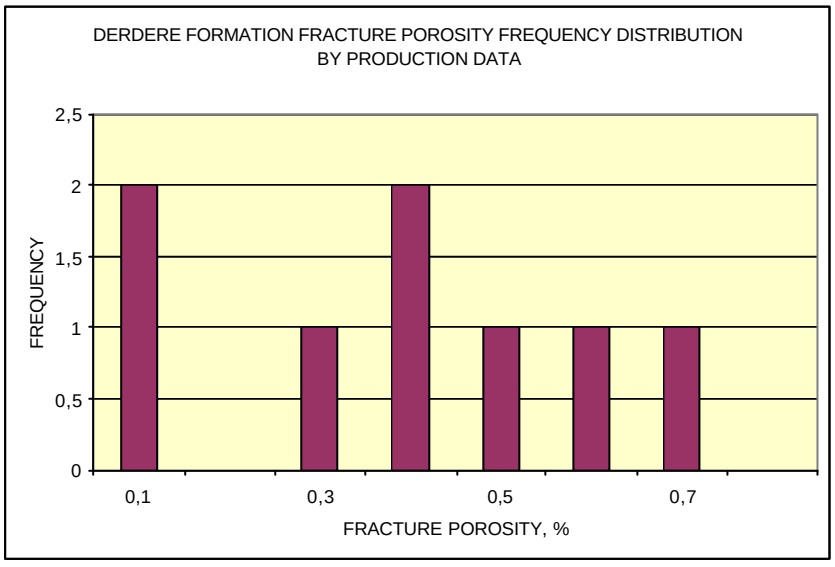

Figure 6.36 Histogram of Derdere Formation fracture porosity obtained by production data

Table 6.9 Probability distributions and summary statistics of fracture porosity obtained by production data.

FRACTURE POROSITY DISTRIBUTION FUNCTION OF PRODUCING FORMATIONS							
Formation	Probability distribution function						
$Ø_f$, %	Minimum	Maximum	Mean	Std Deviation	10% P	50% P	90% P
Karabogaz	0.037	2.571	0.895	0.603	0.168	0.797	1.787
Kbb-C	0.037	2.571	0.895	0.603	0.168	0.797	1.787
Derdere	0.000	1.241	0.414	0.292	0.068	0.365	0.848
Formation	Statistical results						
Karabogaz	RiskTriang(0.03711, 0.03711, 2.6)						
Kbb-C	RiskTriang(0.03711, 0.03711, 2.6)						
Derdere	RiskTriang(0,00060259; 0,00060259; 1,2511)						

Fracture porosities calculated by the proposed method, give results in the range of values defined by FMI interpretations. These values may be affected by technical accuracy of production measurements and log interpretations. These facts must be considered as creating uncertainty. By defining the distribution of the values an idea of fracture potential related to the production trend of a fractured reservoirs can be built but it also must be considered that preference to produce or not from a fractured zone is the main factor in defining the porosity distributions by production values.

6.2 Estimation of OOIP by Monte Carlo Simulation

Field-A original oil in place calculations by volumetric method using statistical technique is performed by Monte Carlo simulation. Variables in Equation 6.1 are evaluated according to their uncertainty by plotting their frequency distributions by the given data sets.

Each variable has its unique distribution function according to the range and mean of the data set. Types of their distributions, mean values, minimum and maximum values are fitted by @Risk software. Given a data set, this program fits the most

representative distribution functions to the data. According to the shape of frequency distribution and the quality of the data set best fitting probability function is selected. The only variables that are accepted constant are original oil formation volume factor (B_{oi}) and fracture water saturation which is at most 1 % in an oil zone. Uncertain variables for each reservoir zone in reserve calculation, their detailed statistical information, probability density function and cumulative distribution functions in graphics are given in Appendix-C.

Uncertain variables that had been attained a distribution function according to their data sets are given in Monte Carlo simulation as input variables and original oil in place (matrix + fracture) for each formation is calculated by 10 000 iterations, giving the all probable values of OOIP as output. Equation 6.4 is used for both matrix and fracture oil in place separately. Equation combining both reserves is as follows :

$$OOIP = A*h*\varnothing_m*(1-S_{mwi})/B_{oi} + A*h*\varnothing_f*(1-S_{fwi})/B_{oi} \qquad 6.4$$

where, A = a random number from the distribution function of the area

h = a random number from the distribution function of the net thickness

$\varnothing_m$ = a random number from the distribution function of the matrix porosity

S_{mwi} = a random number from the distribution function of the matrix initial water saturation

S_{fwi} = 1 % (fracture initial water saturation)

B_{oi} = 1.0921 rbbl/stb (initial oil formation volume factor)

Monte Carlo simulation for calculating OOIP is repeated for each reservoir zone. Matrix reserves of formations and their ranges are given in Table 6.10. Fracture reserves are given in Table 6.11.

Table 6.10 Monte Carlo simulation results of matrix reserves and summary statistics

MATRIX OOIP RESULTS BY MONTE CARLO SIMULATION							
Formation	Statistical results						
OOIP, Mbbl	Minimum	Maximum	Mean	Std Deviation	10% P	50% P	90% P
Karabogaz	20	96,975	13,643	9,920	3,790	11,246	26,452
Kbb-C	129	158,325	19,388	14,547	5,514	15,669	37,680
Derdere	0.975	152,527	15,097	15,009	2,322	10,597	33,176

Table 6.11 Monte Carlo simulation results of fracture reserves and summary statistics

FRACTURE OOIP RESULTS BY MONTE CARLO SIMULATION							
Formation	Statistical results						
OOIP, Mbbl	Minimum	Maximum	Mean	Std Deviation	10% P	50% P	90% P
Karabogaz	1.277	14,455	2.685	2.344	337	2,031	5,963
Kbb-C	2.447	21,683	4,768	4,001	586	3,726	10,646
Derdere	69	12,572	2,011	1,610	507	1,537	4.179

Monte Carlo simulation results showing probability density function and cumulative distribution function plots of each reservoir formation's matrix reserves are given in Figures 6.37, 6.38, 6.39, 6.40, 6.41 and 6.42. Same distribution plots for fracture reserves are given in Figures 6.43, 6.44, 6.45, 6.46, 6.47 and 6.48. Fitted type of probability density function of OOIP of matrix and fractures for each reservoir is log-normal. Detailed Monte Carlo simulation results for reserve estimation are given in Tables B.1, B.2, B.3, B.4, B.5 and B.6.

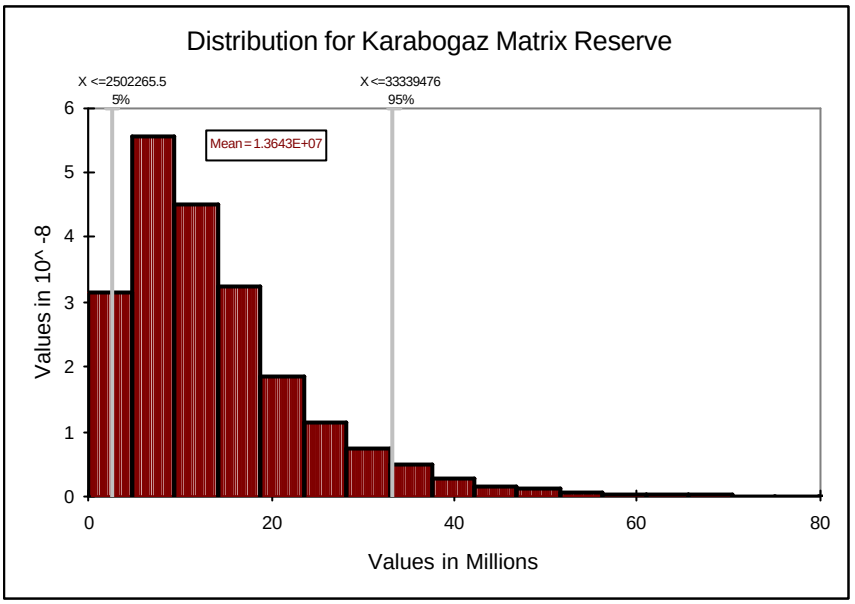

Figure 6.37 Probability density function of Karabogaz Formation matrix reserve (bbl)

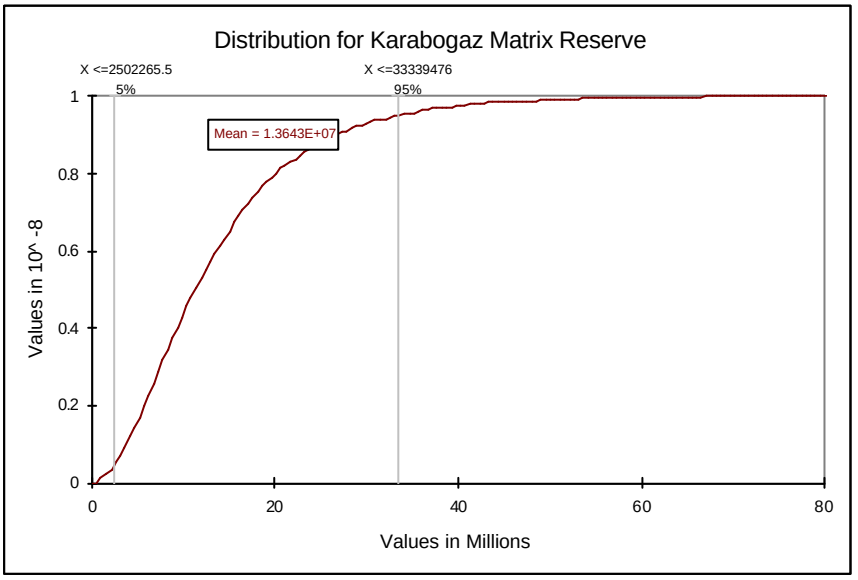

Figure 6.38 Cumulative distribution function of Karabogaz Formation matrix reserve (bbl)

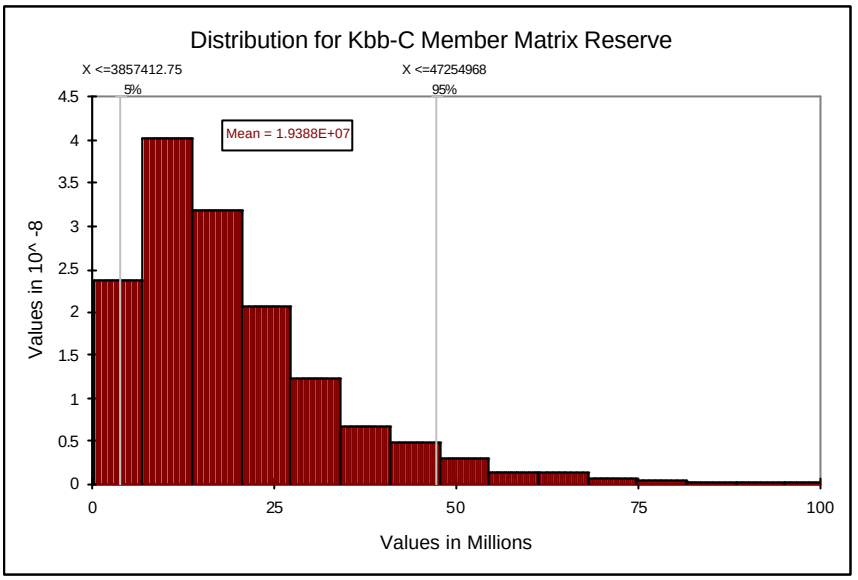

Figure 6.39 Probability density function of Kbb-C Member matrix reserve (bbl)

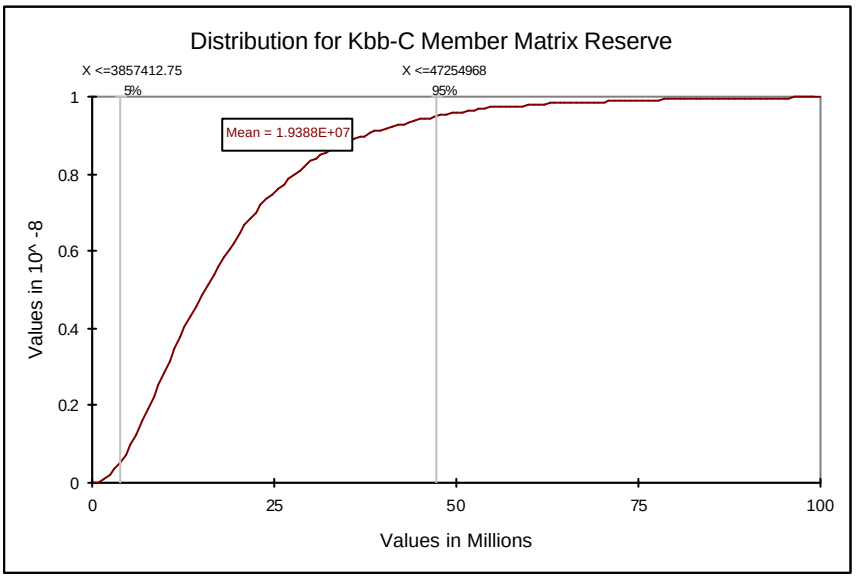

Figure 6.40 Cumulative distribution function of Kbb-C Member matrix reserve (bbl)

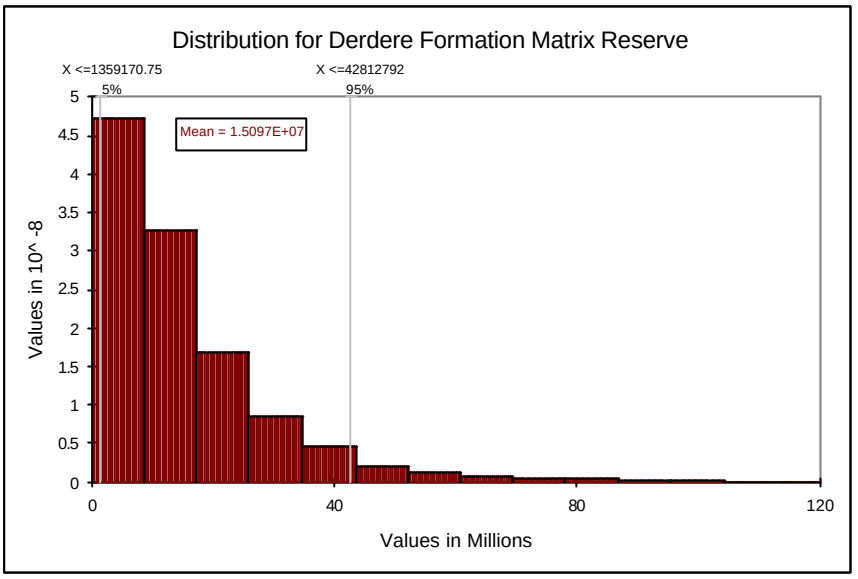

Figure 6.41 Probability density function of Derdere Formation matrix reserve (bbl)

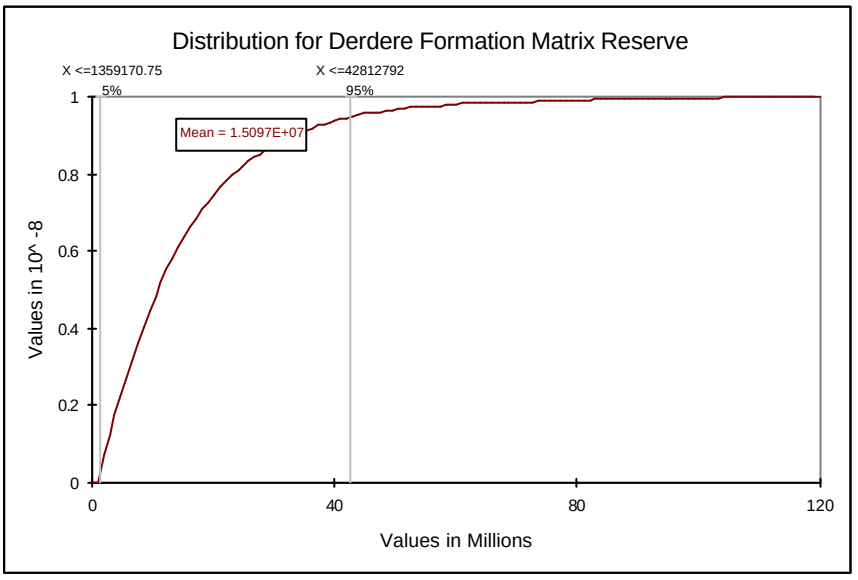

Figure 6.42 Cumulative distribution function of Derdere Formation matrix reserve (bbl)

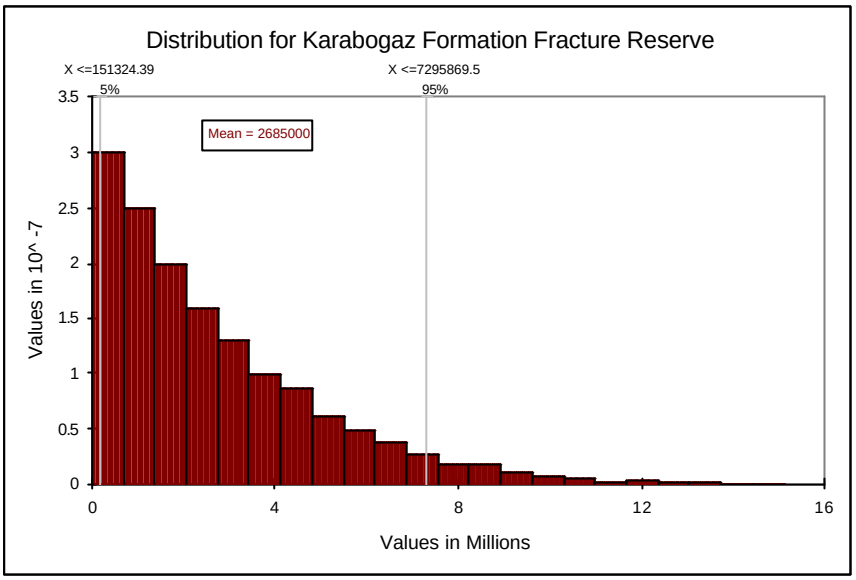

Figure 6.43 Probability density function of Karabogaz Formation fracture reserve (bbl)

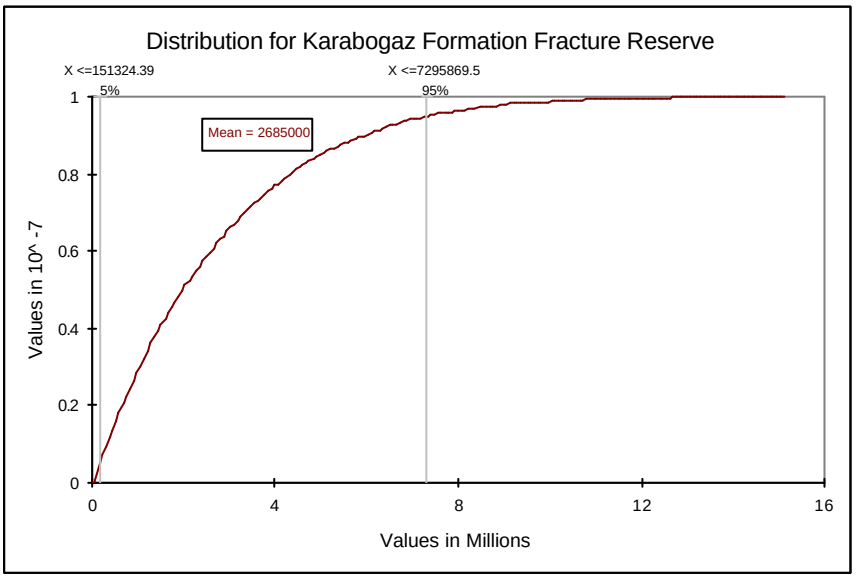

Figure 6.44 Cumulative distribution function of Karabogaz Formation fracture reserve (bbl)

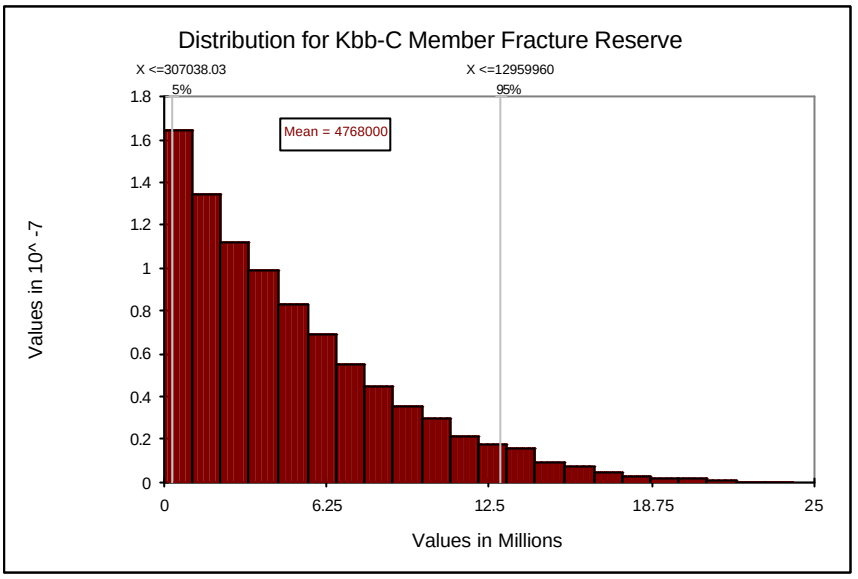

Figure 6.45 Probability density function of Kbb-C Member fracture reserve (bbl)

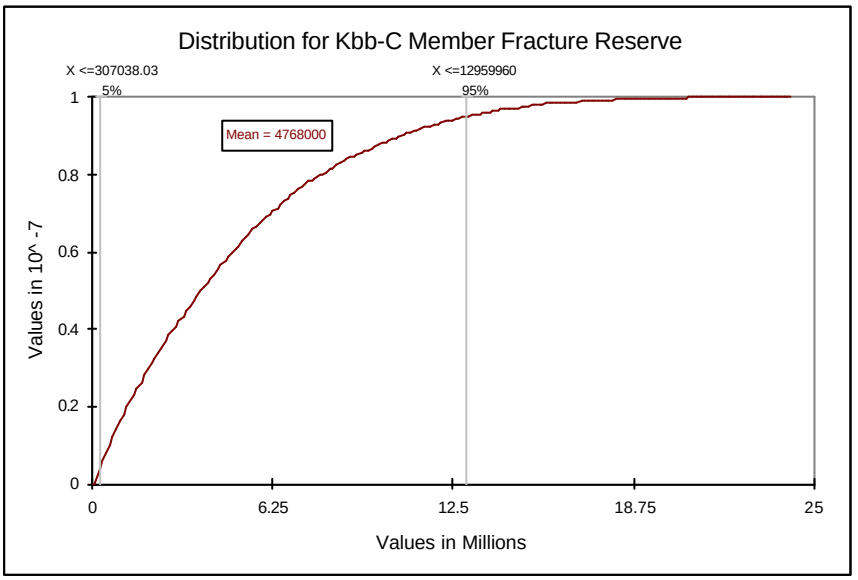

Figure 6.46 Cumulative distribution function of Kbb-C Member fracture reserve (bbl)

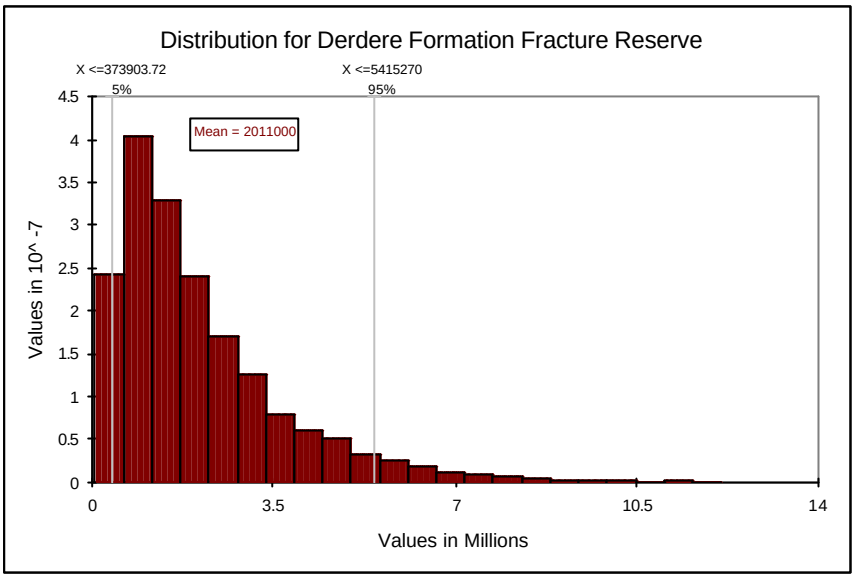

Figure 6.47 Probability density function of Derdere Formation fracture reserve (bbl)

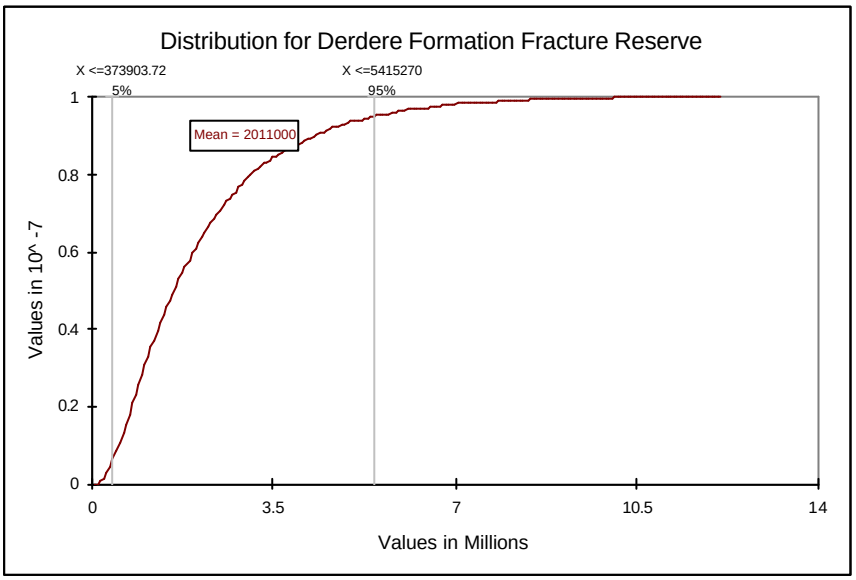

Figure 6.48 Cumulative distribution function of Derdere Formation fracture reserve (bbl)

Statistical results of cumulative distribution function of matrix reserve values simulated by Monte Carlo are given in Tables B.4, B.5 and B.6 for reservoir zones.

Results of Field-A reserve estimation performed by Turkish Oil Company are given in Table 6.12. Reserve calculations are done by deterministic method. Volumetric method is applied by using net thickness, water saturation and porosity maps on a chosen area for matrix reserve estimation [32]. Fracture reserves are estimated by using a single fracture porosity value for each formation according to the FMI interpretations [29]. Reserve estimation in the range of P10-P90 by probabilistic method can be compared by these values. Deterministic calculations are in these ranges and close to the mean of probabilistic distribution of reserves.

Table 6.12 TPAO reserve estimation for Field-A

FIELD-A RESERVE ESTIMATIONS (MMstb), deterministic method		
Formation	Matrix Reserve	Fracture Reserve
Karabogaz	8.7	1.4
Kbb-C	19.3	3.5
Derdere	19.1	5.3

Sensitivity analysis applied on the input variables of reserve estimations. Correlations among the input variables are shown by tornado diagrams. Diagram of Karabogaz Formation matrix reserve shows that matrix porosity and net thickness parameters are equally effecting the reserve estimation in this formation and they are the most significant input variables (Figure 6.49). In Kbb-C Member matrix reserve estimation, matrix porosity is the most significant parameter in reserve volume, and then comes the thickness parameter (Figure 6.50). But, for Derdere Formation matrix reserve estimation, the most influencing parameter is the matrix initial water saturation (Figure 6.51). Since oil-water contact is in Derdere Formation and matrix pores are invaded by the water, oil in place amount

is highly affected by water saturation values. This fact also affects the production trend and recovery of oil from Derdere Formation.

Fracture reserve estimations for these three zones are all affected by most the fracture porosity parameter (Figures 6.52, 6.53 and 6.54). Fracture porosity is a factor of fracture density and width. A network of well connected fracture system in an oil zone increases the storativity of fractures.

Area being the most insignificant parameter in both matrix and fracture reserve estimation may imply that this value is not distributed in a large range as the other parameters have. Uncertainty is less in the area value according to the other parameters because the reserve calculation is not done for probable reserves. A larger area distribution may be chosen for possible reserves beyond the Field-A's drilled, tested and mapped area.

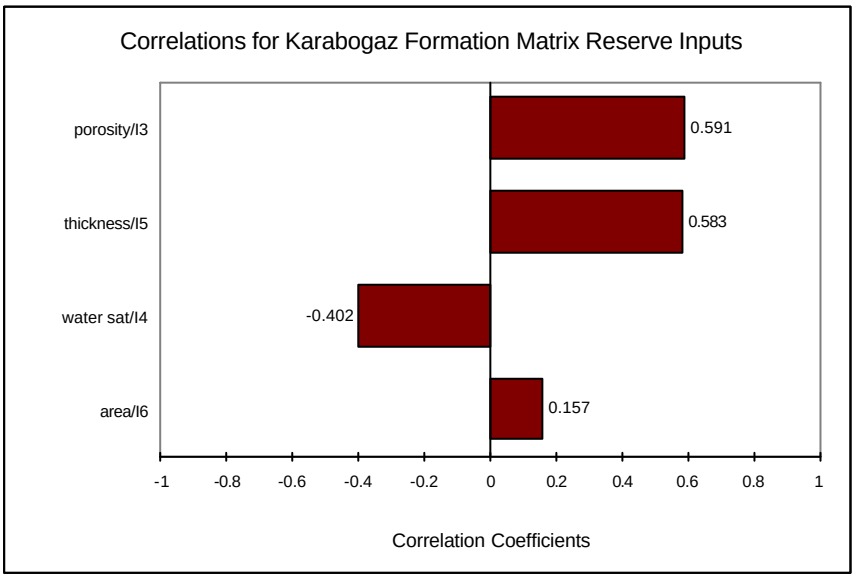

Figure 6.49 Effect of input variables on Karabogaz Formation matrix reserve

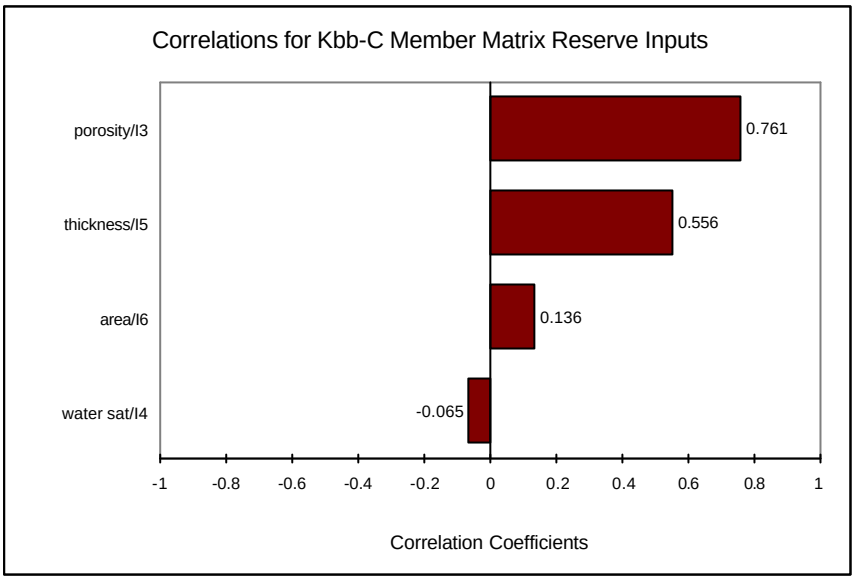

Figure 6.50 Effect of input variables on Kbb-C Member matrix reserve

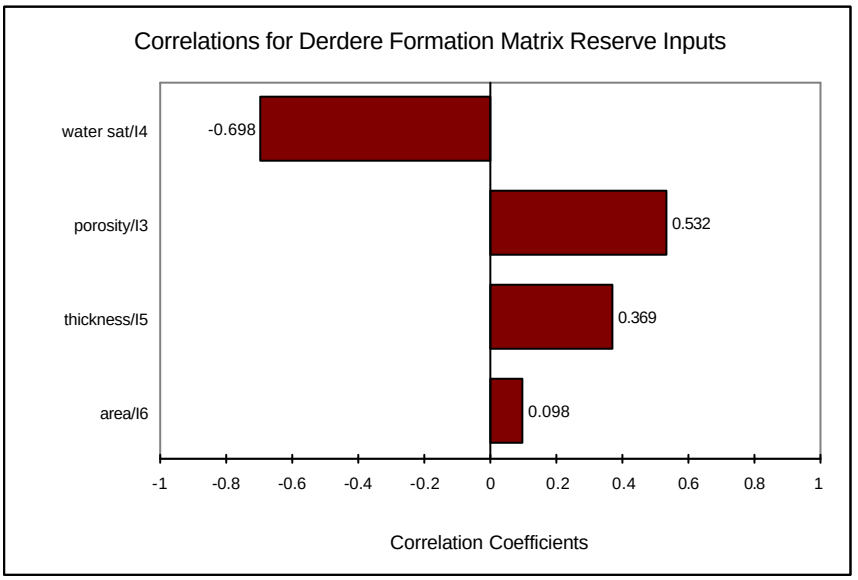

Figure 6.51 Effect of input variables on Derdere Formation matrix reserve

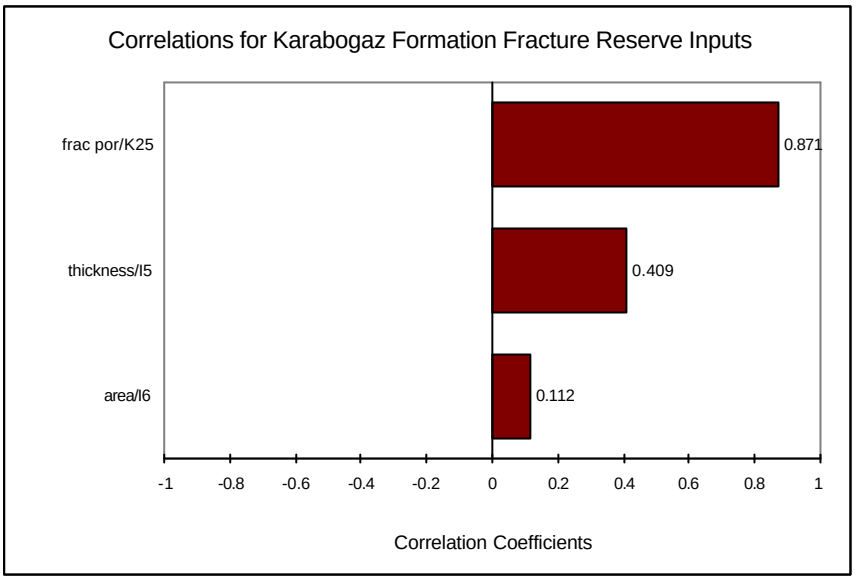

Figure 6.52 Effect of input variables on Karabogaz Formation fracture reserve

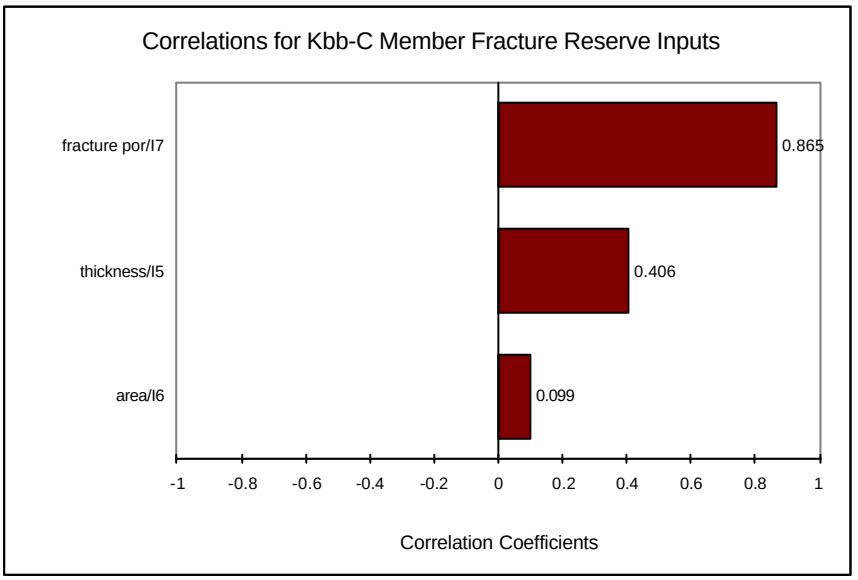

Figure 6.53 Effect of input variables on Kbb-C Member fracture reserve

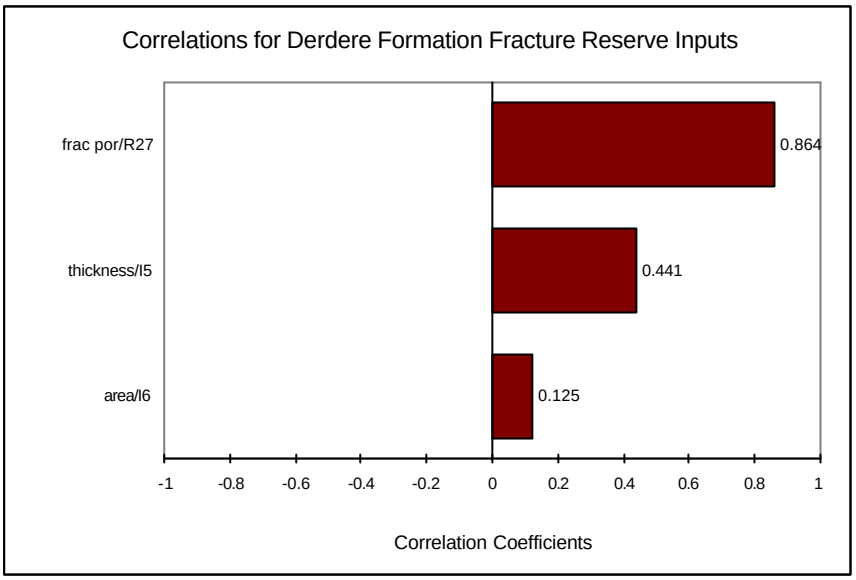

Figure 6.54 Effect of input variables on Derdere Formation fracture reserve

CHAPTER 6

CONCLUSIONS

Naturally fractured reservoirs are extremely heterogeneous due to phases of fracturing as a result of several stress mechanisms taking place in the rock. They are technically not easy to measure but can be modeled by fractures layering between matrix blocks by assuming certain block shapes and fracture network. Assumptions are build on fracture density and width measurements but indirect methods of measurement, lack of detailed data and technical shortcomings lead to uncertainty in their distribution of true values over the field. Defining fracture network's storativity and conductivity is important in optimal production from a reservoir. The following conclusions can be drawn from the results of the current study.

1. Fracture porosity values are in the range of 0-2 %. Fracture porosites calculated by production values support these values also. The mean value of the fracture porosities for Karabogaz Formation and Kbb-C Member is 0.6 while it is 0.3 for Derdere Formation.

2. According to the cumulative distribution function designed for Field-A reserves, P50 reserve estimations are 11.2 MMstb in matrix and 2.0 MMstb in fracture of Karabogaz Formation, 15.7 MMstb in matrix and 3.7 MMstb in fracture of Kbb-C Member and 10.6 MMstb in matrix and 1.6 MMstb in fracture of Derdere Formation. Fracture reserves are 15 % of total reserve in Karabogaz Formation, 19 % in Kbb-C Member and 13 % in Derdere Formation.

3. Sensitivity analysis results on matrix parameters show that for Karabogaz Formation and Kbb-C Member most effective parameters in reserve estimation are matrix porosity and net thickness. Net thickness is related to porosity development in a zone but porosity being more significant than the net thickness

in Kbb-C Member shows that porosity development in this zone is better than Karabogaz Formation. In Derdere Formation most effective parameter is initial water saturation showing that having a large distribution of water saturation values, this zone is invaded by water differently throughout the field. Knowing that water-oil contact varies over naturally fractured reservoirs because of fracture systems differing conductivity and interaction with the matrix, variations in water saturation must be carefully interpreted and modeled as the simulation result tells.

CHAPTER 7

RECOMMANDATIONS

Oil in place estimations have uncertainty depending on the size and quality of reservoir parameters. As the sample pool is enriched inferring the the true population becomes more accurate. For this reason calculations of reserve amount are most certain in later life of a field. To be more certain in estimations in an earlier time, gathered data from a field must be carefully interpreted and understood. As a result following recommendations are proposed:

1. In fields like Field-A which are heterogenous and fractured, data must be collected on the fracture parameters throughout the field so that the areal distribution and true range of these parameters can be used in defining fracture porosity and provide an optimal production. Simulation studies can be performed best by rich and correct data.

2. Probabilistic reserve estimation gives the benefit to see the whole picture regarding the reservoir parameters and their ranges by inferring from a measured data set. But interpreting these values and choosing the appropriate statistical functions for them are important in making a valuable analysis. For this reason data must be analysed by both from a reservoir and statistical point of view.

REFERENCES

1) Etherington, John R., “Can you have Probable Without Proved Reserves”, SPE 90241, presented at the SPE Annual Technical Conference and Exhibition in Houston, Texas, September 26-29, 2004.

2) “Petroleum Resources Classification and Definitions”, approved by SPE, WPC, and AAPG, published by SPE, February 2000.

3) Ross, J. G., “The Philosophy of Reserve Estimation”, SPE 37960, presented at the SPE Hydrocarbon Economics and Evaluation Symposium in Dallas, Texas, March 16-18, 1998.

4) “Determination of Oil and Gas Reserves”, The Petroleum Society of the Canadian Institute of Mining, Metallurgy and Petroleum Monograph 1, ISBN 0-9697990-0-4, 1994.

5) “Petroleum Reserves Definitions”, approved by SPE and WPC, published by SPE, March 1997.

6) Forrest, A. Garb, “Oil and Gas Reserves Classification, Estimation, and Evaluation”, JPT, March 1985.

7) Newendorp, Paul D., and Schuyler, John R., “Decision Analysis for Petroleum Exploration”, Planning Press^{TM}, Aurora, USA, 248-283, 2000.

8) Schuyler, J.R., “Probabilistic Reserves Lead to More Accurate Assessments”, SPE 49032, presented at the SPE Annual Technical Conference and Exhibition in New Orleans, Louisiana, September 27-30, 1998.

9) Capen, E.C., “Probabilistic Reserves! Here at Last?”, SPE 73828, presented at the SPE Hydrocarbon Economics and Evaluation Symposium in Dallas, March 20-23, 1999.

10) Murtha, James A., “Using Pseudocases to Interpret P10 for Reserves, NPV, and Production Forecasts”, SPE 71789, presented at the SPE Hydrocarbon Economics and Evaluation Symposium in Dallas, Texas, April 2-3, 2001.

11) Macary, S.M., Hassan, A., “Better Understanding of Reservoir Statistics is the Key for Reliable Monte Carlo Simulation”, SPE 53624, presented at the 1999 SPE Middle East Oil Show in Bahreyn, February 20-23, 1999.

12) Fylling, A., “Quantification of Petrophysical Uncertainty and Its Effect on In-Place Volume Estimates: Numerous Challenges and Some Solutions”, SPE 77637, presented at the SPE Annual Technical Conference and Exhibition in San Antonio, Texas, September 29-October 2, 2002.

13) Mendenhall, W., and Sincich, T., “A Second Course in Statistics, Regression Analysis”, Prentice-Hall Inc, New Jersey, 2-34, 1996.

14) “Statistics and Probability”, Rike Service Inc. course manual, New Orleans, Louisiana, 1990.

15) Nist, Sematech, www.itl.nist.gov/div898/handbook/index.htm, November 2004.

16) Brighton Webs Ltd., http://www.brighton-webs.co.uk/, November 2004.

17) Walstrom, J.E., Mueller, T.D., McFarlane, R.C., “Evaluating Uncertainty in Engineering Calculations”, JPT, December 1967.

18) Briggs, Arthur R., “Reserve Estimates for Naturally Fractured Reservoirs”, SPE 71037, presented at the SPE Rocky Mountain Petroleum Technology Conference, Keystone, Colorado, May 21-23, 2001.

19) Hensel Jr., W.M., “A Perspective Look at Fracture Porosity”, SPE 16806, presented at the 62nd Annual Technical Conference and Exhibition of the Society of the Petroleum Engineers in Dallas, Texas, September 27-30, 1987.

20) Van Golf-Racht, T.D., “Fundamentals of Fractured Reservoir Engineering”, Elsevier Scientific Publishing Co., New York, 55-180, 1982.

21) Dijk, Janpieter V., “Analysis and Modeling of Fractured Reservoirs”, SPE 50570, presented at the 1998 SPE European Petroleum Conference in Hagua, Netherlands. October 20-22, 1998.

22) Weber, Koenraad Johan, “Fracture and Vuggy Porosity”, SPE 10332, presented at the 56th Annual Fall Technical Conference and Exhibition of SPE of AIME, in San Antonio, Texas, October 5-7, 1981.

23) Aguilera, Roberto, “Naturally Fractured Reservoirs”, PennWell Publishing Co., Tulsa, Oklahoma, 19-25, 1980.

24) Pittman, Edward D., “Porosity, Diagenesis and Productive Capability of Sandstone Reservoirs”, SEPM Special Publication No. 26, 159-173 March 1979.

25) Redwine, Lowell, “Hypothesis Combining Dilation, Natural Hydraulic Fracturing, and Dolomitization to Explain Petroleum Reservoirs in Monterey Shale, Santa Maria Area, California”, The Monterey Formation and Related Siliceous Rocks of California, Society of Economic Paleontologists and Mineralogists, 221-248.

26) Karakeçe, Yildiz, “Temel Log Yorumu ve Rezervuar Mühendisliginde Kullanimi”, Üretim Grubu Baskanligi, TPAO, 1995.

27) Desbrandes, Robert, “Encyclopedia of Well Logging”, Editions Technip, Paris, 182-248, 1985.

28) Sayili, A., Ulu, M., Naz, H., “XII. Bölge Güney Karakus Sahasi Karabogaz Formasyonu ve Mardin Grubu Karbonatlarinin Rezervuar Degerlendirmesi”, Arastirma Merkezi Grubu Baskanligi Litostratigrafi Müdürlügü, TPAO, 1996.

29) Çobanoglu, M., Karakeçe, Y., “G.Karakus Sahasi Degerlendirme Çalismasi”, Üretim Grubu Baskanligi, TPAO, 1998.

30) Smith, Charles R., Tracy, G.W., Farrar, R.Lance, “Applied Reservoir Engineering”, OGCI Publications, Oil and Gas Consultants International Inc., Tulsa, Volume 2, 1992.

31) Scientific Software-Intercomp, Petroleum WorkBench, Reservoir Description, 1995.

32) Schlumberger, “Karakus Field RAPID Field Evaluation Study”, July 2004.

APPENDIX A

PRODUCTION INTERVALS AND FIELD

ROCK AND FLUID ANALYSIS DATA

Table A.1 Production Intervals of Field-A Wells

Well No	Production Interval, m	Formation
1	2609-2626	DERDERE
2	2340-2357	KARABOGAZ + KBB-C
	2467-2497	DERDERE
3	2507-2550	KBB-C
4	2341-2357	KARABOGAZ + KBB-C
	2367-2382	KBB-C
	2399-2405	KBB-C
5	2345-2352	KBB-C
	2360-2375	KBB-C
6	2323-2335	KBB-B+KBB-C
	2345-2360	KBB-C
7	2411-2430	S.DERE
	2485-2498	KARABOGAZ
	2506-2522	KBB-C
	2610-2623	DERDERE
8	2320-2335	KARABOGAZ
	2342-2359	KBB-C
	2455-2480	DERDERE
9	NOT DRILLED	
10	2388-2397	S.DERE
	2422-2440	KARABOGAZ
	2448-2466	KARABOGAZ + KBB-C
	2481-2489	KBB-C
	2512-2520	KBB-B
	2573-2598	DERDERE
11	2466-2477	S.DERE
	2536-2549	KARABOGAZ
	2557-2575	KBB-C
	2595-2628	KBB-B
12	2307-2320	KARABOGAZ
	2333-2352	KBB-C
	2349-2470	KBB-A + DERDERE

Table A.1 Production Intervals of Field-A Wells (continued)

Well No	Production Interval, m	Formation
13	2420-2430	KBB-C
	2439-2457	KBB-C
	2477-2483	KBB-B
	2535-2569	DERDERE
14	2286-2301	KARABOGAZ
	2463-2475	DERDERE
15	2580-2594	KBB-B
	2617-2625	KBB-B
	2674-2684	DERDERE
16	2411-2426	KARABOGAZ
	2431-2439	KARABOGAZ
	2455-2475	KBB-C + KBB-B
	2535-2550	DERDERE
	2562-2578	DERDERE
17	2504-2506	DERDERE
18	2447-2464	KARABOGAZ
	2477-2500	KARABOGAZ + KBB-C
	2521-2528	KBB-C
	2546-2565	KBB-B
	2607-2615	DERDERE
19	2281-2293	KBB-C
	2410-2435	DERDERE
20	2470-2480	S.DERE
	2490-2500	S.DERE
	2538-2550	KARABOGAZ
	2555-2572	KARABOGAZ + KBB-C
21	2413-2435	S.DERE
	2443-2455	S.DERE
	2490-2500	KARABOGAZ
	2508-2525	KBB-C
	2593-2612	DERDERE
22	2393-2413	KARABOGAZ
	2443-2460	KBB-C
	2474-2485	KBB-B
	2535-2554	DERDERE
23	2536-2549	KARABOGAZ
	2557-2575	KBB-C
	2595-2628	KBB-B
24	2650-2671	DERDERE
25	2540-2586	DERDERE
26	2320-2343	KBB-C
	2350-2370	KBB-C

Table A.2 Core Analysis Results of Field-A

Well No	**1**		**2**		**3**		**4**		**5**		**6**		**7**		**10**		**11**	
	$Ø_m$	K_m	$Ø_m$	K_m	$Ø_m$	K_m	$Ø_m$	K_m	$Ø_m$	K_m	$Ø_m$	K_m	$Ø_m$	K_m	$Ø_m$	K_m	$Ø_m$	K_m
Formation	(%)	(md)	(%)	(md)	(%)	(md)	(%)	(md)	(%)	(md)	(%)	(md)	(%)	(md)	(%)	(md)	(%)	(md)
Karabogaz	2.1	0.04													7.54	0.06	0.56	0.03
	1.51	0.05													2.73	0.03		
	7.54	0.06													1.47	0.03		
	2.73	0.03																
	1.47	0.03																
	7.54	0.06																
	2.73	0.03																
	1.47	0.03																
Kbb-C					1.83	0.04	1.01	0.03	12	0.13	2.97	0.06	3.37	0.09			4.74	0.44
					2.95	0.1			12.2	0.29	4.1	0.05	3.55	0.1			0.78	0.03
									5.16	0.05	1.84	0.06	2.34	0.03				
									4.37	0.05			0.93	0.03				
									6.07	0.08								
									4.83	0.24								
									5.58	0.06								
Derdere	10.1	0.62	12	9.72														

Table A.3 Average Log Results of Karabogaz Formation

Well No	Top of formation, m	$Ø_m$, %	S_{mw},%	V_{shale}, %	Net thickness, m
1	2485	3.61	33.95	2.41	9.33
2	2342	4.05	58.26	5.70	11.32
3	2525	3.83	17.37	5.81	9.03
4	2354	4.44	43.44	8.20	13.16
5	2350	7.47	28.56	7.50	9.49
6	2325	6.90	35.40	17.12	6.73
7	2490	4.47	40.82	12.71	13.77
8	2325	3.14	56.06	2.49	10.10
10	2438	4.38	57.71	0.16	15.61
11	2547	5.22	21.33	5.09	2.45
12	2318	6.56	24.23	2.29	16.07
13	2402	4.71	22.49	6.22	20.04
14	2330	3.39	14.14	5.57	11.32
15	2500	4.52	24.47	0.04	14.08
16	2425	3.89	46.08	5.59	10.71
18	2468	6.85	37.80	7.36	11.93
20	2540	5.22	37.88	4.35	23.56
24	2487	2.93	15.68	0.20	10.56
26	2342	4.61	14.81	2.34	9.03

Table A.4 Average Log Results of Kbb-C Member

Well No	Top of formation, m	$Ø_m$, %	S_{mw},%	V_{shale}, %	Net thickness, m
1	2497	3.17	67.64	0.33	22.64
2	2358	4.24	87.36	2.78	8.11
3	2536	4.14	66.13	1.82	26.32
4	2368	5.56	34.91	1.98	31.06
5	2360	7.27	58.29	3.52	28.76
6	2333	5.64	66.31	8.69	33.66
7	2507	4.59	60.38	4.81	26.47
8	2340	4.04	54.62	2.00	34.58
10	2456	4.35	47.90	0.14	37.49
11	2553	4.34	53.97	1.54	31.52
12	2333	11.39	17.12	1.35	31.98
13	2421	5.17	42.90	6.40	34.88
14	2345	2.60	21.23	4.27	31.13
15	2516	5.33	85.44	1.74	4.13
16	2439	4.75	42.92	6.91	28.00
18	2484	4.82	27.63	5.33	33.81
20	2563	7.80	27.37	5.93	8.57
24	2499	2.14	50.89	0.26	37.79
26	2351	4.65	22.83	5.53	36.87

Table A.5 Average Log Results of Derdere Formation

Well No	Top of formation, m	$Ø_m$, %	S_{mw},%	V_{shale}, %	Net thickness, m*
1	2593	3.21	61.37	1.03	21.88
2	2467	3.83	65.22	6.02	22.03
6	2446	3.32	40.50	3.71	5.97
8	2457	3.92	47.40	3.18	34.27
10	2575	4.11	60.49	0.34	12.70
12	2439	5.13	41.64	0.12	42.08
13	2536	6.96	67.64	2.79	49.11
14	2460	4.35	59.23	1.30	9.03
16	2519	7.49	60.00	1.71	40.24
18	2604	5.78	52.66	6.63	17.44
20	2620	4.19	52.45	0.02	24.02

* : In wells, W-3,4,5,7,15 and 24 Derdere Formation top is under the oil-water contact (-1860 m. sub sea). For this reason they are discarded from the table. In wells, W-11 and 26 Derdere Formation is not penetrated.

Table A.6 PVT Analysis Results of Field-A Oil

Pressure (psig)	Viscosity (cp)	Rs (scf/stb)	Bo rbbl/stb
3100	3.39	34.81	1.0921
2500	3.21	34.81	1.0942
2000	3.06	34.81	1.0972
1500	2.93	34.81	1.1014
1000	2.74	34.81	1.1059
750	2.72	34.81	1.109
600	2.64	34.81	1.1091
500	2.61	34.81	1.1097
P_{bp}=400	2.56	34.81	1.1128
0	3.47	0	1.0784

Table A.7 Formation Gross Thickness Values of Field-A Wells

Well No	KARABOGAZ		KBB-C		KBB-B	KBB-A	DERDERE**	
	Gross thickness, m	ntg	Gross thickness, m	ntg	Gross thickness, m	Gross thickness, m	Gross thickness, m	ntg
1	43	0.22	31	0.73	40	25	116	3.74
2	47	0.24	35	0.23	45	29	65	1.86
3	45	0.20	34	0.77	41	25	29	0.85
4	52	0.25	36	0.86	43	27	48	1.33
5	41	0.23	31	0.93	45	28	35	1.13
6	42	0.16	31	1.09	45	27	94	3.03
7	50	0.28	35	0.76	45	23	15	0.43
8	51	0.20	38	0.91	45	34	42	1.11
10	60	0.26	39	0.96	47	33	25	0.64
11	46	0.05	36	0.88	41	10	0	0.00
12	56	0.29	36	0.89	41	31	51	1.42
13	56	0.36	37	0.94	45	33	67	1.81
14	47	0.24	39	0.80	43	33	35	0.90
15	66	0.21	46	0.09	47	22	12	0.26
16	47	0.23	28	1.00	26	26	56	2.00
17	44	0.00	30	-	42	29	34	1.13
18	54	0.22	43	0.79	46	35	34	0.79
19	44	0.00	25	-	38	28	33	1.32
20	45	0.52	19	0.45	30	18	35	1.84
21	46	*	28	*	43	23	24	0.86
22	31	*	29	*	32	28	28	0.97
23	81	*	43	*	57	35	42	0.98
24	50	0.21	31	1.22	54	30	44	1.42
25	61	*	30	*	51	30	117	3.90
26	53	0.17	39	0.95	26	0	0	0.00

ntg: net to gross thickness ratio

* : These wells have no interpreted log

DERDERE** : Only W-1 fully penetrated this formation. Wells with zero gross thickness values have no penetration.

APPENDIX B

RESULTS OF MONTE CARLO SIMULATION

Table B.1 Karabogaz Formation Matrix Reserve Simulation by Monte Carlo

Name	Matrix reserve, Mstb	Net thickness, m	Area, m2	$Ø_m$, %	S_{wmi} , %
Minimum	20.424	1.347	4,020,873	0.867	1.003
Maximum	9.7E+04	25.255	7,240,757	17.437	99.861
Mean	1.4E+04	12.295	5,667,686	4.905	30.367
Std Deviation	9,920	4.969	669,367	2.270	19.715
Variance	9.8E+07	24.690	4.48E+11	5.155	388.690
Skewness	1.682	0.208	-4.27E-02	1.292	1.151
Kurtosis	7.621	2.407	2.368	5.348	3.967
Errors Calculated	0	0	0	0	0
Mode	7,341	18.580	4,740,188	4.406	13.159
5% Perc	2,516	4.522	4,534,950	2.123	7.598
10% Perc	3,790	5.904	4,757,728	2.474	9.998
15% Perc	4,804	7.005	4,925,246	2.785	12.040
20% Perc	5,729	7.854	5,059,402	3.046	13.838
25% Perc	6,621	8.640	5,186,893	3.297	15.612
30% Perc	7,508	9.381	5,295,769	3.517	17.335
35% Perc	8,408	10.001	5,393,403	3.738	19.208
40% Perc	9,311	10.580	5,490,048	3.998	21.072
45% Perc	10,213	11.233	5,593,442	4.218	23.131
50% Perc	11,246	11.934	5,682,008	4.453	25.331
55% Perc	12,345	12.649	5,768,078	4.706	27.587
60% Perc	13,484	13.316	5,854,606	4.996	30.166
65% Perc	14,796	14.077	5,946,079	5.285	33.172
70% Perc	16,255	14.919	6,041,908	5.597	36.427
75% Perc	18,165	15.847	6,152,577	5.973	40.216
80% Perc	20,188	16.842	6,268,381	6.442	44.785
85% Perc	22,779	17.907	6,405,525	7.056	50.690
90% Perc	26,452	19.244	6,571,538	7.918	59.071
95% Perc	32,760	21.015	6,779,711	9.324	71.946

Table B.2 Kbb-C Member Matrix Reserve Simulation by Monte Carlo

Name	Matrix reserve, Mstb	Net thickness, m	Area, m2	$Ø_m$, %	S_{wmi} , %
Minimum	128.754	0.260	4,020,873	0.453	35.454
Maximum	1.6E+05	37.676	7,240,757	27.523	56.973
Mean	1.9E+04	21.803	5,667,686	4.969	45.736
Std Deviation	1.5E+04	7.999	669,367	3.051	2.754
Variance	2.1E+08	63.979	4.48E+11	9.308	7.582
Skewness	1.916	-0.391	-4.27E-02	1.853	0.004
Kurtosis	9.049	2.397	2.368	8.373	2.992
Errors Calculated	0	0	0	0	0
Mode	9,028	27.331	4,740,188	2.769	42.198
5% Perc	3,785	7.078	4,534,950	1.631	41.181
10% Perc	5,514	10.156	4,757,728	2.017	42.205
15% Perc	6,824	12.570	4,925,246	2.327	42.888
20% Perc	8,154	14.535	5,059,402	2.605	43.388
25% Perc	9,339	16.061	5,186,893	2.879	43.893
30% Perc	10,570	17.657	5,295,769	3.148	44.301
35% Perc	11,828	19.133	5,393,403	3.400	44.688
40% Perc	13,038	20.391	5,490,048	3.656	45.052
45% Perc	14,336	21.636	5,593,442	3.969	45.406
50% Perc	15,669	22.848	5,682,008	4.247	45.746
55% Perc	17,220	23.892	5,768,078	4.562	46.082
60% Perc	18,876	24.986	5,854,606	4.893	46.436
65% Perc	20,654	25.984	5,946,079	5.275	46.795
70% Perc	22,631	27.042	6,041,908	5.707	47.183
75% Perc	25,226	28.003	6,152,577	6.203	47.583
80% Perc	28,189	29.085	6,268,381	6.797	48.037
85% Perc	32,079	30.258	6,405,525	7.577	48.602
90% Perc	37,680	31.601	6,571,538	8.718	49.233
95% Perc	48,080	33.510	6,779,711	10.838	50.260

Table B.3 Derdere Formation Matrix Reserve Simulation by Monte Carlo

Name	Matrix reserve, Mstb	Net thickness, m	Area, m2	$Ø_m$, %	S_{wmi} , %
Minimum	0.976	5.282	3,168,439	0.555	9.418
Maximum	152,527	49.589	5,151,636	20.572	99.986
Mean	15,097	26.860	4,279,881	5.205	56.661
Std Deviation	15,008	9.288	424,938	2.963	23.772
Variance	2.3E+08	86.260	1.8E+11	8.777	565.116
Skewness	0.002	0.093	-0.349	1.465	-7.6E-02
Kurtosis	0.013	2.406	2.385	5.850	1.942
Errors Calculated	0	0	0	0	0
Mode	4,860	23.767	4,047,438	2.525	41.436
5% Perc	1,280	11.761	3,516,687	1.807	17.706
10% Perc	2,322	14.548	3,672,153	2.226	23.038
15% Perc	3,247	16.742	3,790,292	2.521	28.275
20% Perc	4,163	18.509	3,887,150	2.815	33.108
25% Perc	5,074	20.124	3,974,565	3.086	37.475
30% Perc	6,043	21.652	4,059,051	3.358	41.533
35% Perc	6,985	22.981	4,131,010	3.646	45.652
40% Perc	8,090	24.233	4,200,076	3.924	49.457
45% Perc	9,252	25.333	4,267,929	4.189	53.474
50% Perc	10,597	26.492	4,331,290	4.478	57.308
55% Perc	12,011	27.744	4,389,832	4.822	61.076
60% Perc	13,682	29.014	4,446,100	5.199	64.773
65% Perc	15,666	30.349	4,500,660	5.572	68.561
70% Perc	17,698	31.885	4,553,461	6.081	72.414
75% Perc	20,046	33.420	4,605,345	6.587	76.566
80% Perc	23,203	35.227	4,661,176	7.185	80.773
85% Perc	27,166	37.355	4,729,645	7.577	84.842
90% Perc	33,176	39.712	4,804,717	8.718	88.941
95% Perc	43,848	42.722	4,912,563	10.838	93.479

Table B.4 Karabogaz Formation Fracture Reserve Simulation by Monte Carlo

Name	Fracture reserve, Mstb	Net thickness, m	Area, m2	Fracture width, mm	Fracture density, 1/mm	$Ø_f$, %
Minimum	1.277	1.208	4,020,873	5E-06	0.030	4.5E-04
Maximum	14,455	25.124	7,240,757	0.999	0.050	1.986
Mean	2,685	12.371	5,667,686	0.273	0.040	0.670
Std Deviation	2,344	4.959	669,367	0.231	0.004	0.470
Variance	5.5E+06	24.595	4.5E+11	0.053	1.7E-05	0.221
Skewness	1.322	0.170	-4.3E-02	1.034	-0.011	0.553
Kurtosis	4.739	2.397	2.368	3.370	2.412	2.381
Errors Calculated	0	0	0	0	0	0
Mode	2,659	10.794	4,740,188	0.125	0.033	0.895
5% Perc	157	4.515	4,534,950	0.016	0.033	0.051
10% Perc	337	5.900	4,757,728	0.034	0.034	0.105
15% Perc	516	7.045	4,925,246	0.052	0.035	0.157
20% Perc	690	7.896	5,059,402	0.069	0.036	0.215
25% Perc	872	8.748	5,186,893	0.088	0.037	0.272
30% Perc	1,077	9.465	5,295,769	0.108	0.038	0.330
35% Perc	1,291	10.148	5,393,403	0.131	0.038	0.393
40% Perc	1,531	10.751	5,490,048	0.154	0.039	0.455
45% Perc	1,770	11.382	5,593,442	0.179	0.040	0.523
50% Perc	2,031	12.044	5,682,008	0.208	0.040	0.588
55% Perc	2,319	12.784	5,768,078	0.240	0.041	0.660
60% Perc	2,640	13.490	5,854,606	0.273	0.041	0.743
65% Perc	3,011	14.220	5,946,079	0.312	0.042	0.822
70% Perc	3,404	15.069	6,041,908	0.354	0.042	0.906
75% Perc	3,864	15.936	6,152,577	0.403	0.043	1.005
80% Perc	4,402	16.933	6,268,381	0.458	0.044	1.113
85% Perc	5,068	17.999	6,405,525	0.530	0.044	1.225
90% Perc	5,963	19.200	6,571,538	0.620	0.046	1.364
95% Perc	7,460	20.924	6,779,711	0.762	0.047	1.552

Table B.5 Kbb-C Member Fracture Reserve Simulation by Monte Carlo

Name	Fracture reserve, Mstb	Net thickness, m	Area, m2	Fracture width, mm	Fracture density, 1/mm	$Ø_f$, %
Minimum	2.447	0.202	4,020,873	5E-06	0.030	4E-04
Maximum	2.2E+04	37.778	7,240,757	0.999	0.050	1.986
Mean	4,768	21.798	5,667,686	0.273	0.040	0.670
Std Deviation	4,001	8.001	669,367	0.231	0.004	0.470
Variance	1.6E+07	64.008	4.48E+11	0.053	1.7E-05	0.221
Skewness	1.100	-0.403	-4.27E-02	1.034	-0.011	0.553
Kurtosis	3.823	2.384	2.368	3.370	2.412	2.381
Errors Calculated	0	0.000	0	0	0	0
Mode	2,576	19.103	4,740,188	0.125	0.033	0.895
5% Perc	279	7.199	4,534,950	0.016	0.033	0.051
10% Perc	586	10.277	4,757,728	0.034	0.034	0.105
15% Perc	908	12.468	4,925,246	0.052	0.035	0.157
20% Perc	1,244	14.287	5,059,402	0.069	0.036	0.215
25% Perc	1,582	16.006	5,186,893	0.088	0.037	0.272
30% Perc	1,938	17.595	5,295,769	0.108	0.038	0.330
35% Perc	2,337	19.075	5,393,403	0.131	0.038	0.393
40% Perc	2,761	20.450	5,490,048	0.154	0.039	0.455
45% Perc	3,236	21.697	5,593,442	0.179	0.040	0.523
50% Perc	3,726	22.867	5,682,008	0.208	0.040	0.588
55% Perc	4,235	24.024	5,768,078	0.240	0.041	0.660
60% Perc	4,825	25.079	5,854,606	0.273	0.041	0.743
65% Perc	5,464	26.100	5,946,079	0.312	0.042	0.822
70% Perc	6,140	27.037	6,041,908	0.354	0.042	0.906
75% Perc	6,985	28.010	6,152,577	0.403	0.043	1.005
80% Perc	7,969	29.067	6,268,381	0.458	0.044	1.113
85% Perc	9,164	30.219	6,405,525	0.530	0.044	1.225
90% Perc	10,646	31.594	6,571,538	0.620	0.046	1.364
95% Perc	12,817	33.446	6,779,711	0.762	0.047	1.552

Table B.6 Derdere Formation Fracture Reserve Simulation by Monte Carlo

Name	Fracture reserve, Mstb	Net thickness, m	Area, m2	Fracture width, mm	Fracture density, 1/mm	$Ø_f$, %
Minimum	69	5.282	3,168,439	0.000	0.000	1.7E-02
Maximum	12,572	49.589	5,151,636	1.000	0.034	1.025
Mean	2,011	26.860	4,279,881	0.288	0.018	0.306
Std Deviation	1,610	9.288	424,938	0.241	0.007	0.204
Variance	2.6E+06	86.260	1.8E+11	0.058	0.000	4.2E-02
Skewness	1.703	0.093	-0.349	0.952	-0.023	1.142
Kurtosis	6.691	2.406	2.385	3.085	2.397	3.878
Errors Calculated	0	0	0	0	0	0
Mode	689	23.767	4,047,438	0.006	0.020	0.227
5% Perc	367	11.761	3,516,687	0.016	0.006	7.3E-02
10% Perc	507	14.548	3,672,153	0.033	0.008	9.7E-02
15% Perc	631	16.742	3,790,292	0.052	0.010	0.115
20% Perc	748	18.509	3,887,150	0.071	0.011	0.133
25% Perc	865	20.124	3,974,565	0.093	0.013	0.152
30% Perc	994	21.652	4,059,051	0.115	0.014	0.170
35% Perc	1,113	22.981	4,131,010	0.139	0.015	0.189
40% Perc	1,242	24.233	4,200,076	0.163	0.016	0.208
45% Perc	1,381	25.333	4,267,929	0.190	0.017	0.230
50% Perc	1,537	26.492	4,331,290	0.222	0.018	0.252
55% Perc	1,705	27.744	4,389,832	0.254	0.019	0.275
60% Perc	1,898	29.014	4,446,100	0.291	0.019	0.300
65% Perc	2,108	30.349	4,500,660	0.330	0.020	0.331
70% Perc	2,367	31.885	4,553,461	0.374	0.022	0.367
75% Perc	2,669	33.420	4,605,345	0.730	0.023	0.411
80% Perc	3,053	35.227	4,661,176	0.493	0.024	0.461
85% Perc	3,530	37.355	4,729,645	0.566	0.025	0.527
90% Perc	4,179	39.712	4,804,717	0.661	0.027	0.608
95% Perc	5,279	42.722	4,912,563	0.791	0.029	0.726

APPENDIX C

PRODUCTION GRAPHICS OF WELLS IN FRACTURE POROSITY

INTERPRETATION BY PRODUCTION DATA

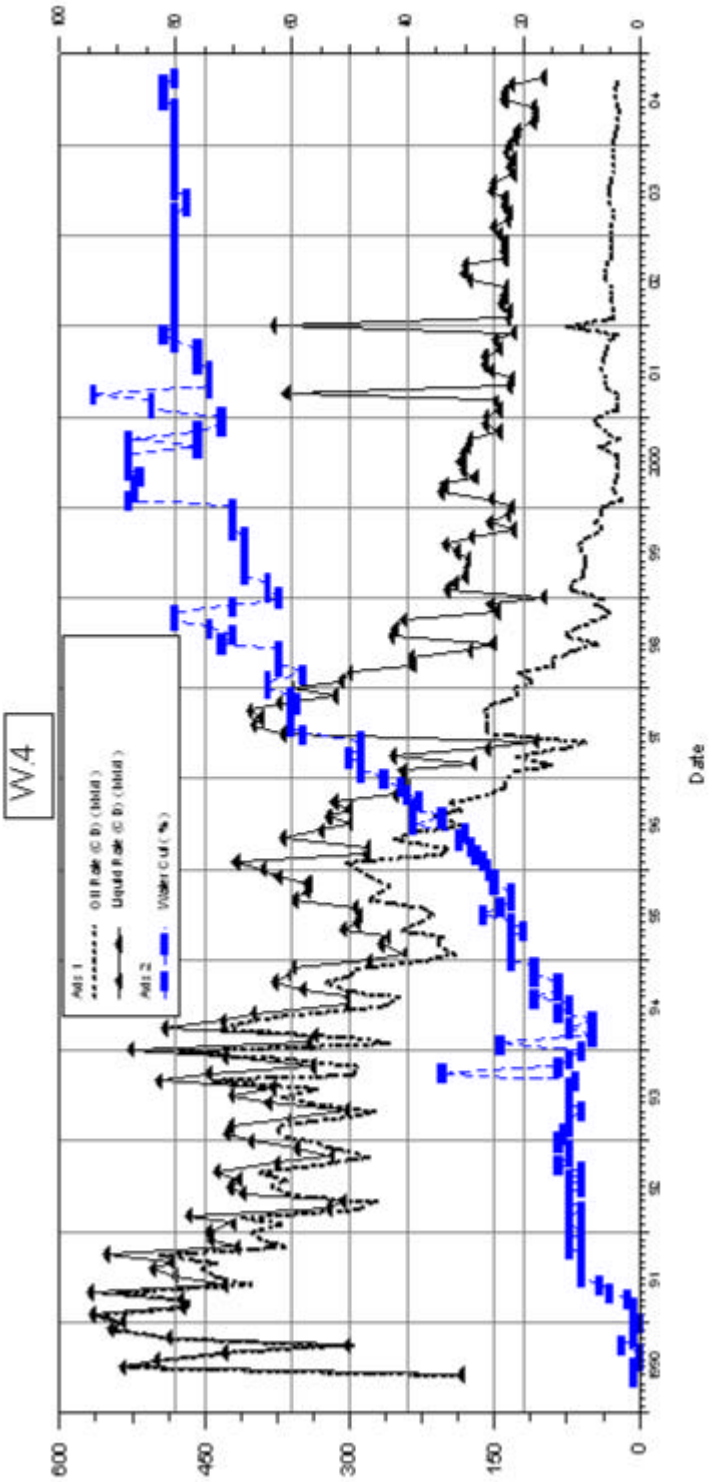

Figure C.1 W-4 Production graphic

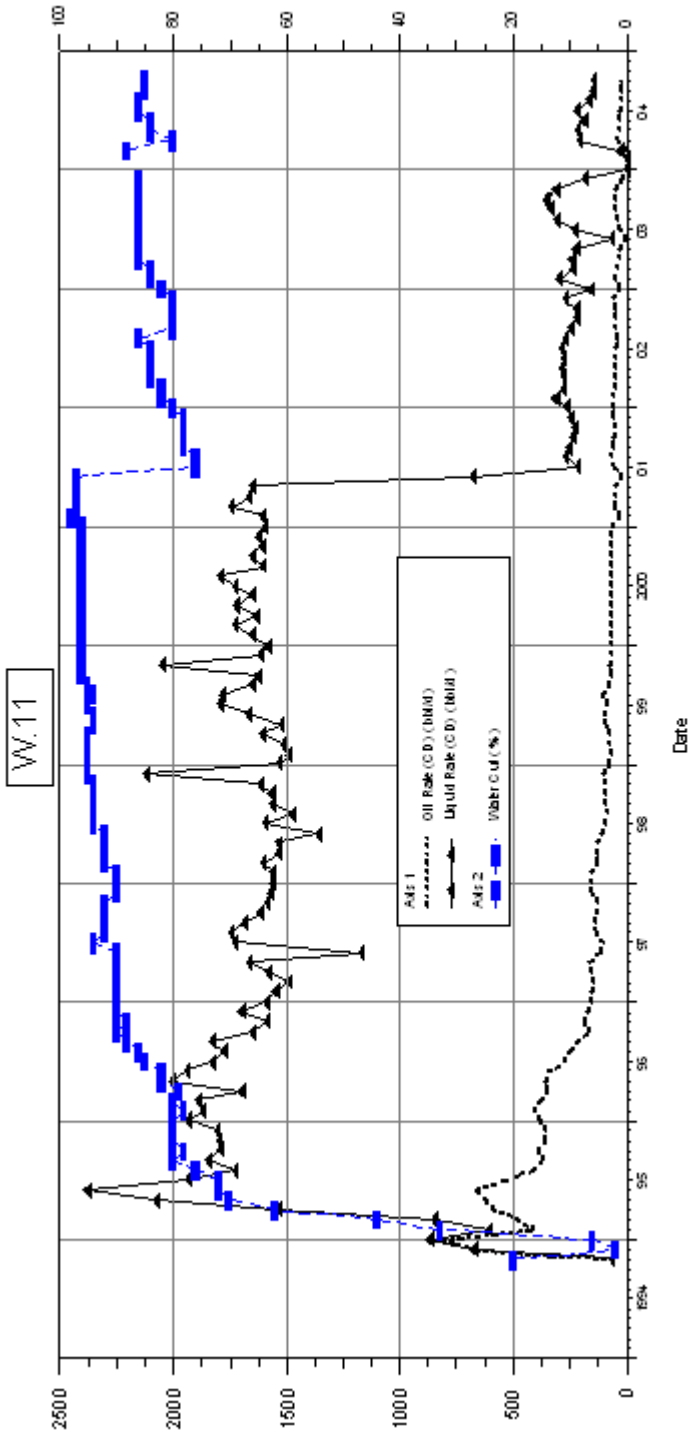

Figure C.2 W-11 production graphic

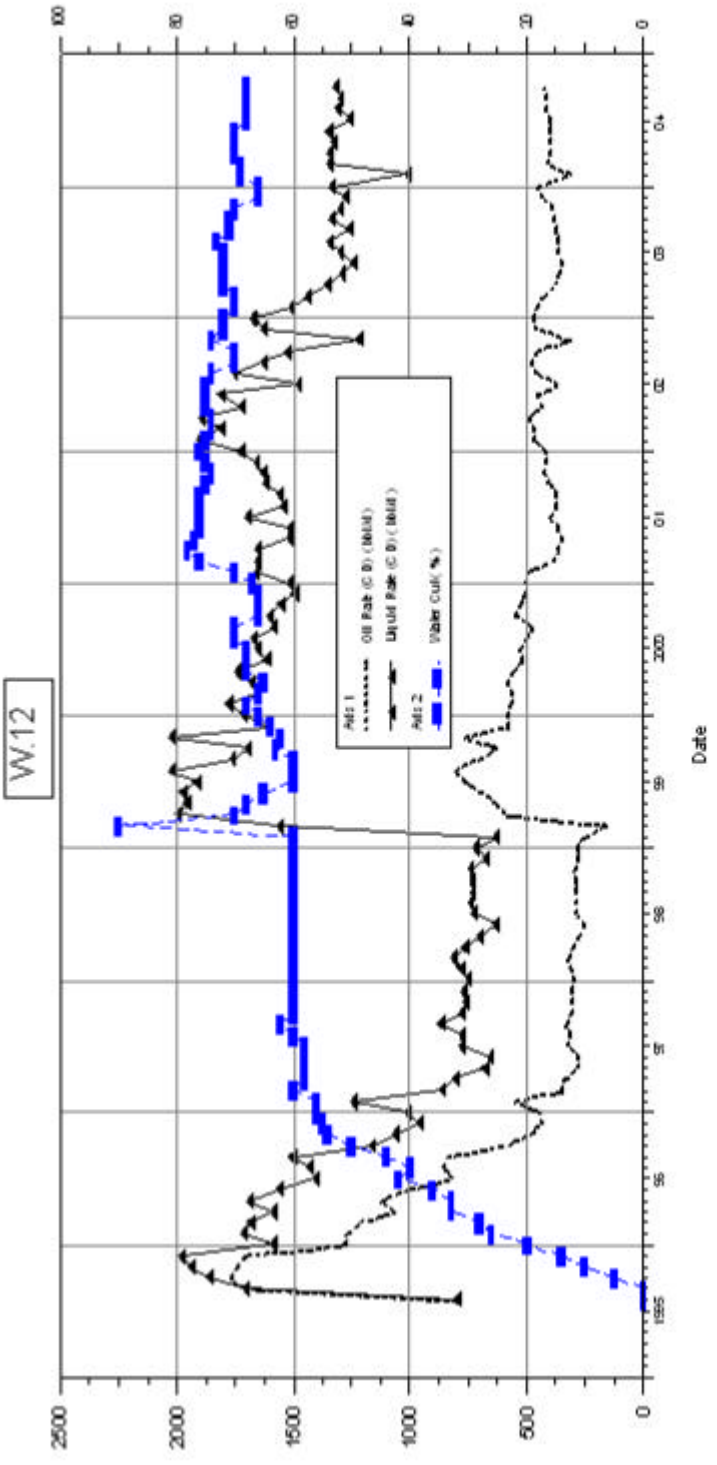

Figure C.3 W-12 production graphic

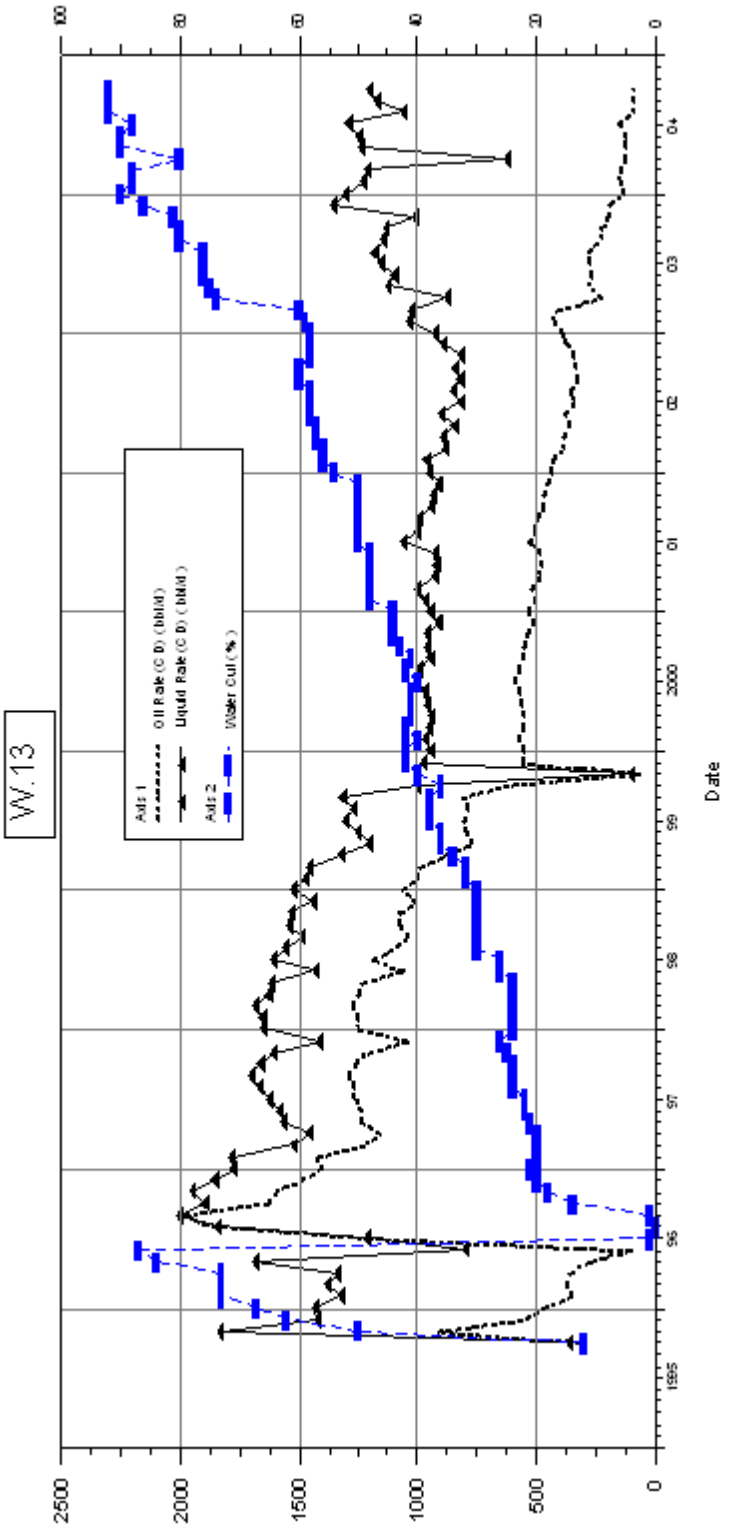

Figure C.4 W-13 production graphic

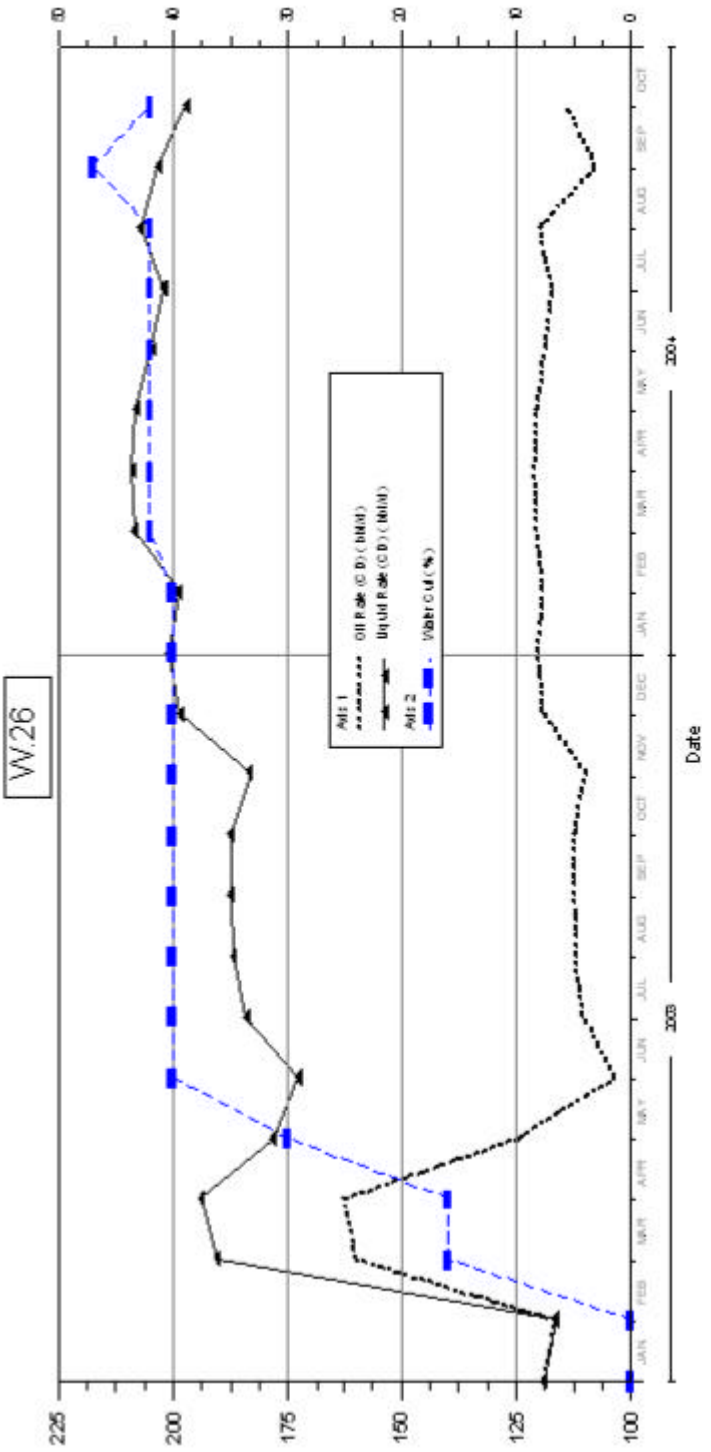

Figure C.5 W-26 production graphic

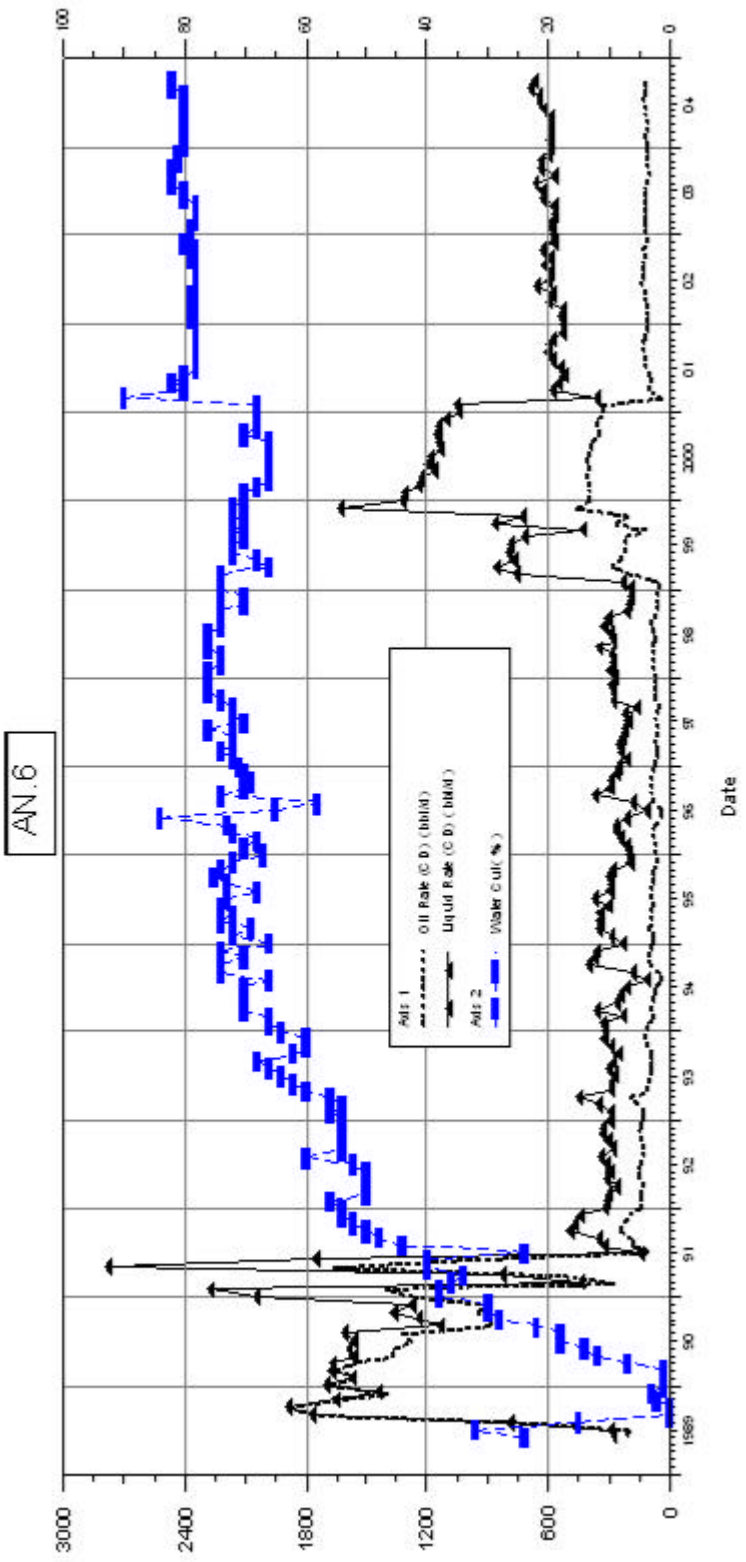

Figure C.6 AN-6 production graphic

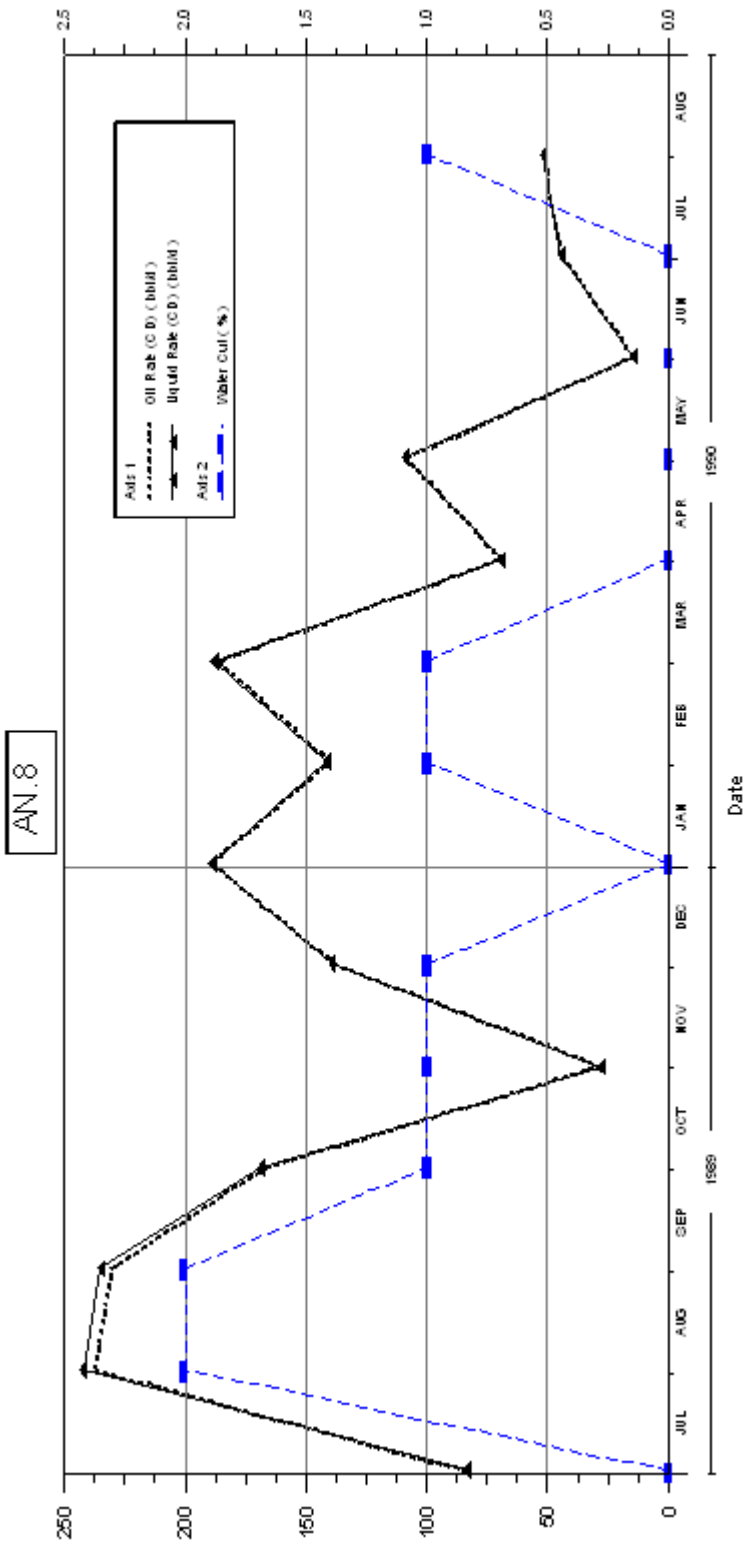

Figure C.7 AN-8 production graphic

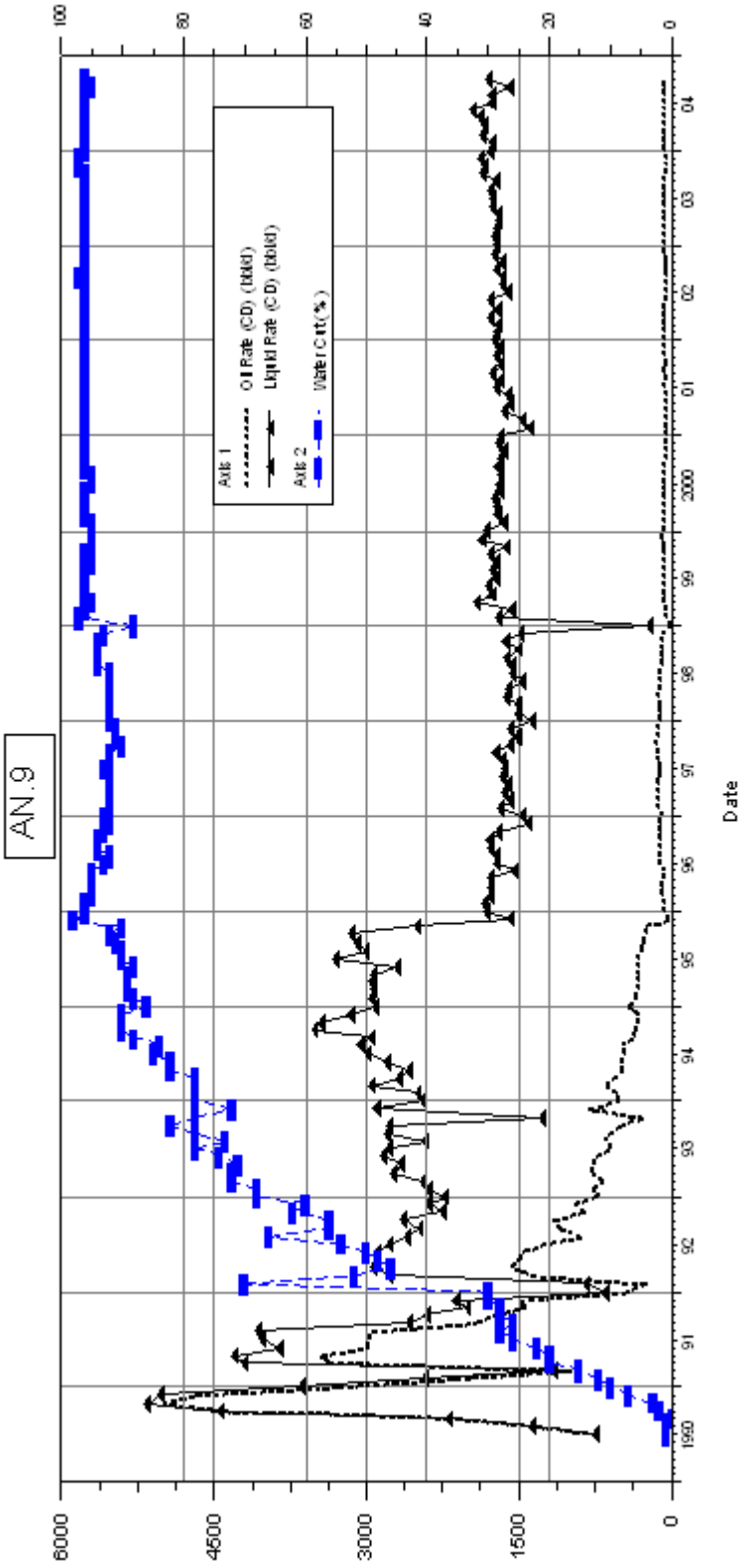

Figure C.8 AN-9 production graphic

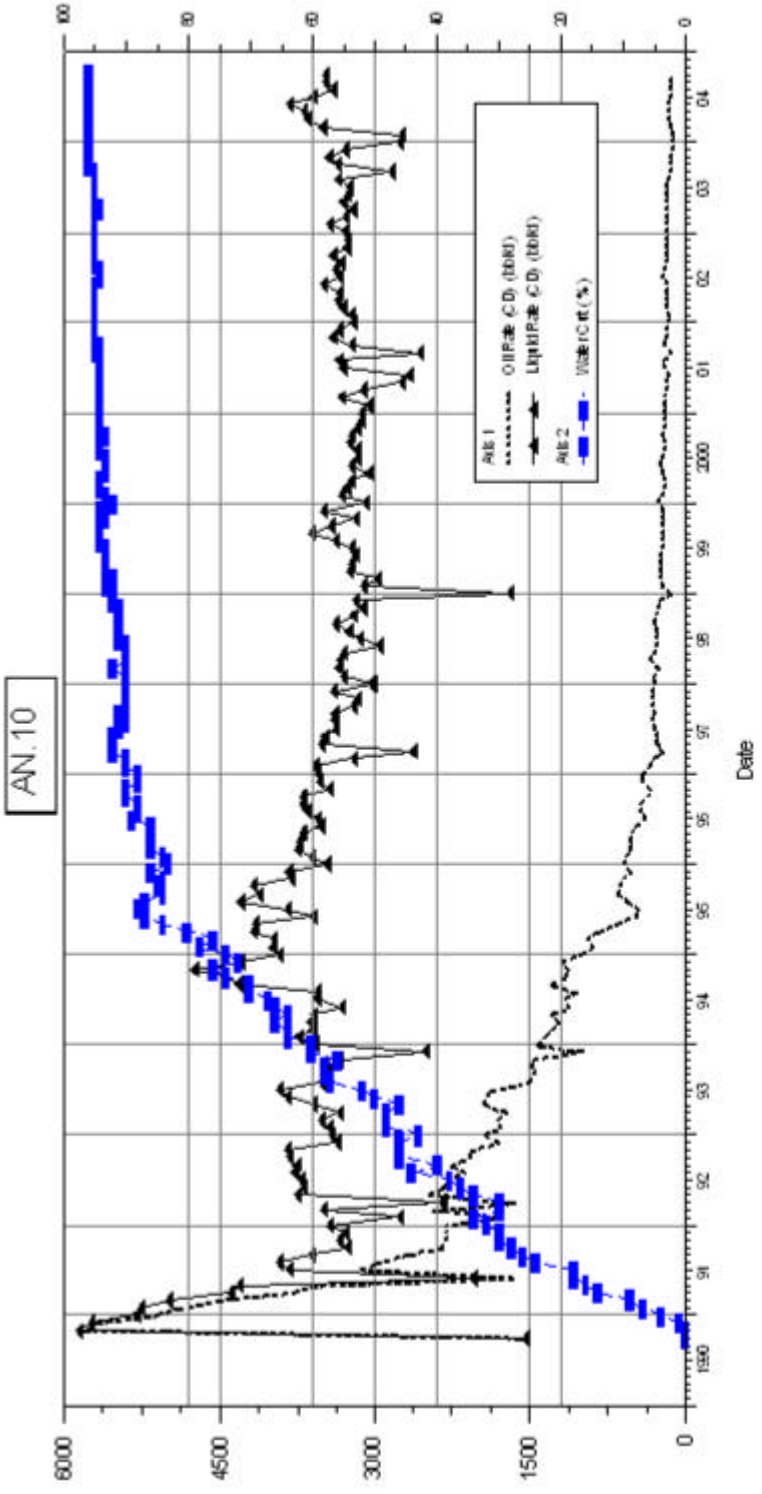

Figure C.9 AN-10 production graphic

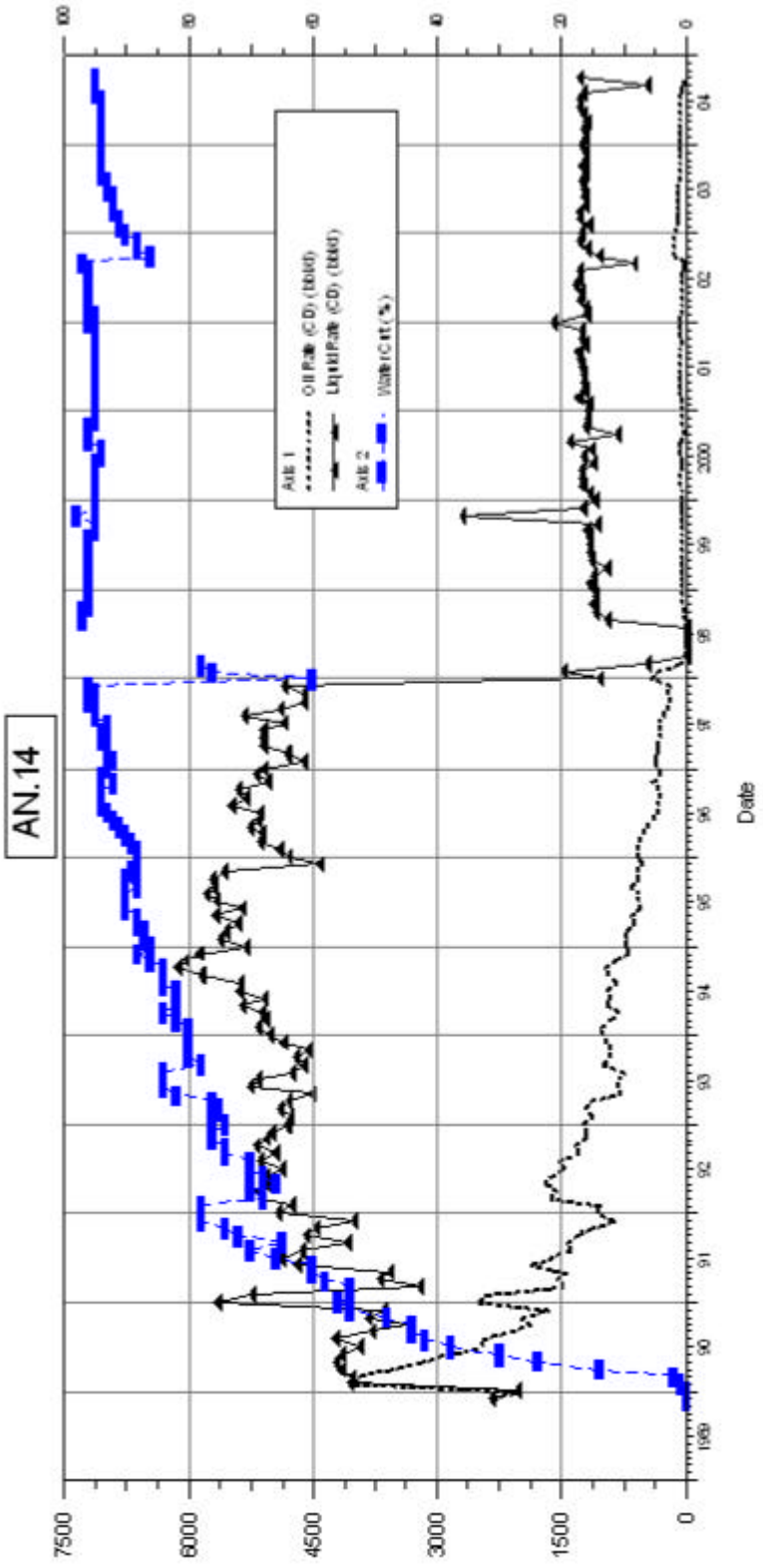

Figure C.10 AN-14 production graphic

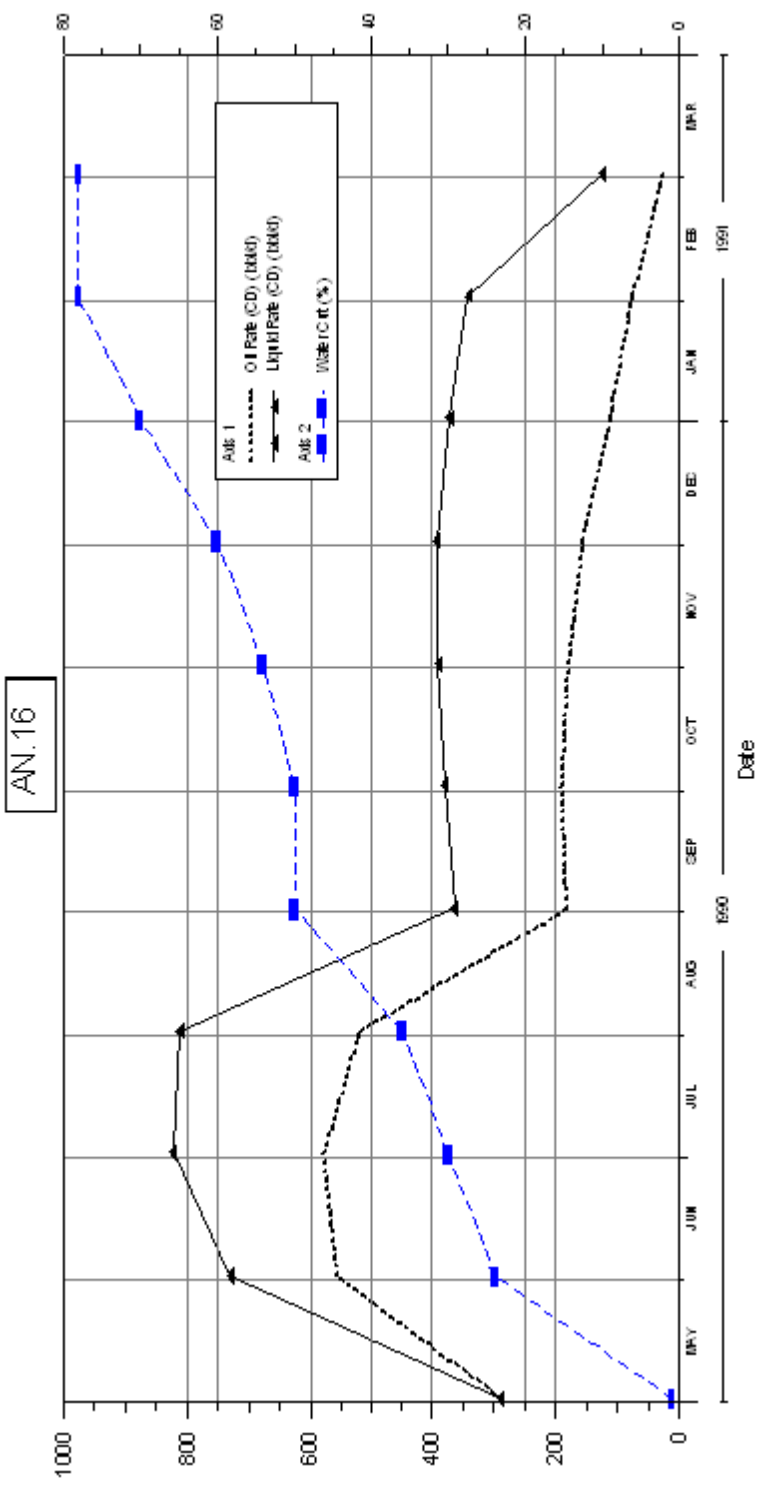

Figure C.11 AN-16 production graphic

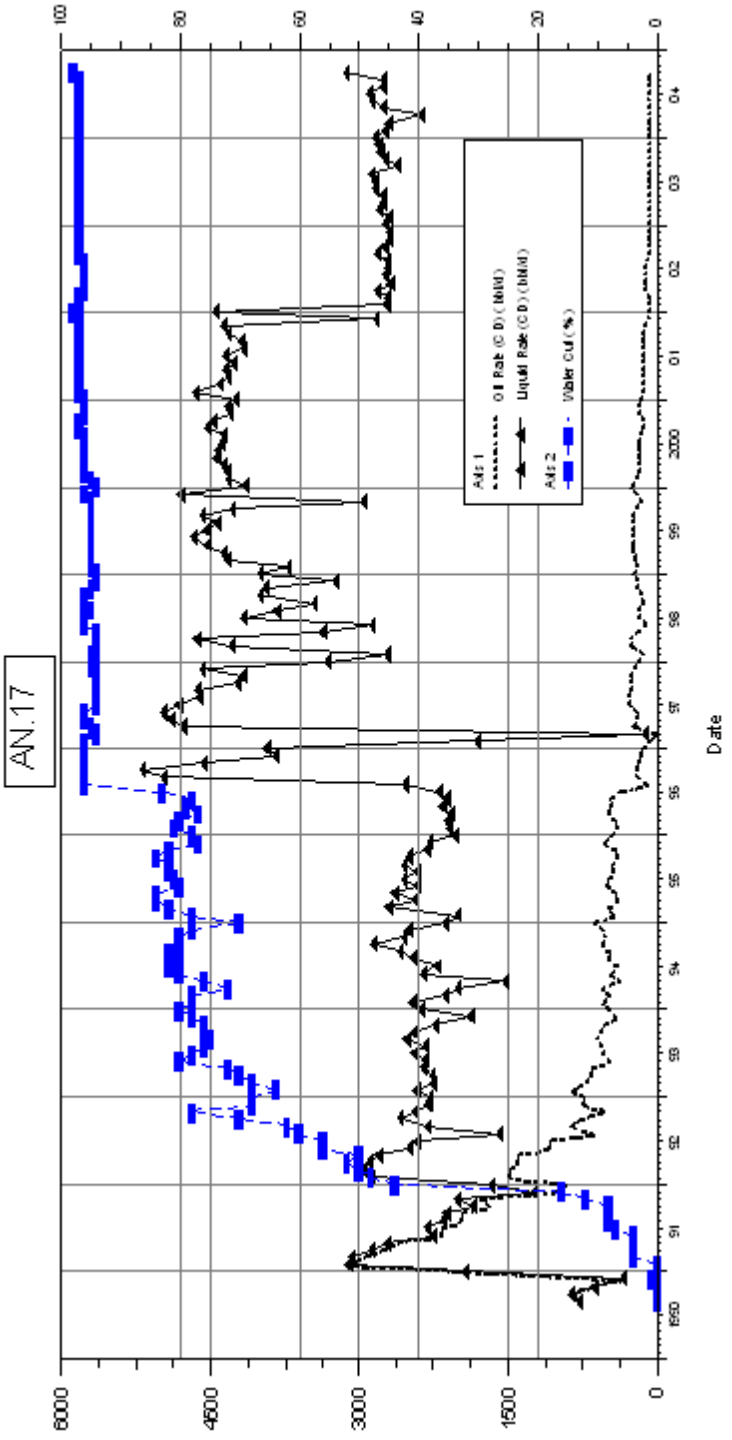

Figure C.12 AN-17 production graphic

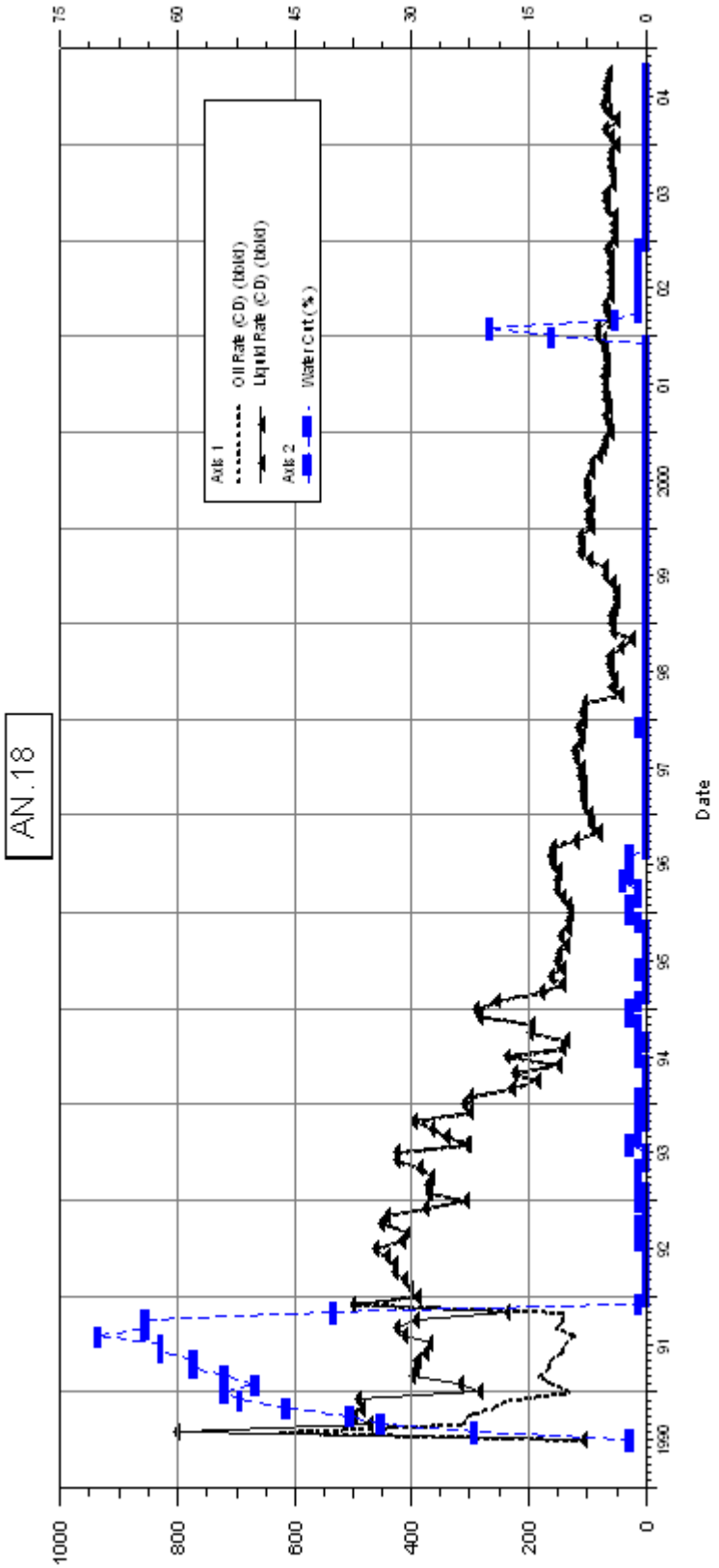

Figure C.13 AN-18 production graphic

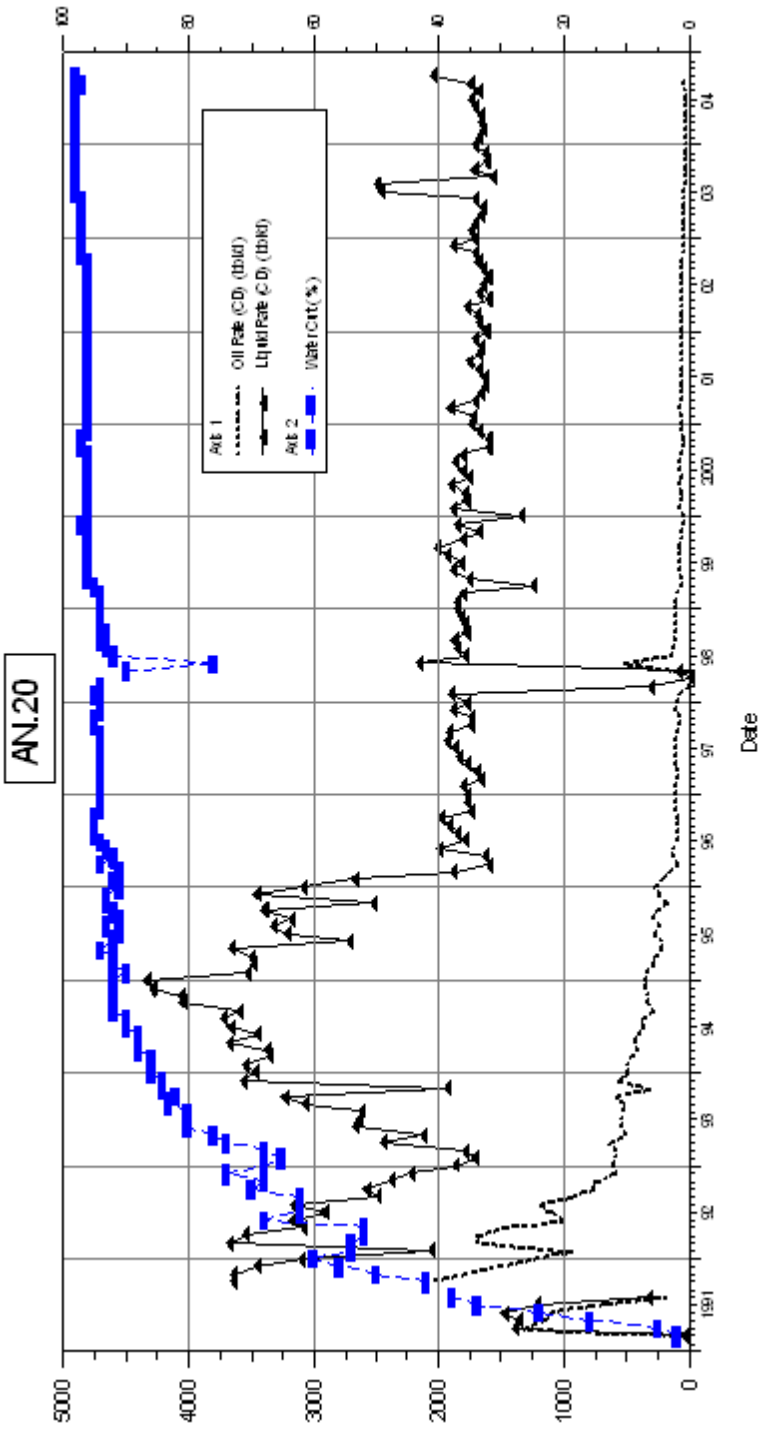

Figure C.14 AN-20 production graphic

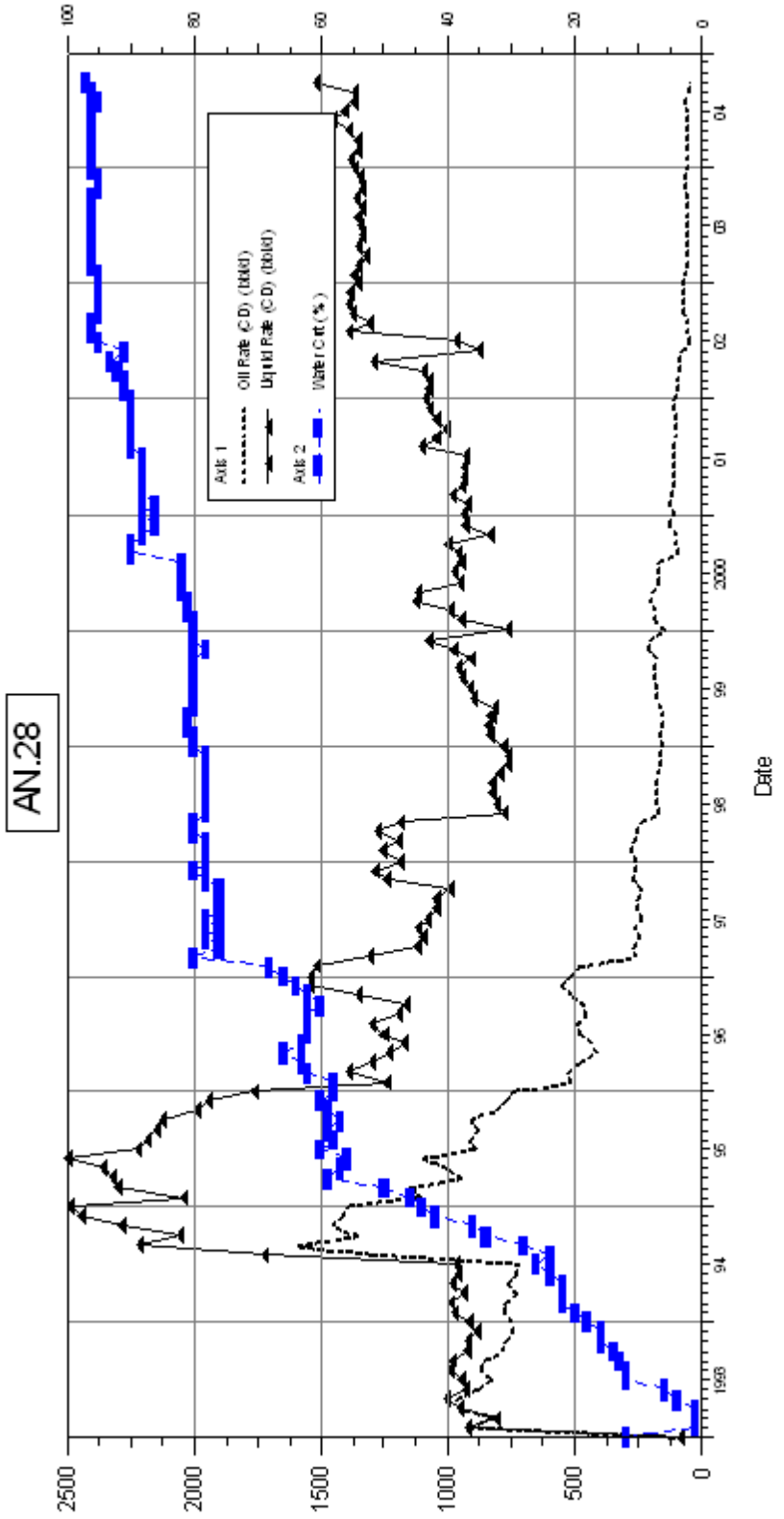

Figure C.15 AN-28 production graphic

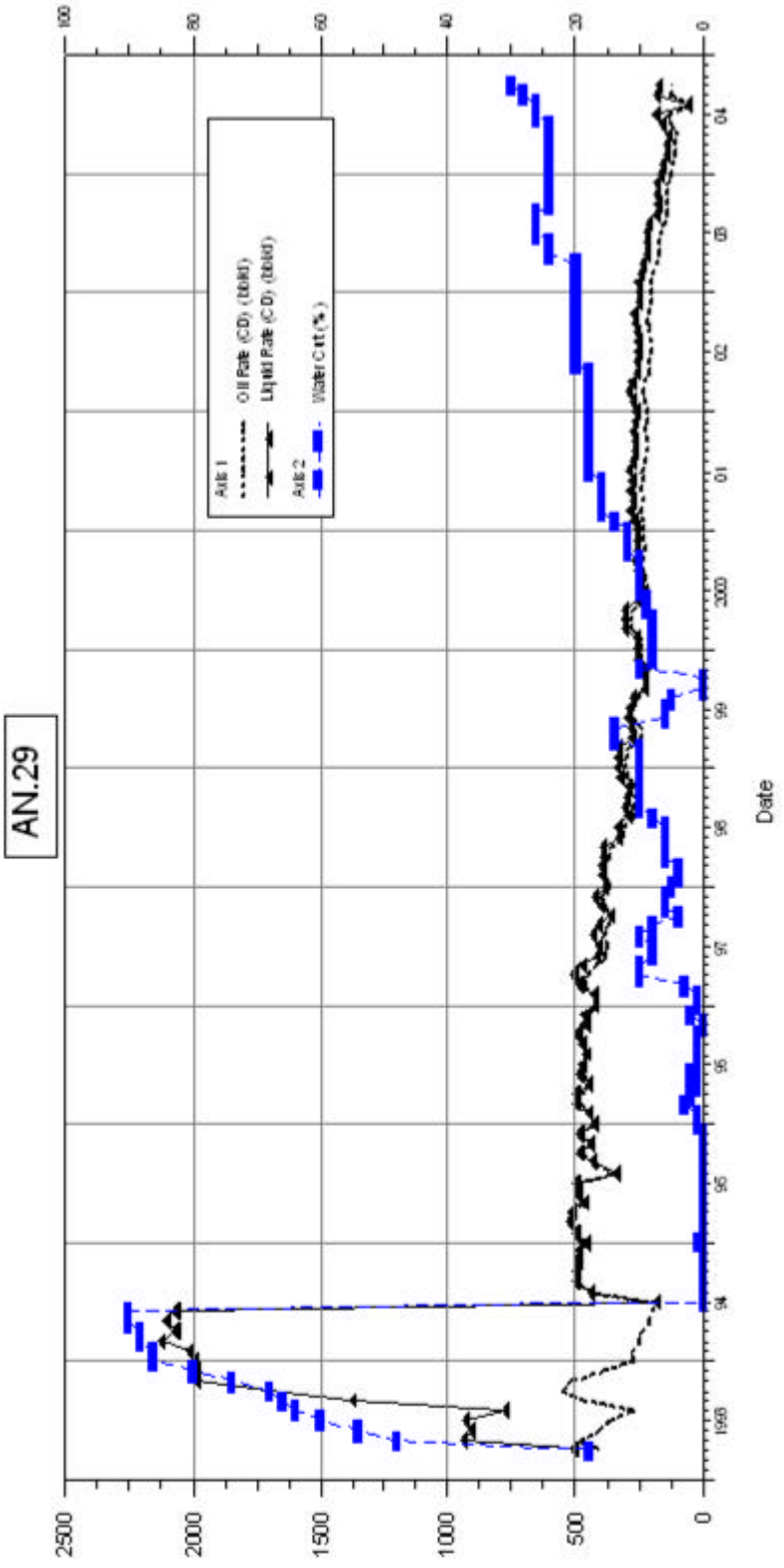

Figure C.16 AN-29 production graphic

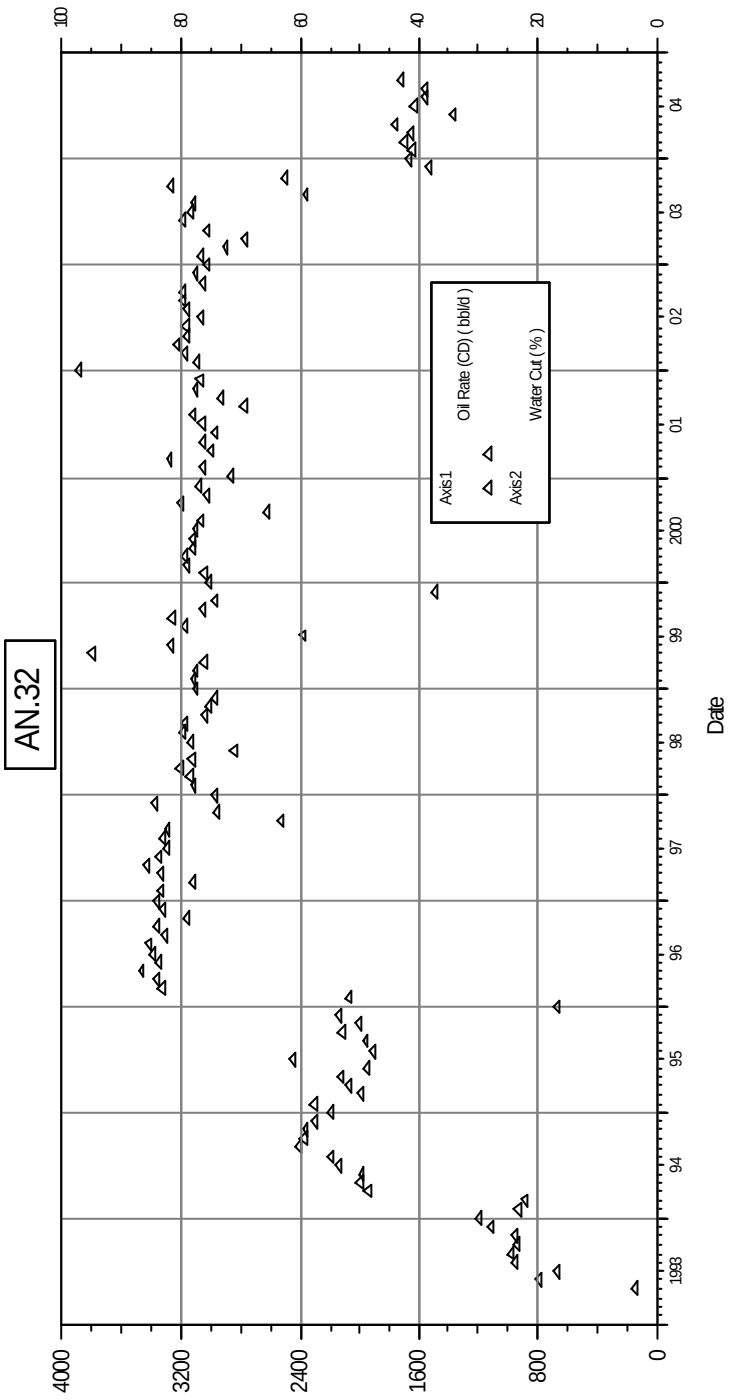

Figure C.17 AN-32 production graphic

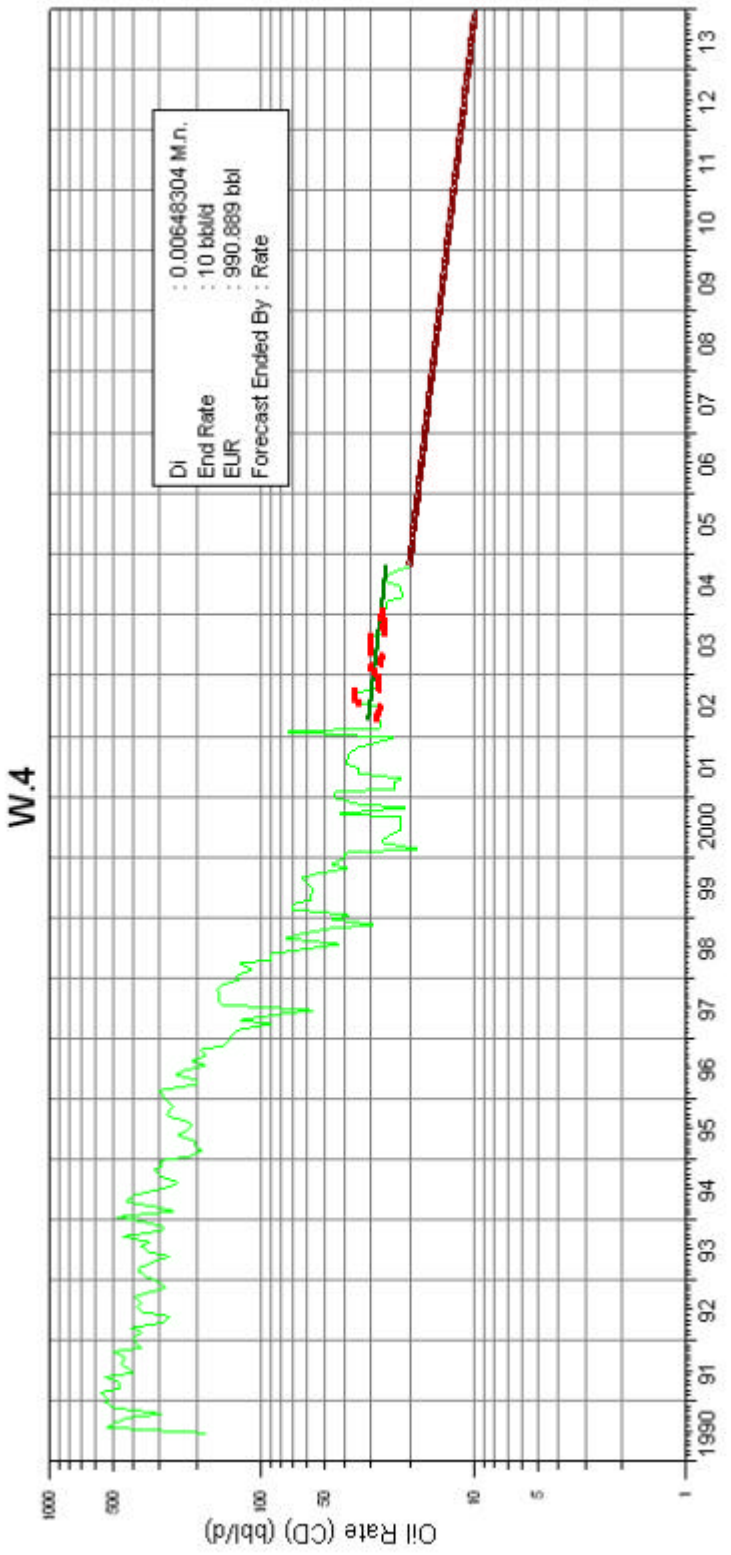

Figure C.18 W-4 decline curve graphic

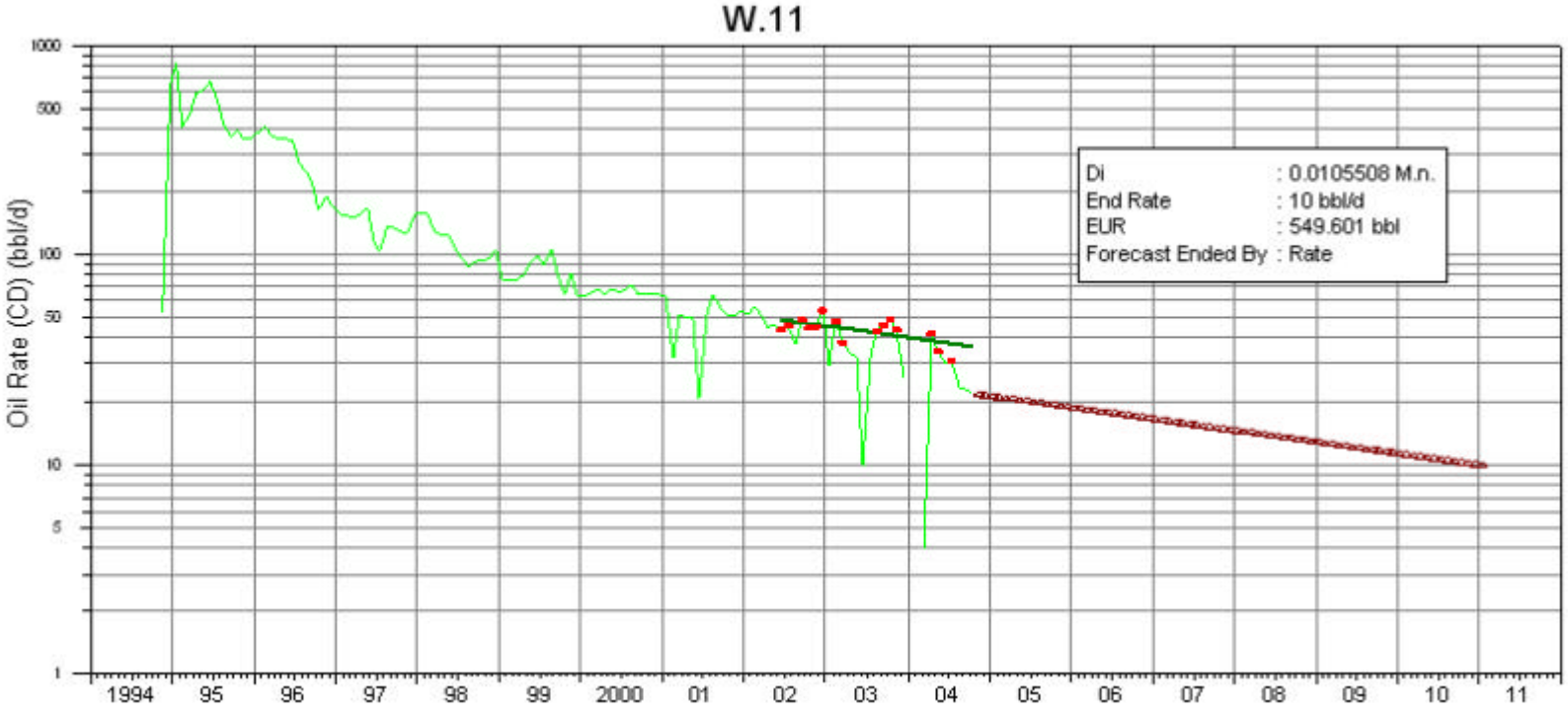

Figure C.19 W-11 Decline curve graphic

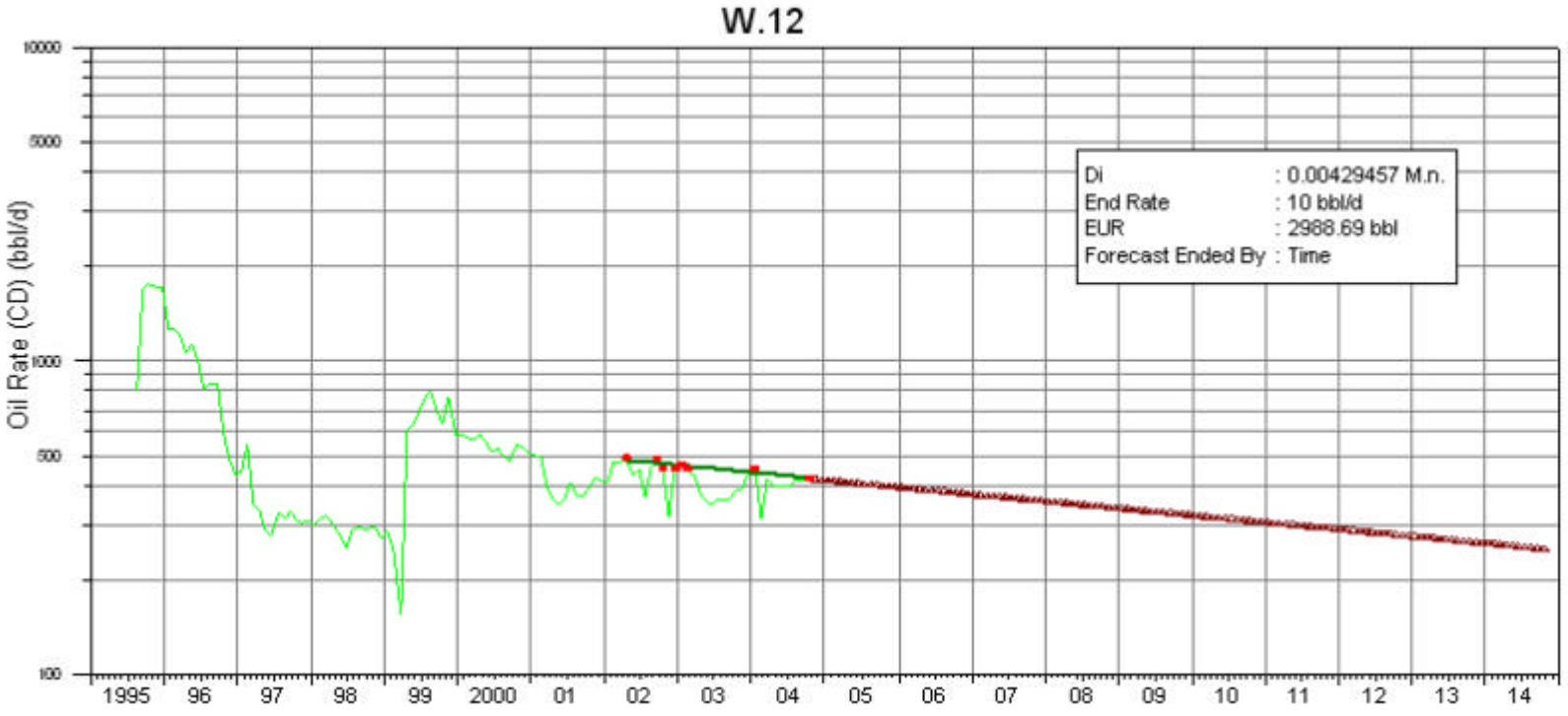

Figure C.20 W-12 Decline curve graphic

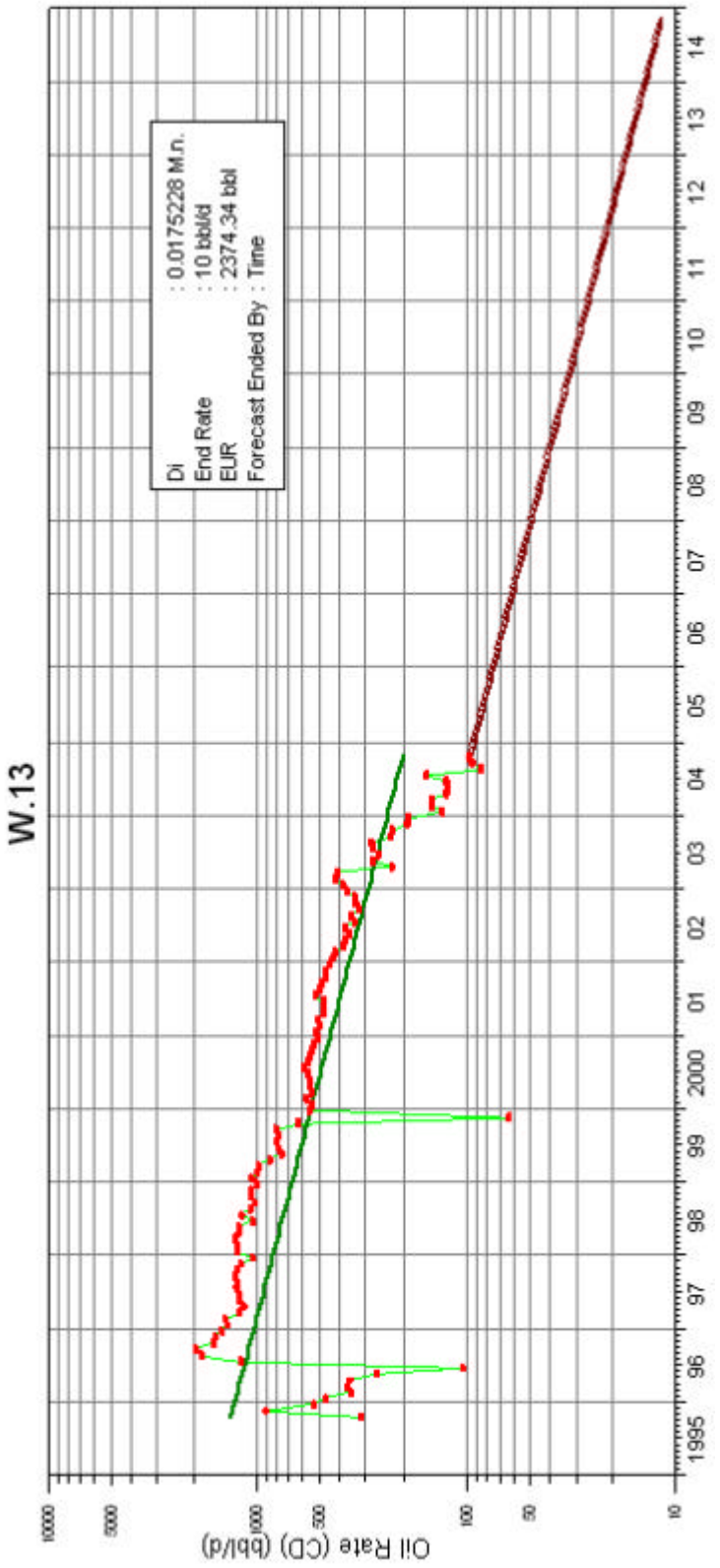

Figure C.21 W-13 Decline curve graphic

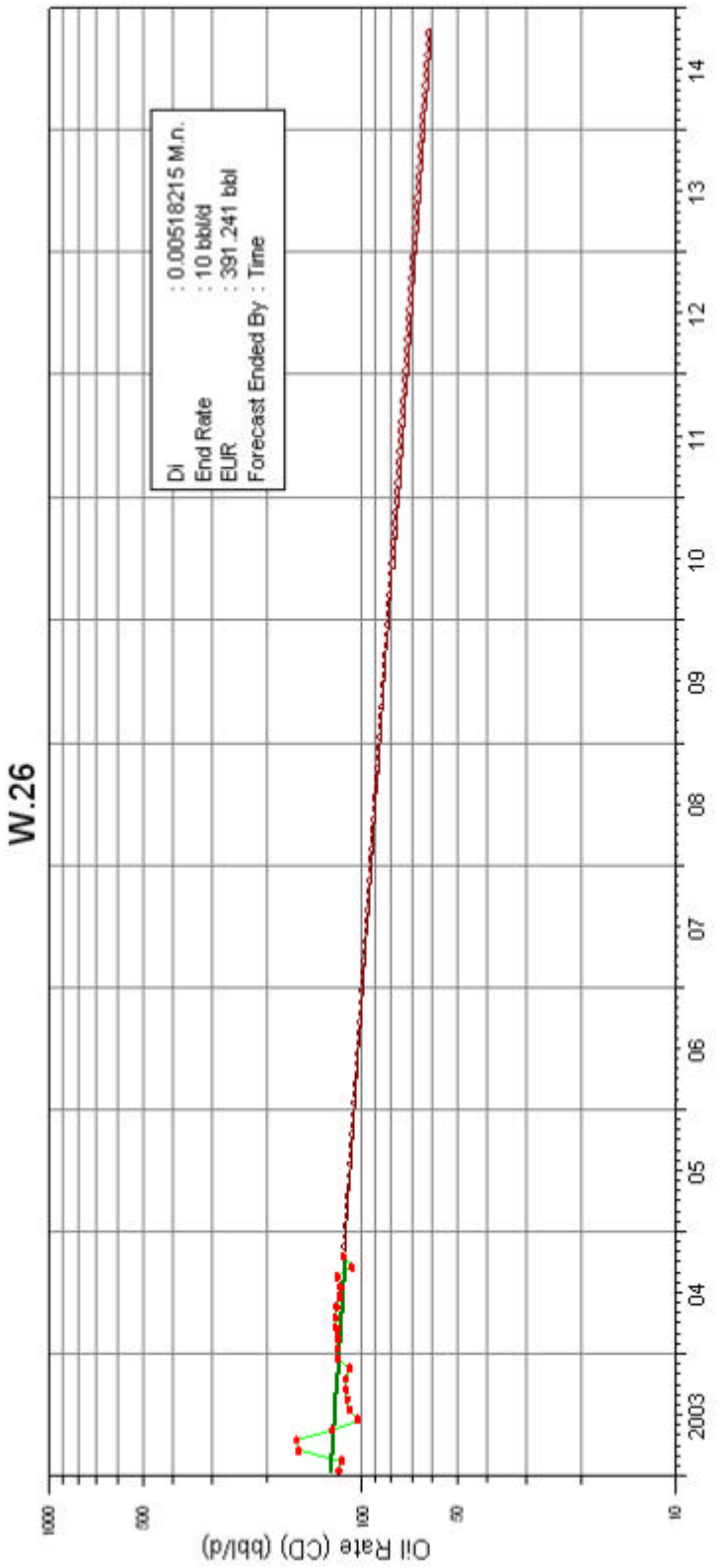

Figure C.22 W-26 Decline curve graphic

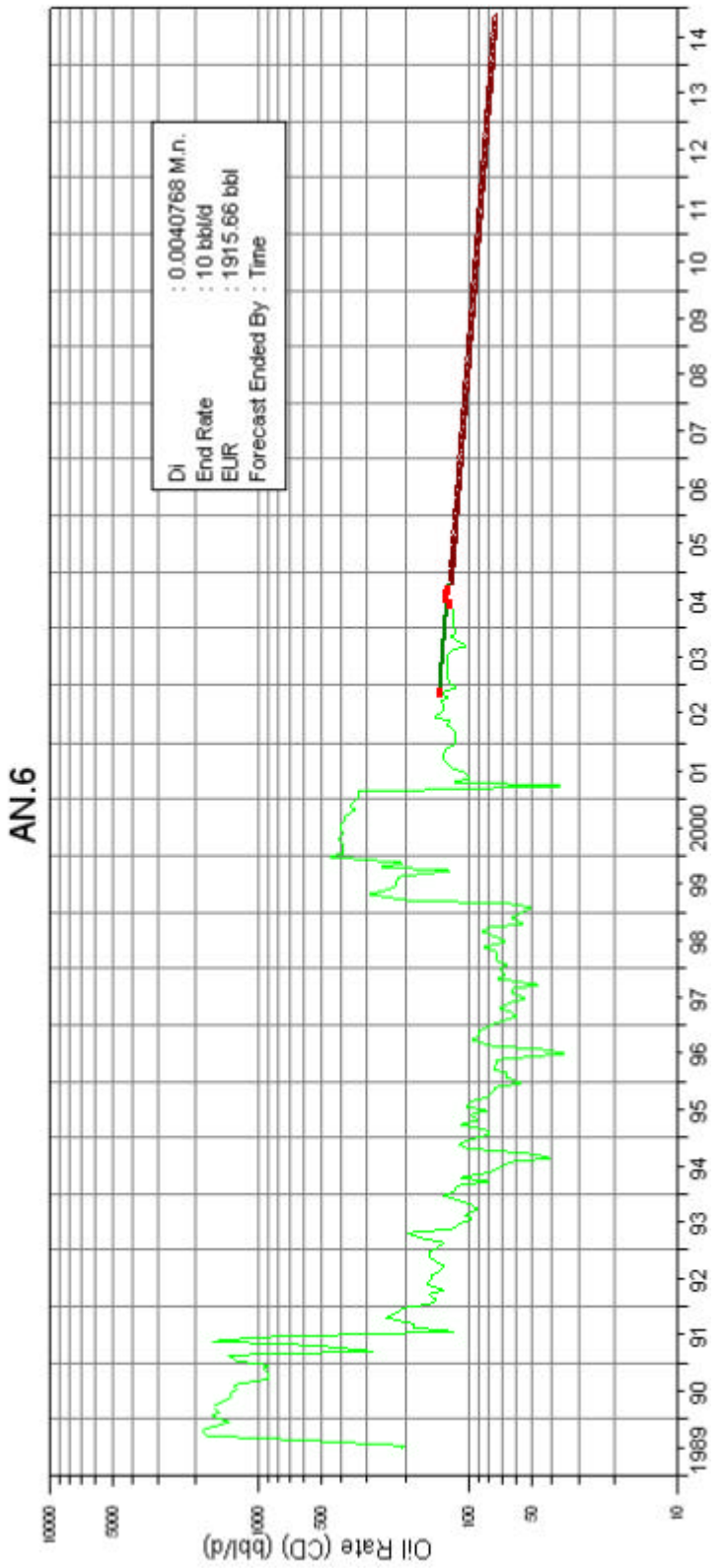

Figure C.23 AN-6 Decline curve graphic

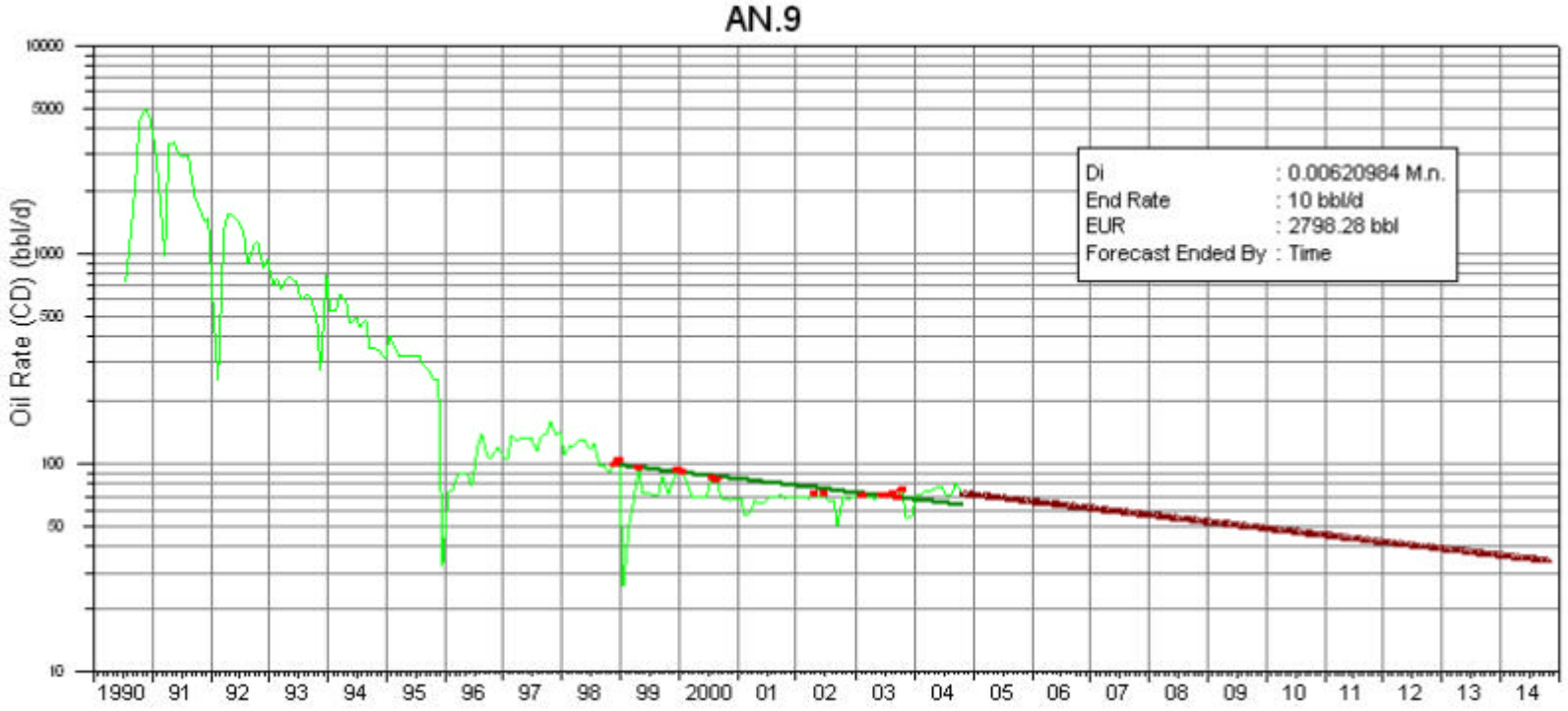

Figure C.24 AN-9 Decline curve graphic

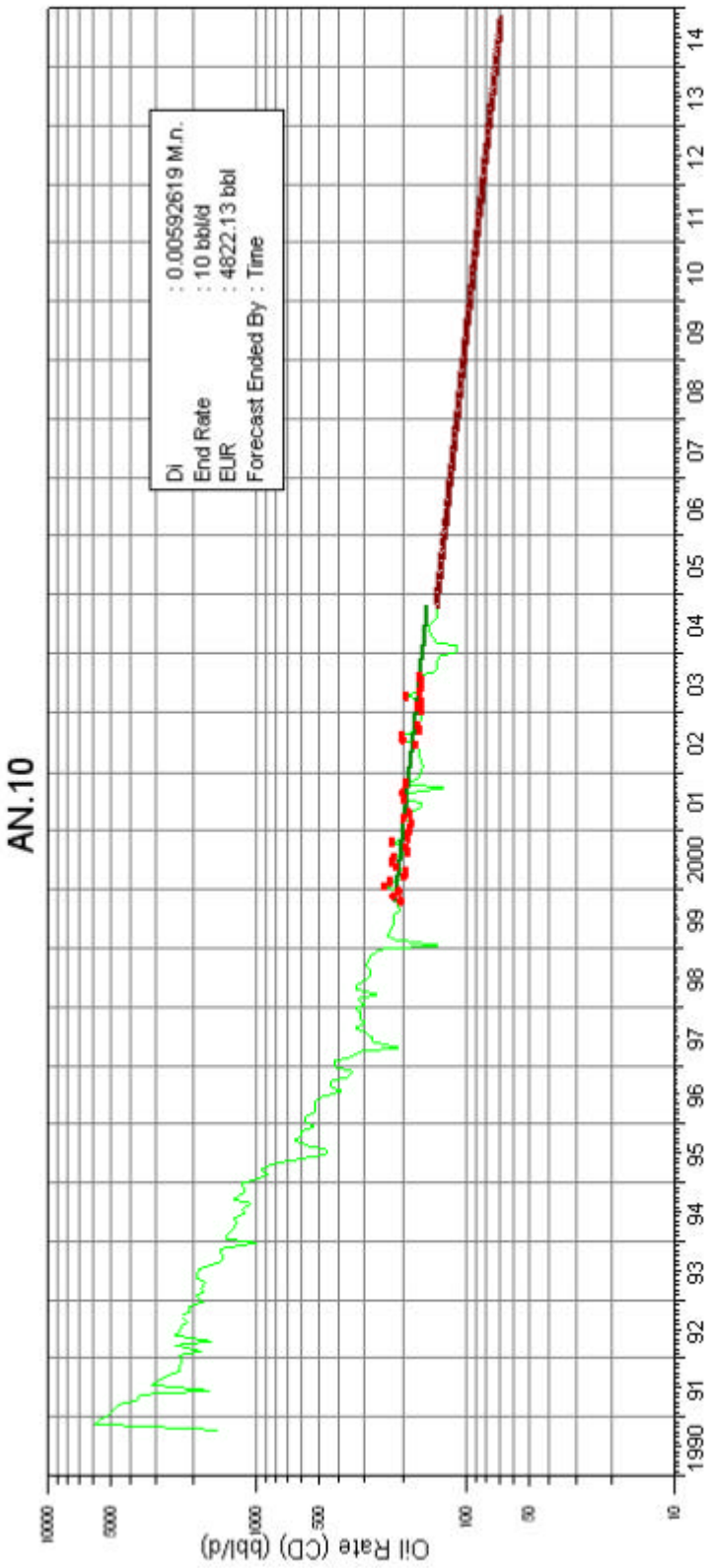

Figure C.25 AN-10 Decline curve graphic

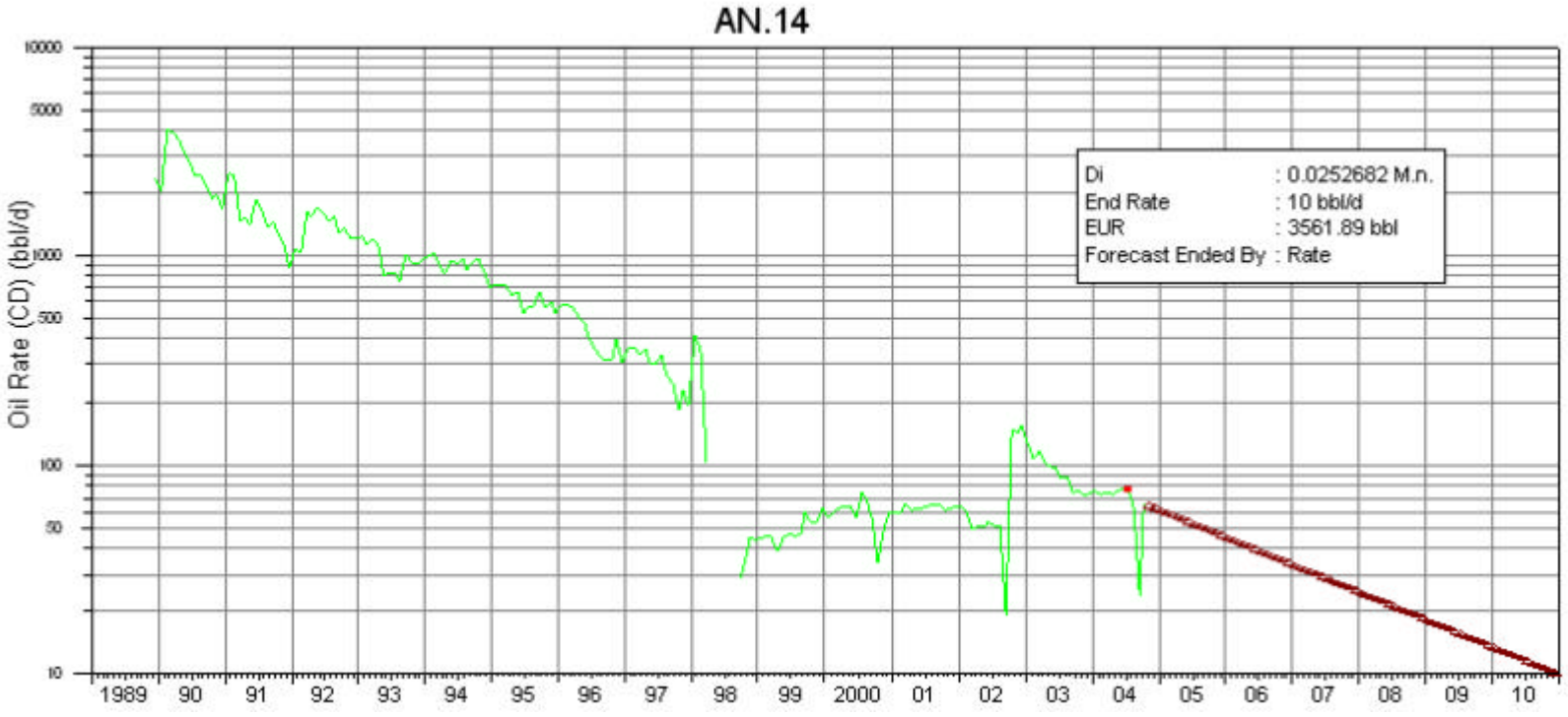

Figure C.26 AN-14 Decline curve graphic

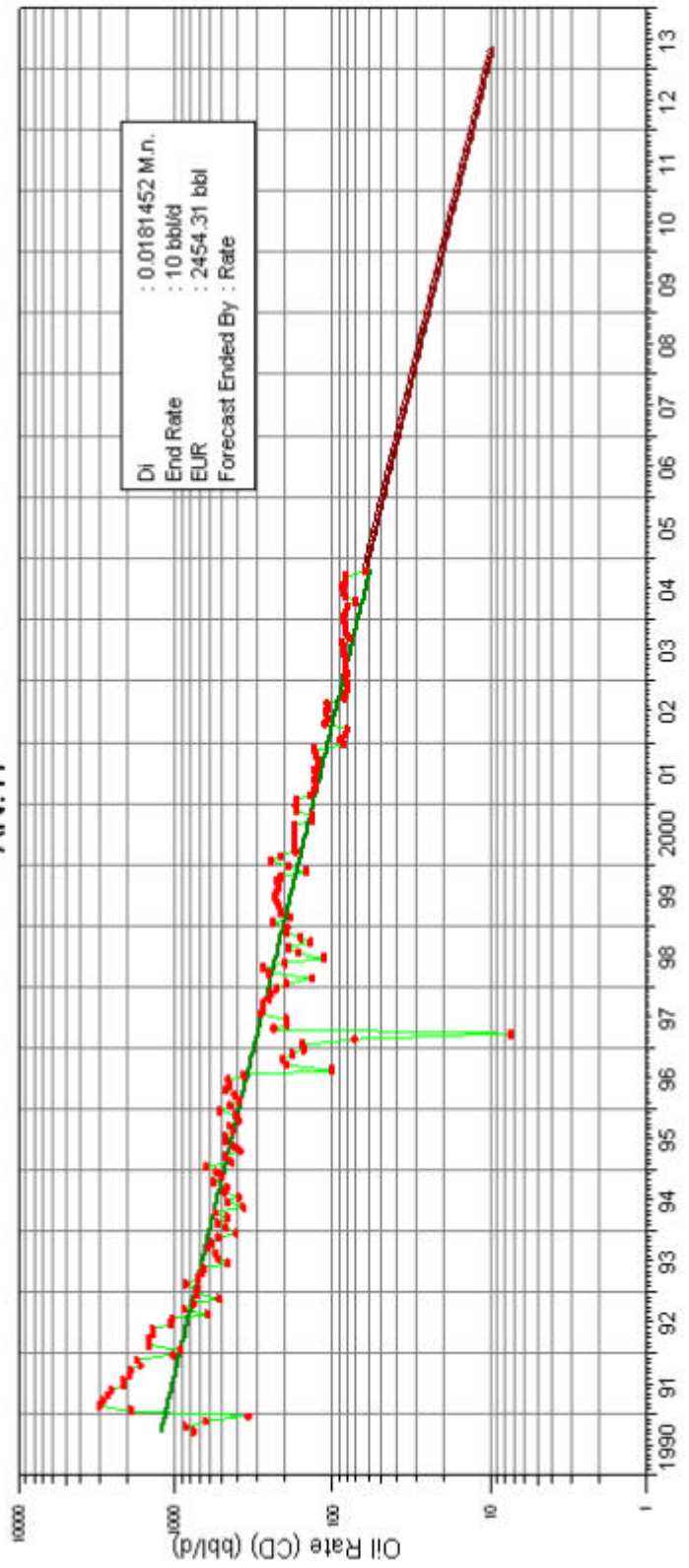

Figure C.27 AN-17 Decline curve graphic

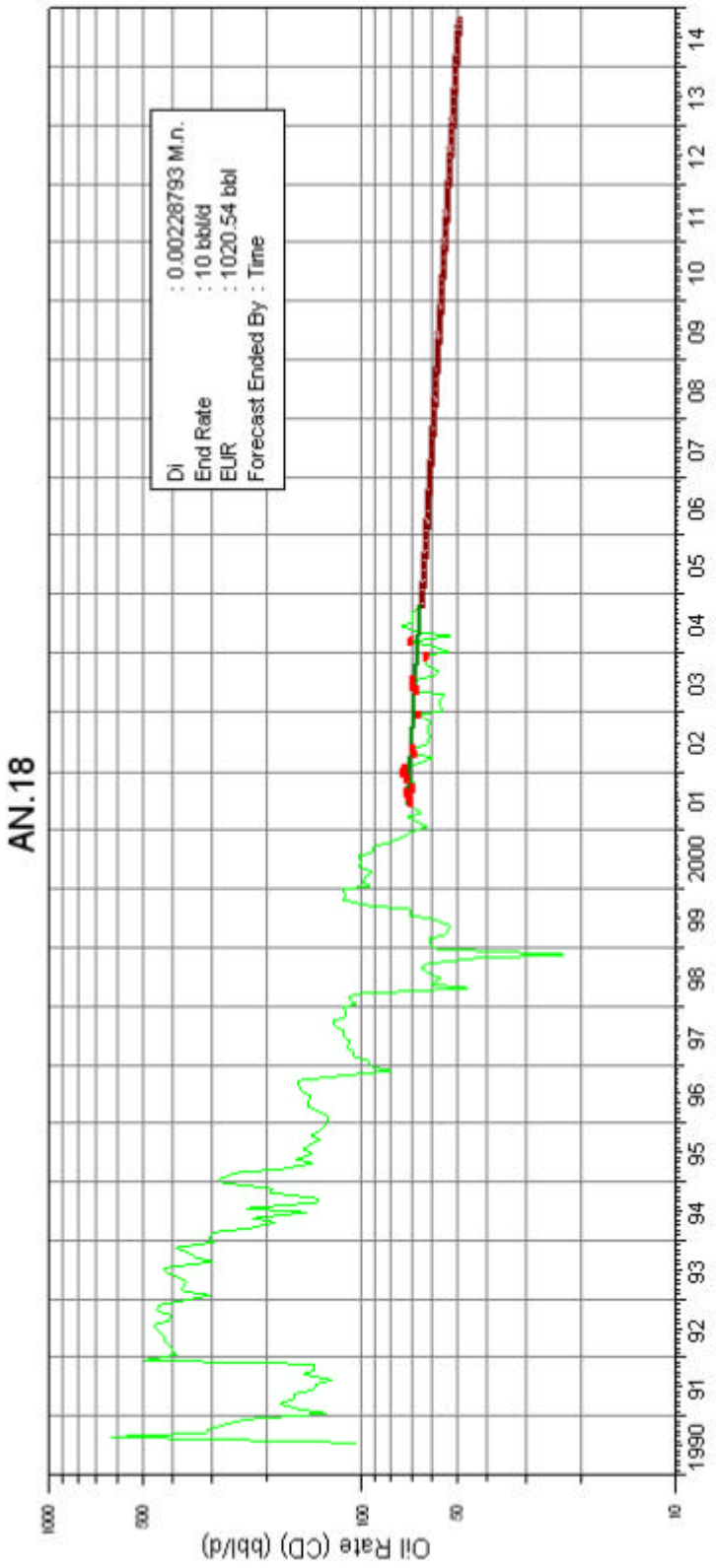

Figure C.28 AN-18 Decline curve graphic

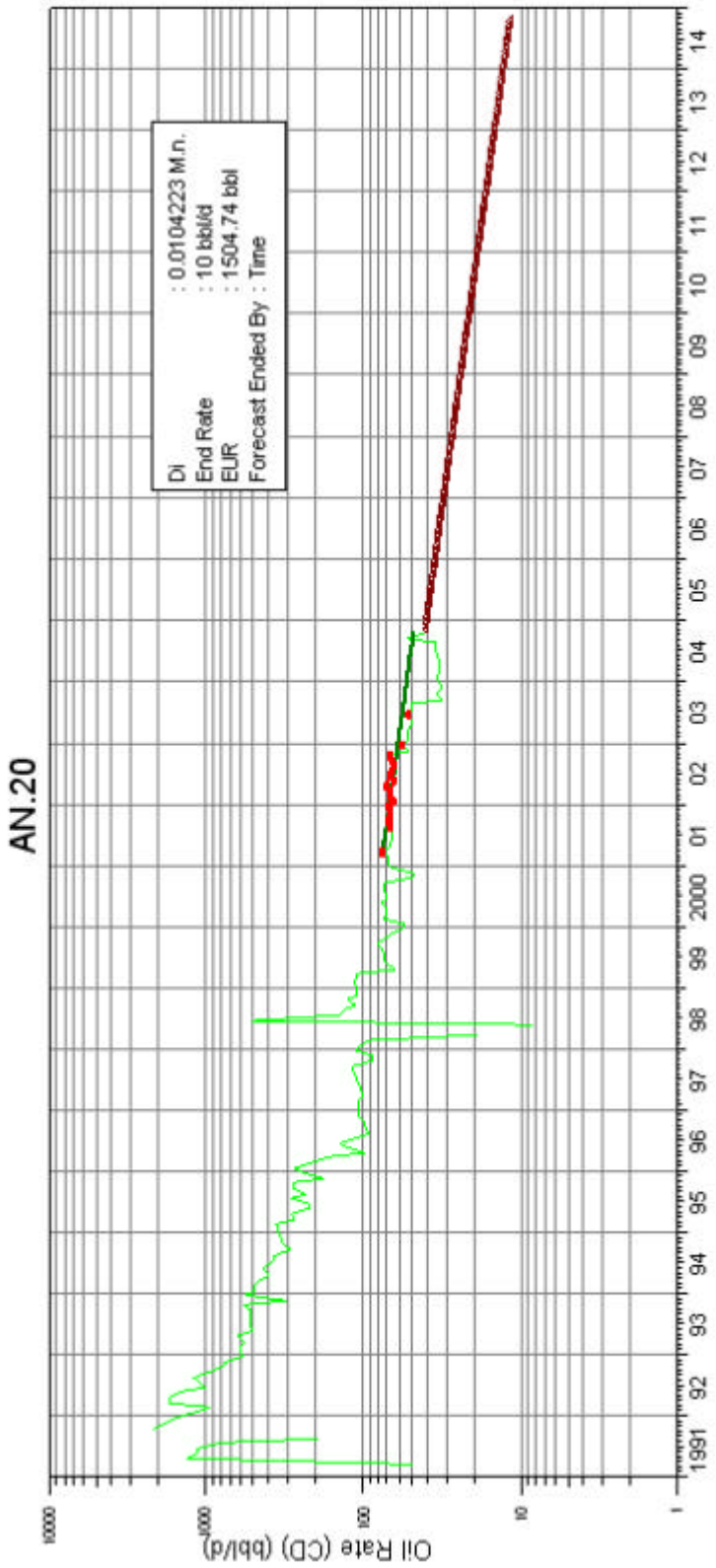

Figure C.29 AN-20 Decline curve graphic

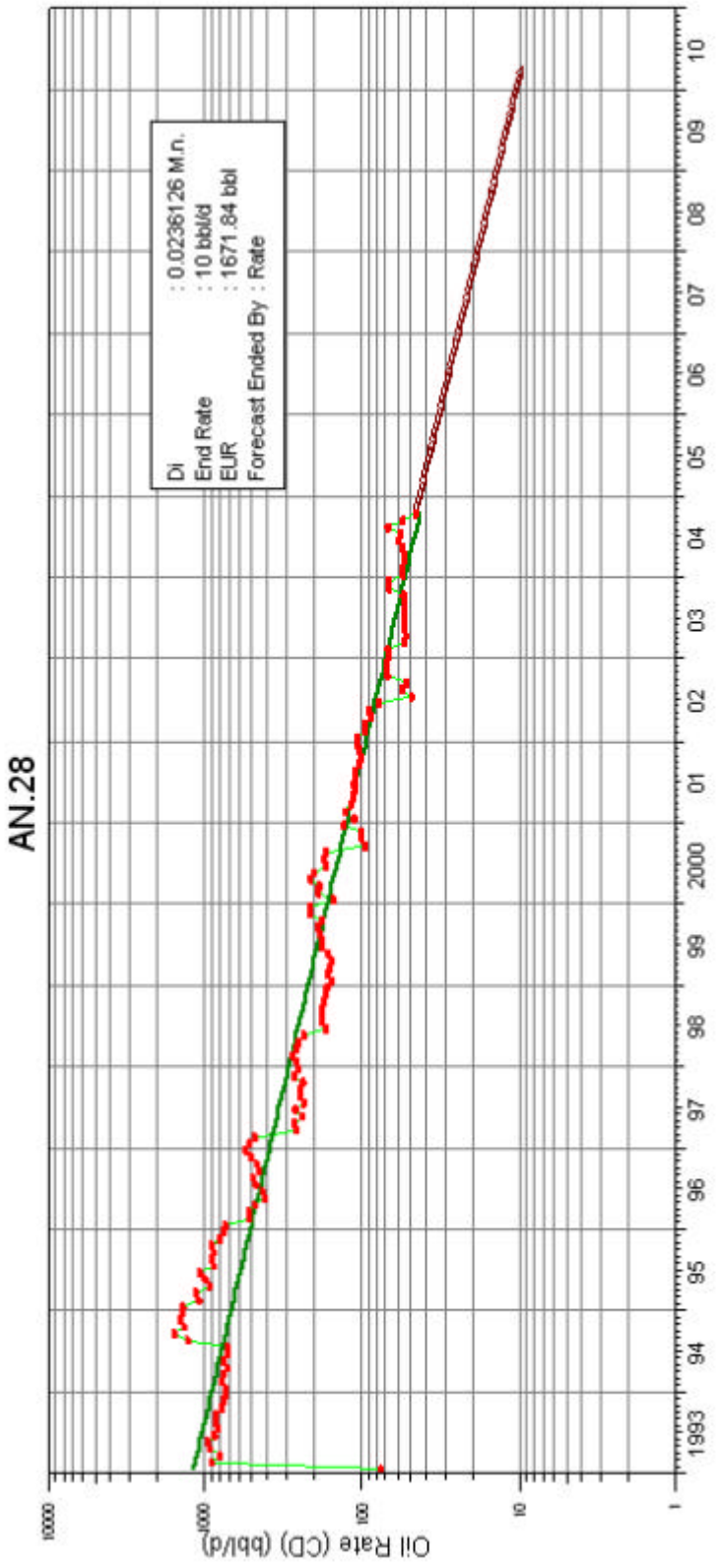

Figure C.30 AN-28 Decline curve graphic

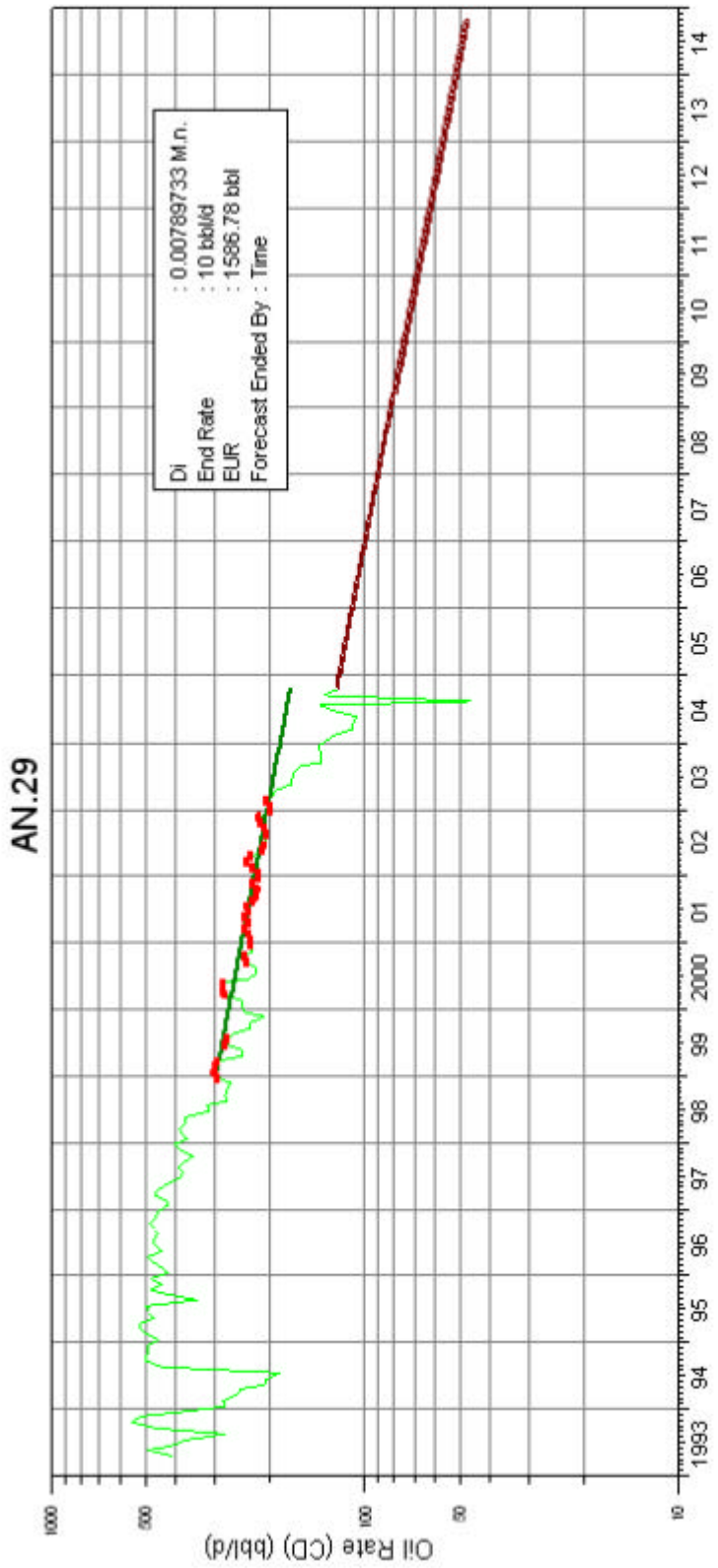

Figure C.31 AN-29 Decline curve graphic

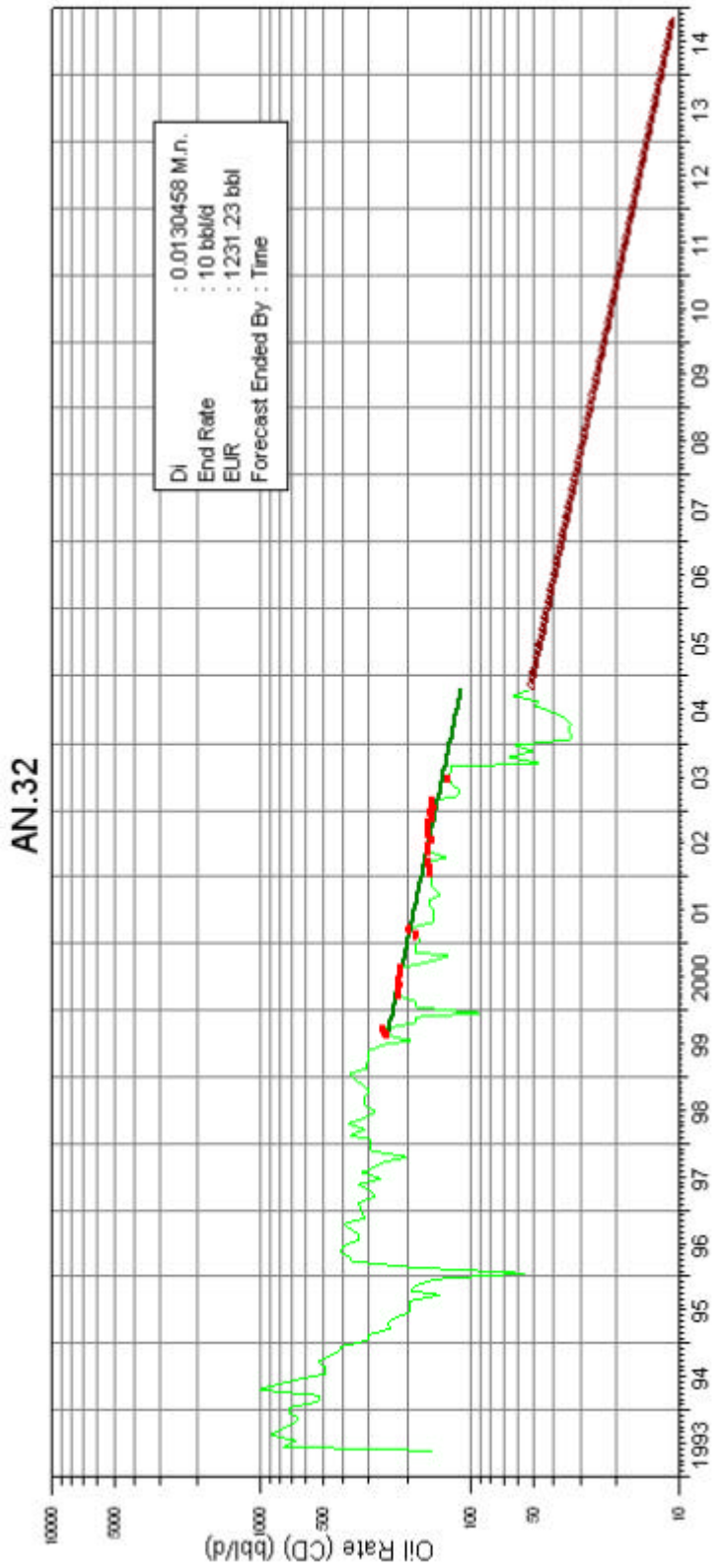

Figure C.32 AN-32 Decline curve graphic